PRODUCTION AND PURIFICATION OF XYLITOL

FROM SUGARCANE BAGASSE

Nguyen Cao Cuong

A Thesis Submitted in Partial Fulfillment of the Requirements for the

Degree of Master of Science in Biotechnology

Suranaree University of Technology

Academic Year 2020

การผลิตและการทำบริสุทธิ์ไซลิทอลจากกากชานอ้อย

เหงียน เกา เกือง

PRODUCTION AND PURIFICATION OF XYLITOL

FROM SUGARCANE BAGASSE

Suranaree University of Technology has approved this thesis submitted in partial fulfillment of the requirements for a Master's Degree.

Thesis Examining Committee

_____

(Assoc. Prof. Dr. Mariena Ketudat-Cairns)

Chairperson

_____

(Assoc. Prof. Dr. Apichat Boontawan)

Member (Thesis Advisor)

_____

(Assoc. Prof. Dr. Kaemwich Jantama)

Member

_____

(Assoc. Prof. Dr. Theppanya Charoenrat)

Member

_____   _____

(Assoc. Prof. Flt. Lt. Dr. Kontorn Chamniprasart)   (Prof. Dr. Neung Teaumroong)

Vice Rector for Academic Affairs   Dean of Institute of Agricultural Technology

and Internationalization

เหงียน เกา เกือง : การผลิตและการทำบริสุทธิ์ไซลิทอลจากกากชานอ้อย (PRODUCTION AND PURIFICATION OF XYLITOL FROM SUGARCANE BAGASSE) อาจารย์ที่ปรึกษา : รองศาสตราจารย์ ดร.อภิชาติ บุญทาวัน, 129 หน้า

ไซลิทอลเป็นน้ำตาลแอลกอฮอล์ที่มีจำนวนคาร์บอน 5 อะตอม มีการประยุกต์ใช้ได้หลากหลาย ในการศึกษานี้ได้ทำการผลิตด้วยเชื้อ Candida guilliermondii TISTR 5068 และทำบริสุทธิ์จากกากชานอ้อย แทนที่จะใช้น้ำตาลไซโลสทางการค้า กากชานอ้อยได้ถูกย่อยด้วยด่างเพื่อที่จะได้ของผสมระหว่างน้ำตาลไซโลสและน้ำตาลกลูโคส น้ำตาลกลูโคสได้ถูกกำจัดโดยการหมักให้เป็นเอทานอล กระบวนการหมักน้ำตาลไซลิทอลได้ถูกดำเนินการด้วยถังหมักขนาด 500 ลิตร ซึ่งผลการทดลองแสดงให้เห็นว่าสามารถผลิตน้ำตาลไซลิทอลได้ 23.24 กรัมต่อลิตร โดยมีค่าผลผลิตและผลิตผลอยู่ที่ 0.87 กรัม$_\text{ไซลิทอล}$/กรัม$_\text{ไซโลส}$ และ 0.14 กรัมต่อลิตรต่อชั่วโมงตามลำดับ ซึ่งถัดมาน้ำหมักได้ถูกทำบริสุทธิ์ด้วยการใช้เทคนิคเยื่อแผ่นบางและเรซิ่นแลกเปลี่ยนประจุ โดยในช่วงแรกได้มีการศึกษาการใช้อิเลคโตรไดอะไลซีส แต่วิธีการนี้ไม่สามารถกำจัดสีได้ ผลการทดลองการทำบริสุทธิ์ที่มีประสิทธิภาพดีที่สุดนั้น ได้จากการทำงานต่อเนื่องระหว่างไมโครฟิวเตรชั่น อัลต้าฟิวเตรชั่น นาโนฟิวเตรชั่น เรซิ่นแลกเปลี่ยนประจุ และขั้นตอนการตกผลึก โดยไมโครฟิวเตรชั่นได้มุ่งเน้นการแยกเซลล์และองค์ประกอบที่มีขนาดใหญ่ในน้ำหมัก ส่วนอัลต้าฟิวเตรชั่นและนาโนฟิวเตรชั่นมุ่งเน้นการกำจัดสิ่งปนเปื้อนที่เป็นสารอินทรีย์ อนินทรีย์ โปรตีนและสารโมเลกุลใหญ่อื่น ๆ เรซิ่นแลกเปลี่ยนประจุใช้ในการกำจัดเกลือและสีของน้ำหมัก ซึ่งคุณประโยชน์เหล่านี้ได้ส่งผลต่อการทำบริสุทธิ์เป็นอย่างมาก โดยกระบวนการทำการบริสุทธิ์ขั้นสุดท้ายด้วยการตกผลึก ได้ผลึกไซลิทอลที่มีความบริสุทธิ์ที่ร้อยละ 99.64 และประสิทธิภาพการกู้คืนที่ร้อยละ 85.03 จากการทดลองการล่อผลึกที่ร้อยละ 1 โดยน้ำหนัก ซึ่งผลการทดลองแสดงให้เห็นถึงความสำเร็จในการผลิตผลึกไซลิทอลคุณภาพสูงในระดับโรงงานต้นแบบจากกากชานอ้อยด้วยเชื้อ Candida guilliermondii TISTR 5068

สาขาวิชาเทคโนโลยีชีวภาพ   ลายมือชื่อนักศึกษา_____

ปีการศึกษา 2563   ลายมือชื่ออาจารย์ที่ปรึกษา_____

ลายมือชื่ออาจารย์ที่ปรึกษาร่วม_____

NGUYEN CAO CUONG : PRODUCTION AND PURIFICATION OF
XYLITOL FROM SUGARCANE BAGASSE. THESIS ADVISOR :
ASSOC. PROF. APICHAT BOONTAWAN, Ph.D. 129 PP.

XYLITOL/SUGARCANE HEMICELLULOSIC HYDROLYSATE/MEMBRANE
FILTRATION/ION EXCHANGE RESIN/CRYSTALLIZATION

Xylitol is five-carbon sugar alcohol widely applied in many different fields. In this study, the production using *Candida guilliermondi* TISTR 5068 and purification of xylitol from sugarcane bagasse instead of commercial xylose were investigated. Bagasse was alkaline hydrolyzed to recover the xylose-glucose mixture. Glucose was removed from the xylose-glucose mixture by ethanol fermentation. Batch-batching xylitol fermentation was performed using a 500 L bioreactor. The results showed that xylitol titer of 23.24 g/L with the yield of 0.87 $g_{xylitol}/g_{xylose}$ and productivity of 0.14 g/L.h were obtained for batch fermentation. Subsequently, the fermentation broth was purified by membranes and ion exchange chromatography techniques. Electrodialysis was initially investigated. However, the color removal capacity was not good. Highly efficient purification results were obtained by conducting a series of microfiltration (MF), ultrafiltration (UF), nanofiltration (NF), ion exchange chromatography, and crystallization steps. MF was used to remove cells and large size insoluble components in the fermentation broth. UF and NF were used to eliminate potential foulants including organic and inorganic substances, proteins, and macromolecules. The ion exchange

chromatography was highly effective in the desalination and decolorization of the clarified fermentation broth. Crystallization was performed as a final step to maximize purity of the final crystal product. The xylitol crystal purity of 99.64% with a recovery efficiency of 85.03% was obtained for a 1% (w/v) seeding crystallization experiment. These results showed that very high-quality xylitol crystal production at a pilot scale could be achieved from sugarcane bagasse using *Candida guilliermondi* TISTR 5068.

School of Biotechnology

Academic Year 2020

Student's Signature_____

Advisor's Signature_____

Co-advisor's Signature_____

ACKNOWLEDGEMENT

CONTENTS

CONTENTS (Continued)

CONTENTS (Continued)

LIST OF TABLES

LIST OF FIGURES

LIST OF FIGURES (Contiued)

Figure   **Page**

LIST OF FIGURES (Contiued)

Figure   **Page**

LIST OF FIGURES (Contiued)

LIST OF ABBREVIATIONS

ºC	=	Degree Celsius
%	**=**	Percent
w/w	=	Weight per Weight
v/v	=	Volume per Volume
g/L	=	Gram per Liter
g/L.h	=	Gram per Liter per H
g	=	Gram
g/g	=	Gram per Gram
L	=	Liter
mL	=	Milliliter
rpm	=	Round per Minute
vvm	=	Volume per Volume per Liter
min	=	Minute
h	=	Hour
et al.,	=	and others
NF	=	Nanofiltration
UF	=	Ultrafiltration
MF	=	Microfiltration
ED	=	Electrodialysis
EV	=	Evaporation

LIST OF ABBREVIATIONS (Continued)

DI	=	Deionized water
HMF	=	Hydroxymethylfurfural
OD_{600}	=	Optical density measured at 600 nm
DO	=	Dissolved oxygen
P_x	=	Volumetric rate of xylose consumption (g/L.h)
XDH	=	Xylitol dehydrogenase
XR	=	Xylose reductase
Y_x	=	Xylitol yield from xylose (g/g)
XBS	=	Xylose from Sugarcane hemicellulosic hydrolysate
PSD	=	Particle Size Distribution
FBRM	=	Focused Beam Reflectance Measurement
PVM	=	Particle Vision and Measurement

CHAPTER I

INTRODUCTION

1.1   Significant of this study

Xylitol is regarded as a sugar-alcohol widely used in food, and pharmaceutical industries. Xylitol contains high sweetness and low energy value compared to sucrose, which is suitable for dieters, obese people or diabetics. On the other hand, its antibacterial properties can be applied in several functional foods with preventive and treatment properties so-called oral, cardiovascular, and anti-oxidant. Therefore, the demand for xylitol is continuously increasing every year. According to research and market reports, the global xylitol market in 2018 is estimated at US $ 823.6 million, and will reach US$ 1.15 billion by 2023 with an annual compound growth of approximately 5.7% from 2018 to 2023 (Markets 2018). With that momentum, the xylitol market is estimated to reach US$ 1.37 billion ($4-5/kg by 2025 (Felipe Hernandez-Perez, de Arruda *et al.* 2019).

Direct xylitol fermentation from xylose produced from bagasse seems to be an essential step to continue improving the value chain of biological materials in the context of Thailand being a country with the fourth largest sugar industry in the world. The efficiency of the fermentation process, the ability to recover the product, is influenced by subsequent downstream processes, which will determine the quality, yield and economic value of the product. The post-fermentation downstream processes

can be referred to as separation, crystallization process (Martínez, de Almeida e Silva *et al.* 2007); centrifugation and supercritical extraction with CO_2 (Silva, Dussán *et al.*

2020); membrane separation processes (Kresnowati, Desiriani *et al.* 2017); ion exchange membrane (Kumar, Sandhu *et al.* 2019); combined ultrafiltration and ion exchange membranes (Kresnowati, Regina *et al.* 2019). However, most studies tend to stop increasing the xylitol concentration in the fermented liquid solution, whereas, the commercial application of xylitol is primarily in the crystalline state through crystallization. On the other hand, previous studies are mainly at the laboratory scale, there is no pilot study to fully access of the industrial application and this is an important step to encourage commercial production system.

In this study, *Candida guilliermondi* TISTR 5068 with fast growth characteristics, capable of producing high-yield xylitol was used to ferment in 500 L bioreactor. Next, process purification including combination of membrane filtration and ion exchange membrane as well as vacuum evaporation and crystallization was investigated. The goal of this research is to obtain high yield and purity of xylitol production.

1.2   Research objectives

The main objectives of this study are listed as follows:

To design an efficient xylitol fermentation: process optimization

To obtain high xylitol content from fermentation broth using a combination of membrane filtration, ion exchange resin and crystallization

1.3   Research hypothesis

High yield of xylitol can be fermented from xylose by using *Candida guilliermondi* TISTR 5068.

Membrane and ion exchange resin techniques can be used to remove unwanted components especially salts, and color from the fermentation broth.

The crystallization process can be applied to obtain high purity of xylitol crystal.

1.4 Scope of the thesis

This research consist of two parts. The first one is the xylitol fermentation by *Candida guilliermondi* TISTR 5068 with two main carbon sources which are glucose and xylose. In particular, glucose plays a role in biomass development while xylose acts as a raw material for xylitol production. The fermentation process was carried out in 500 L bioreactor. The next section is the downstream processing of xylitol from fermentation broth using microfiltration (MF), nanofiltration (NF), electrodialysis (ED), ion exchange resin, evaporation (EV), and crystallization techniques. After fermentation, the fermentation broth was cleaned with the help of microfiltration (MF) to remove all of the cells. For proteins and polymeric compounds, salts can be separated by combining nanofiltration (NF) and electrodialysis (ED) and Ion exchange resin. The solution was evaporated to increase the concentration of xylitol. The methods of crystallization used include cooling, seeding, or a combination of the two to obtain a high crystallization yield.

1.5 Expected results

High efficiency of xylitol fermentation with high content, yield, and productivity was obtained by combining suitable carbon sources (glucose and xylose).

The high purity of xylitol will be obtained using membrane separation,

evaporation, and crystallization processes.

The downstream process can be applicable for industrial-scale production with high-purity xylitol production.

CHAPTER II

LITERATURE REVIEWS

2.1   Xylitol

Xylitol, a sugar alcohol with five carbon atoms ($C_5H_{12}O_5$), is obtained by replacing the aldehyde group with a hydroxy group (Hernández-Pérez, Jofre *et al.* 2020). Xylitol containing a 152.15 g/mol molecular weight is often used as a sweetener in sugar-free confectionery. Xylitol is found naturally in small amounts in various fruits and vegetables such as prunes, strawberries, cauliflower, and pumpkins. It is the sweetest sugar of all polyols and is equivalent to the sweetness of sucrose but contains low energy (2.4 cal/gram compared to 4.0 cal/gram of sucrose). Xylitol was first synthesized in 1890 by German scientist Hermann Emil Fischer (Salli, Lehtinen *et al.* 2019).

The molecular structure and physical and chemical properties of xylitol are indicated in Fig 2.1. and Table 2.1, respectively.
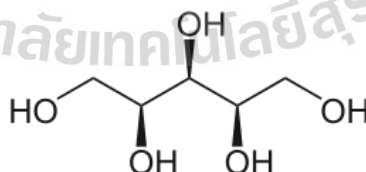
Figure 2.1 Molecular structure of xylitol (Salli, Lehtinen *et al.* 2019)

Xylitol tends not to be considered as sugar but only as a sugar-free sweetener in the same group as other popular diet sweeteners such as sorbitol, mannitol, and maltitol. The xylitol molecule which has 5 hydroxyl (OH) groups linked to 5 carbon atoms. Non-

caramelized xylitol at temperatures that are close to the boiling point for a short time (216 ^{o}C). Xylitol is well soluble in water and is dependent on temperature, sparingly soluble in alcohol (1.2 grams/100 grams of ethanol) (Mussatto 2012).

GRAS (Generally Recognized As Safe) status for xylitol was granted by the U.S. Food and Drug Administration in 2016, which means apart from being used as medicines, xylitol is also allowed to be used for both food and drinks. The xylitol market has been growing rapidly in recent years because people are concerned about their health, demanded for sugar-free gum, confectionery and pharmaceuticals. The global xylitol market in 2019 is 40 times larger than in 1978 and is expected to reach US$ 1.37 billion by 2025 (Felipe Hernandez-Perez, de Arruda *et al.* 2019). Currently, the xylitol market is estimated to reach 242 thousand metric tons, valued at US$ 1 billion (Delgado Arcaño, Valmaña García *et al.* 2020). Production of xylitol is primarily in the Asia Pacific, followed by Europe, the United States and Australia (Markets 2018).
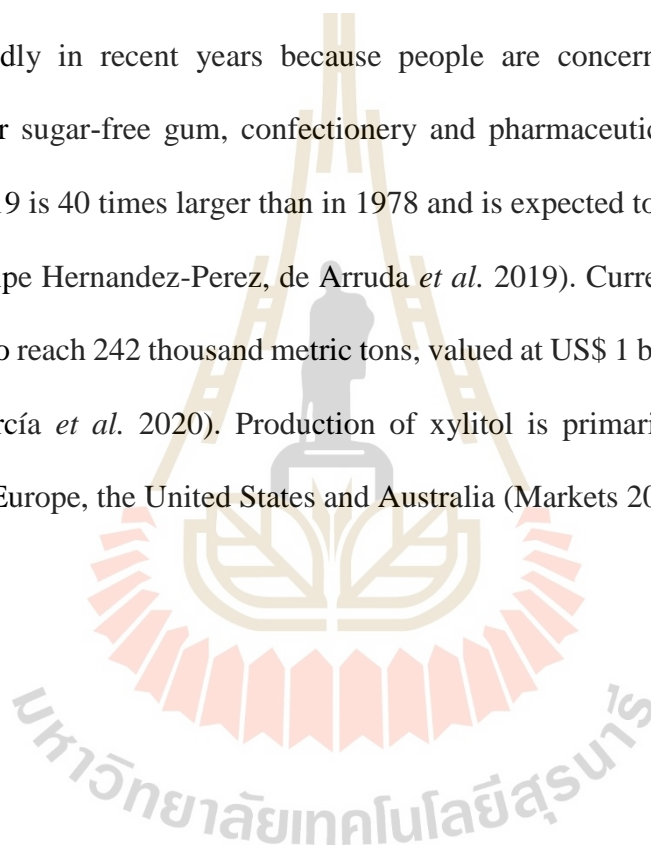
Table 2.1 Chemical and physical properties of xylitol (Ur-Rehman, Mushtaq *et al.* 2015)

Properties	
Formula	$C_5H_{12}O_5$
Molecular weight, $g.mol^{-1}$	152.15
Appearance	White, crystalline powder
Solubility at 20 ºC, g/100 g water	169
pH in water, 1 g/10 mL	5–7
Melting point, ºC	93–94.5
Boiling point (at 760 mmHg), ◦C	216
Caloric value, cal/g	2.4
Density of aqueous solution 10% (at 20 ºC), $g.cm^{-3}$	1.03
Viscosity (CP) 10% (at 20 ºC)	1.23

2.1.1 Application of xylitol

As mentioned above, xylitol is a natural sweetener with high sweetness, low energy without causing any disease. Hence, xylitol is widely applied in life and becomes the most typical type, especially its application on food and pharmaceuticals in practical. Figure 2.2. illustrates some of the current popular applications of xylitol (Lugani and Sooch 2018)
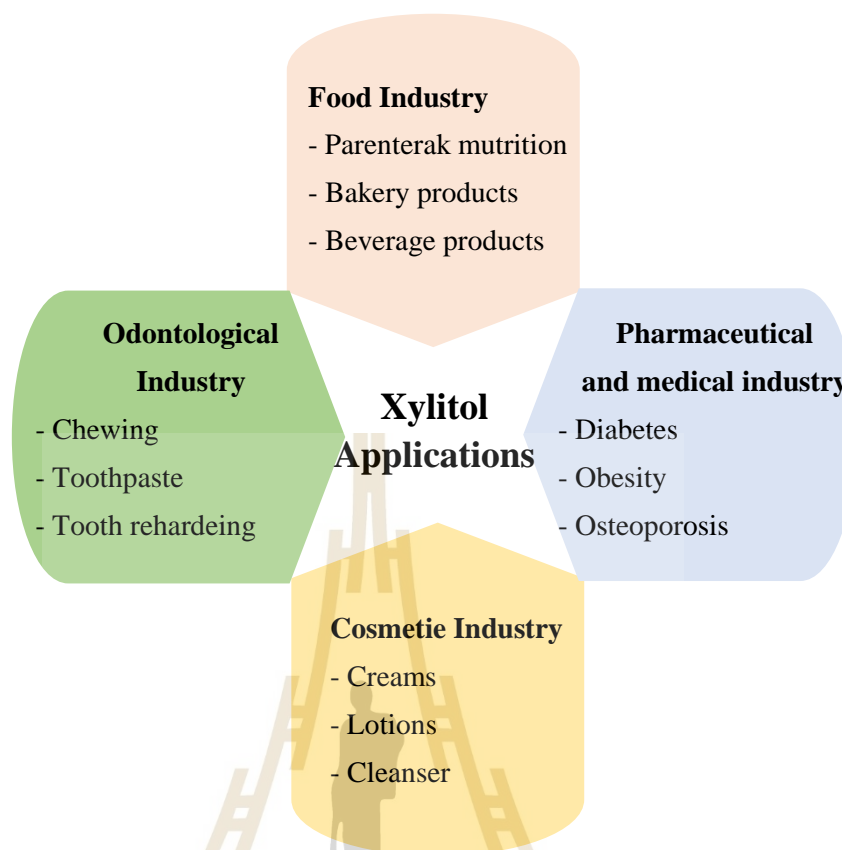
Figure 2.2 Industrial applications of xylitol (Lugani and Sooch 2018)

In the food industry, xylitol is primarily used of as a sweetener in the manufacture of candy, chocolate, beverages, jams, and snacks; while in the pharmaceutical industry, it is used in adjuvant therapy to treat diabetes and dental disease (Mohamad, Mustapa Kamal *et al.* 2014, Lugani, Oberoi *et al.* 2017, Xu, Liu *et al.* 2018). Numerous studies have demonstrated the benefits of xylitol to human health, especially for those who need tobe on a diet, obese or diabetic. Additionally, by its natural antiseptic properties, xylitol is also applied a lot in products to deter tooth decay so-called sugarless gum, toothpaste, etc.

According to Ly and colleagues, xylitol is capable of reducing *Streptococcus* levels in dental plaque, and saliva, which can reduce cavities. Xylitol-containing food products with the function of preventing tooth decay are increasingly

being accessed by consumers (Ly, Milgrom *et al.* 2006).

Apart from benefiting from the prevention of dental diseases, xylitol has also been shown to be a viable solution in other health-related problems (Salli, Lehtinen *et al.* 2019). For example, xylitol improves skin function and prevents the growth of germs on the surface of the skin (Umino, Ipponjima *et al.* 2019). In other studies, it is thought to be like a prebiotic, which is poorly digested in the small intestine and goes down to the colon as a source of nutrients for probiotics that help improve digestion absorption, laxative and reduce constipation (Yunhui Gong, Qianwen Zhang *et al.* 2015, Lenhart and Chey 2017). Researches on the role of xylitol on the health of people's ears, nose and throat have also been conducted. Thereby, xylitol has been proved to enhance respiratory function for patients with non-allergic nasal congestion if using xylitol-containing nasal spray twice a day (Cingi, Birdane *et al.* 2014). The effects of xylitol on sore throat were also demonstrated when using a 15% xylitol gum solution for 3 months, resulting in improved swallowing ability and reduced inflammation effectively (Little, Stuart *et al.* 2017).

2.1.2 Production of xylitol

In recent years, with the result of the positive effects of xylitol on health, together with the increasing number of diabetic patients and people's concerns, xylitol has been produced and widely applied. Xylitol can be produced through three methods: direct extraction, chemical hydrogenation, and biotransformation.

It can be easy to extract xylitol directly from fruits and vegetables; however, this method it not often due to its low xylitol content and high production costs. Xylose hydrogenated is a traditional method for producing xylitol, but it is expensive and energy-

intensive. Biological methods are commonly used to produce xylitol, in which xylose is converted into xylitol under the action of xylose reductase enzyme of microorganisms during fermentation (Xu, Liu *et al.* 2018).

Figure 2.3 and Table 2.2 compare the two methods of manufacturing xylitol currently used.
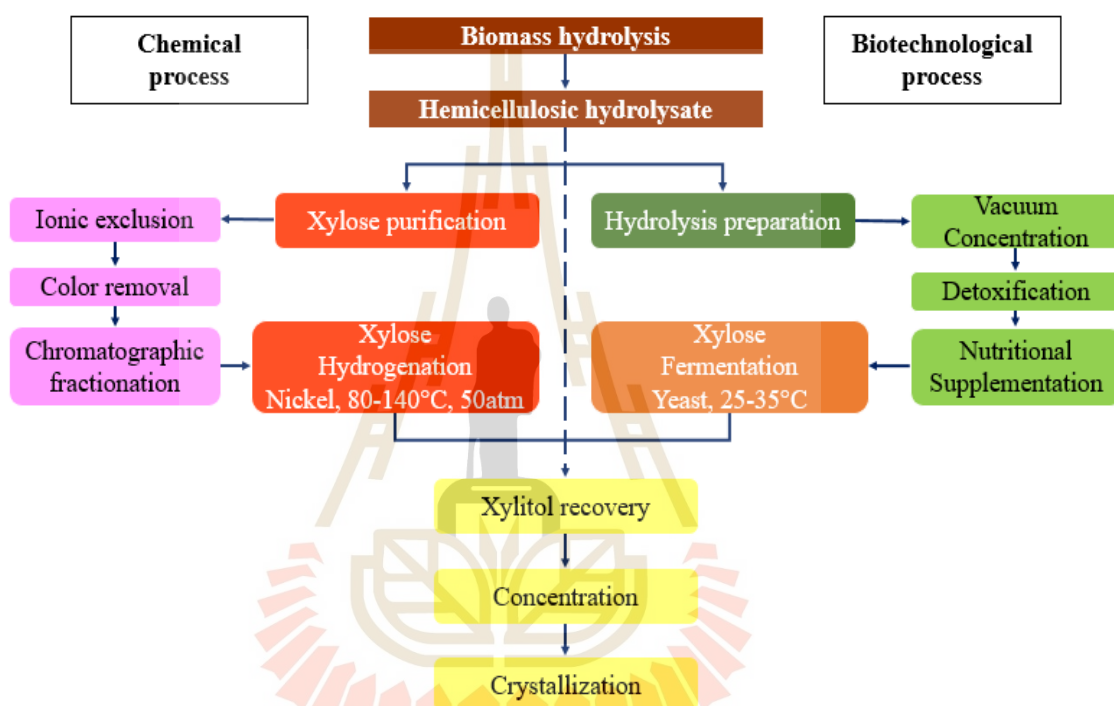
Figure 2.3 Comparison of the main steps of the chemical and biotechnological processes for the production of xylitol from vegetable biomasses (Hou-Rui 2012, Canilha, Lacerda Brambilla Rodrigues *et al.* 2013, Pal, Mondal *et al.* 2016)

Table 2.2 Factors of biological and chemical processes for xylitol production (Mohamad, Mustapa Kamal *et al.* 2014)

Factor	Biological	Chemical
Carbon source	Xylose from lignocellulose	Pure xylose Xylose from lignocellulose
Catalyst	Yeast/bacteria/fungi that required xylose reductase and xylitol dehydrogenase enzyme	Nickel and hydrogenation
Process steps	1. Acid or enzymatic hydrolysis of lignocellulose 2. Detoxification of hydrolysate 3. Fermentation of hydrolysate to xylitol 4. Xylitol purification	1. Acid hydrolysis of lignocellulose 2. Purification of hydrolysate to obtain pure xylose 3. Hydrogenation of xylose to xylitol 4. Xylitol crystallization
Purification	Complex downstream process because of different microbial by-products	Ion-exchange resins
Cost	Lower energy and mild temperature	High (need two steps of purification process, high energy required, and laborious)

1. Production of xylitol by chemical process

Producing xylitol by the chemical method is highly productive but energy-consuming because chemical reactions occur in high temperatures and require the necessary catalysts, which increases production costs, resulting in low economic efficiency. On the other hand, this way will also cause environmental concerns (Yi and

Zhang 2012, Rafiqul and Sakinah 2013, Pulicharla, Lonappan *et al.* 2016)

Production of industrial xylitol by chemical methods originates from the hydrolysis of lignocellulose materials to obtain xylan, which was metabolized to produce xylose and then xylitol (Pal, Mondal *et al.* 2016, Delgado Arcaño, Valmaña García *et al.* 2020).

4 basic steps can be listed as follows:

(1) Hydrolyze lignocellulose materials to obtain xylan, continuing to hydrolyze xylan to obtain high-concentration xylose

(2) Purify xylose, improve concentration and remove inhibitors

(3) Hydrogenated xylose to forms xylitol at high temperature and pressure with the participation of chemical catalysts.

(4) Refine and crystallize to create xylitol products

Hydrolysis of the lignocellulosic biomass

There are some basic components including in Lignocellulose materials such as hemicellulose, cellulose, lignin and others. The hydrolysis process is often used with dehydrated acid (0.5-1.5% w/w) at high temperatures (121-160 $^{\circ}$C) to break down the material structure, then release 70-95% of the simple sugars of hemicellulose to the environment. Products obtained in hydrolysate include xylose, glucose. The non-hydrolytic components such as lignin and cellulose are removed in solid form (de Cássia Lacerda Brambilla Rodrigu, Canettieri *et al.* 2012, Yi and Zhang 2012, Abril and Navarro 2013, Rafiqul and Sakinah 2013). Despite its high hydrolytic efficiency and high sugar content, the disadvantage of this method is the formation of undesirable by-products, making it difficult to refine xylose afterwards. The undesirable products are (i) non-sugar products when hydrolyzed hemicellulose (acetic acid), (ii)

sugar by-products (furfural and hydroxymethylfurfural (HMF)) and (iii) secondary products of lignin (phenolics) (Fehér, Fehér *et al.* 2018).

Xylose Purification

To raise the xylose concentration, which is the raw material for the next process, the undesirable auxiliary components including salts formed after the neutralization process have to be eliminated. The common method is making use of activated carbon or ion exchange resins. These methods are capable of removing 73% furfural, 96% acetic acid, 70% HMF, and 91% phenolic (Ur-Rehman, Mushtaq *et al.* 2015)

Xylose hydrogenation

The xylose hydrogenation takes place under high temperature and pressure conditions with the catalytic participation of metals. Hydrogenation reaction is a redox reaction, metal ions acting as effective electron transfer agents to attach two hydrogen atoms to organic molecules. Under these conditions, besides xylitol, other sugars are also hydrophobic to produce the corresponding polyols such as arabinitol, mannitol, galactitol, sorbitol (Hyvönen, Koivistoinen *et al.* 1982).

Schematic diagram of the reaction of xylose hydrogenation into xylitol is depicted in Fig. 2.4.
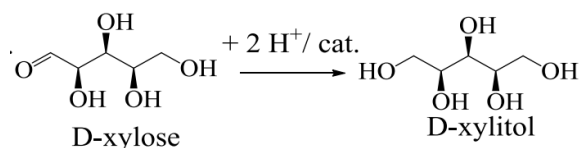
Figure 2.4 Catalytic hydrogenation of D-xylose to D-xylitol (Delgado Arcaño, Valmaña García *et al.* 2020)

Xylitol purification

After the end of chemical hydrogenation, the catalyst was removed by filtration and ion exchange processes to enhance the xylose concentration. Refining processes were then carried out to raise the xylitol concentration to close to saturation to crystallize. Crystal nucleation can be demonstrated under vacuum, low temperature, addition of organic solvents (ethanol or tetrahydrofuran) or addition of crystal germ. This process depends on the solubility and saturation of xylitol at different temperature conditions (de Cássia Lacerda Brambilla Rodrigu, Canettieri *et al.* 2012). In addition, cooling or stirring speed, atmospheric pressure will also affect the ability to germinate crystals, cultivate crystals and stabilize crystal size (Martínez, Canettieri *et al.* 2015). Crystallization yield and purity, quantity and crystal size are important indicators to assess the final product quality.

2. Production of xylitol by bioprocess

Fig. 2.3 and Table 2.2 point out the advantages of biological methods in xylitol production. An important difference between the two methods is the process of converting xylose to xylitol. Using biological methods to convert xylose to xylitol is "milder", less energy-consuming, cheaper and minimizes environmental pollution.

Production of xylitol by biological methods from lignocellulose materials undergoes various stages such as hydrolysis of biomass, detoxification, bioconversion of xylitol production and downstream processes. In this section we will cover the process of bioconversion of xylitol from xylose. The biological metabolic method referred here is the fermentation process, which can be done intermittently or continuously. Two issues to consider in the fermentation process are the microorganism strain and the fermentation environment.

Different types of microorganisms can be used during fermentation process such as bacteria and fungi, but yeasts are thought to be the most effective. The metabolism occurred in two directions with the participation of xylose reductase (XR) reducing xylose and xylitol dehydrogenase (XDH) enzymes that oxidize xylulose (Fig. 2.5). The xylulose is then phosphorylated into xylulose-5-phosphate by the enzyme xylulokinase (XK) (Venkateswar Rao, Goli *et al.* 2016). For XR and XDH work, $NAD^+/NADH$ or $NADH^+/NADPH$ pyridines are needed. Besides, the metabolism of these two factors requires the participation of oxygen. Therefore, oxygen plays a very important role in the fermentation process: under anaerobic conditions, yeasts cannot convert xylose to xylitol due to the redox imbalance between NAD^+ and $NADH$; Under low oxygen conditions, $NADH$ is not completely oxidized, increasing xylitol digestion; At too high oxygen concentration, an imbalance occurs when the $NAD^+/NADH$ couple has a larger ratio than $NADP^+/NADPH$, which will lead to the xylitol-to-xylulose oxidation occurring more strongly, consuming much more desired products (Martínez, Silva *et al.* 2003)
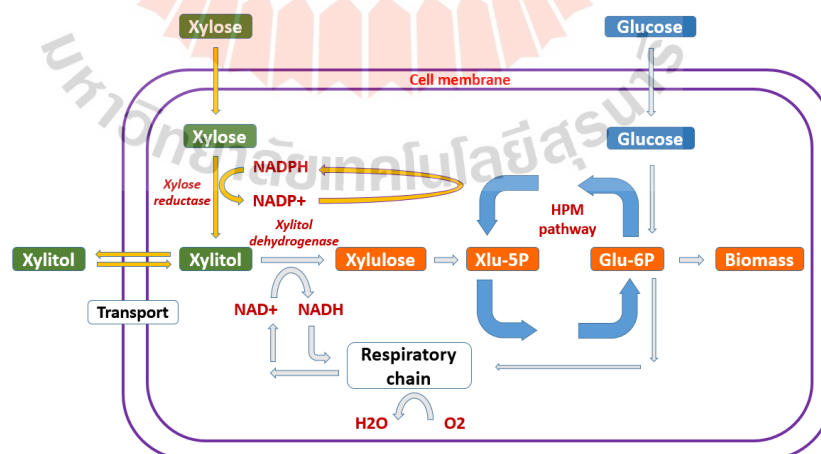
Figure 2.5 Metabolic pathways for xylitol production (Mohamad, Mustapa Kamal *et al.* 2014)

Yeast can be used in the fermentation process to convert xylose into xylitol. Among the yeasts, *Candida* sp. rated as the most effective. *Candida* types can be listed, which are so-called *Candida tropicalis, Candida magnoliae, Candida peltata, Candida boidinii, Candida guilliermondii*. In the study of Jeon et al., *Candida tropicalis* was able to convert 80-90% xylose into xylitol, yielding xylitol 3 g/L.h (Jeon, Shin *et al.* 2011). Tada et al. showed that *Candida magnoliae* was able to convert 18/25 g xylose into xylitol with carbon from corn stalks, yielding 0.6 g xylitol/1g xylose (Tada, Kanno *et al.* 2012). Research by Saha et al. shows that *Candida peltata* can give a maximum xylitol metabolism of 52% after 14 days (Bothast 1999). Studies on *Candida guilliermondii* have also been proved to be effective in fermenting xylitol production (Silva, Mancilha *et al.* 2007, Vaz de Arruda, dos Santos *et al.* 2017), (Lopez-Linares, Romero *et al.* 2018, Hernández-Pérez, Chaves-Villamil *et al.* 2019).

Apart from yeasts, several bacteria such as *Mycobacterium smegmatis, Glucunobacter oxydans* (Izumori and Tuzaki 1988, Suzuki, Sugiyama *et al.* 2002) and *Aspergillus, Penicillium* (Sampaio:, Silveira; *et al.* 2003) are also used to ferment xylitol.

It can be seen that most of the studies focused on yeast, other microorganisms were less studied because of low effectiveness. Nowadays, scientists are looking for ways to improve the conversion efficiency of xylitol by creating mutant strains or combining strains together. Table 2.3 summarizes some recent studies on the use of yeast in the production of xylitol.

Through Table 2.3, it can be seen:

Carbon source: Used mainly as xylose obtained from various lignocellulose material sources. Depending on the treatment method and biomass source, the composition of the solution before fermentation and the product after fermentation

are different. In addition, there are also studies of direct fermentation from commercial xylose supplemented with glucose (Wannawilai, Lee *et al.* 2017).

Nitrogen source: is mainly used in form of organic nitrogen such as yeast extract, peptone; Sources of inorganic nitrogen such as ammonium sulfate, nitrate salt, ammonium chloride salt and casamino acid. Zhang et al. (2012) studied the effects of different nitrogen sources and concluded the combination of yeast extract and urea for maximum fermentation performance (Zhang, Geng *et al.* 2012).

Oxygen condition: the presence of oxygen is expressed by the volumetric oxygen transfer coefficient (kLa). As mentioned, oxygen plays an important role in influencing the activity of the enzymes xylose reductase and xylitol dehydrogenase. Aeration intensity ranges from 0.1-0.25 vvm.

Temperature, pH: most fermentation is done at 30-37 $^{\circ}$C. Some heat-resistant yeasts can perform optimal fermentation at 40-45 $^{\circ}$C. The fermentation medium pH ranges from 5.0-6.5, however, the most common is that fermentation is performed at pH values 5.0-5.5.

Besides, the mixing process is also one of the indispensable factors affecting fermentation performance.

Table 2.3. Different strains of yeast were used in recent studies

Hydrolysate source	Yeast	Fermentation conditions	Xylitol production			Reference
			Titer (g/L)	Yp/s (g/g)	Qp (g/L.h)	
Corncob Dilute-acid hydrolysis Xylose 50 g/L	*C. tropicalis* MTCC 6192	Batch, 14 L STR pH 5.0, 30 ºC, 175 rpm, 0.25 vvm	33.4	0.66	1.2	(Kumar, Krishania *et al.* 2018)
Rapeseed straw Dilute-acid hydrolysis Xylose 41.51 g/L	*C. guilliermondii* FTI 20037	Batch Shaker flasks pH 5.0, 30 ºC, 200 rpm	20.2	0.54	0.14	(Lopez-Linares, Romero *et al.* 2018)
Sugarcane bagasse Dilute-acid hydrolysis Xylose 60 g/L	*C. guilliermondii* FTI 20037	Batch 125 L STR pH 5.5, 30 ºC, 150 rpm, 0.1 vvm	41.8	0.66	0.29	(Vaz de Arruda, dos Santos *et al.* 2017)
Poplar wood Dilute-acid hydrolysis Xylose 50.3 g/L	*C. guilliermondii* FTI 20037	Batch Shaker flasks pH 5.0, 32 ºC, 150 rpm	28.3	0.59	0.81	(Dalli, Patel *et al.* 2017)
Corncob Dilute-acid hydrolysis Xylose 54 g/L	*S. cerevisiae* GRE3	Fed-batch 1 L STR pH 5.5, 30 ºC, 150 rpm, 0.2 vvm	47	0.87	0.32	(Kogje and Ghosalkar 2017)
Corn stover Dilute-acid hydrolysis Xylose 16.4 g/L	*C. tropicalis* XK12K	Batch Shaker flasks pH 6.0, 30 ºC, 200 rpm	16.1	0.98	0.57	(Hong, Kim *et al.* 2016)
Sugarcane bagasse Autohydrolysis Xylose 104.1 g/L	*C. tropicalis*	Batch Shaker flasks pH 5.0, 30 ºC, 200 rpm	32.0	0.46	0.27	(Vallejos, Chade *et al.* 2016)

Table 2.3. Different strains of yeast were used in recent studies (continued)

Hydrolysate source	Yeast	Fermentation conditions	Xylitol production			Reference
			Titer (g/L)	Yp/s (g/g)	Px (g/L.h)	
Waste xylose from xylose purification during xylitol chemical production Xylose 127 g/L	*C. tropicalis* X828	Batch 5 L STR pH 6.0, 39 ºC, 60 rpm, 0.2 vvm	95	0.73	0.86	(Wang, Li *et al.* 2016)
Rice straw Liquid hot water Xylose 59.3 g/L	*S. cerevisiae* YPH499	Batch Shaker bottles pH 5.0, 35 ºC, 150 rpm	37.9	0.63	0.39	(Guirimand, Sasaki *et al.* 2016)
Corncob Patented acid pretreatment Xylose 40-60 g/L	*C. tropicalis*	Repeated batch Shaker flasks pH 6.5, 30 ºC, 150 rpm	41	0.73	0.43	(Yewale, Panchwagh *et al.* 2016)
Corncob Dilute-acid hydrolysis Xylose 160 g/L	*C. maltose* XU316	Repeated batch Shaker flasks pH 5.0, 30 ºC, 200 rpm	120	0.81	2.50	(Jiang, He *et al.* 2016)
Sugarcane straw Dilute-acid hydrolysis Xylose 57 g/L	*C. guilliermondii* FTI 20037	Batch Shaker flasks pH 5.5, 30 ºC, 200 rpm	36.1	0.65	0.75	(Hernandez-Perez, Costa *et al.* 2016)

Explication:

Titer: xylitol product (g xylitol/l media); Qp: average volumetric productivity of xylitol (g xylitol/l per h); $Y_{P/S}$: xylitol yield (g of xylitol produced/g of xylose utilized)

2.2 Downstream processing of xylitol

It is estimated that downstream accounts for 50% of the cost of producing chemicals (Chandel, Garlapati *et al.* 2018). Therefore, downstream plays an important role in determining the quality and price of products.

In the context of this thesis, downstream processes for xylitol produced by biological methods are taken into consideration. The fermentation fluid contains various inorganic and unwanted organic components such as residual sugar, metal ions, fermentation byproducts, proteins, polypeptides, furfural, HMF, etc. Obviously, xylitol accounts for low content that makes it difficult to be purified (Sampaio, Passos *et al.* 2006). Purification processes play an indispensable role in determining the purity of the product after crystallization. Various different processes have been used for xylitol purification such as centrifugal methods, chromatography, membrane separation, activated carbon, ion exchange resins, concentrates, etc. (Martínez, Canettieri *et al.* 2015, Felipe Hernandez-Perez, de Arruda *et al.* 2019).

The downstream processes after fermentation can be summarized through the diagrams of Fig. 2.7 and Table 2.5 will be summarized recent studies on xylitol purification process before crystallization.
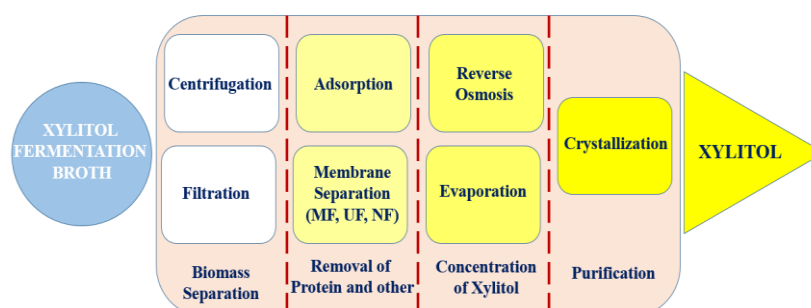
Figure 2.7 Basic downstream processes for xylitol purification

After purifying to increase the fermentation solution's concentration, xylitol is crystallized to create crystals of high purity. The crystallization process is a physicochemical process, in which, xylitol under the effect of different factors reaches the state of saturation and crystal formation.

The most commonly used crystal nucleation methods can be known as cooling, adding existing crystal beads or adding precipitant (ethanol, methanol) (Hao, Hou *et al.* 2006). The crystallization process is assessed by quantity, crystal size, crystalline yield and the end product purity. The crystallization process depends on the initial xylitol concentration, the solution's cooling rate and the saturation temperature, time (Fig. 2.8). Table 2.6 describes a number of studies on xylitol crystallization process on a laboratory scale. Thereby, it can be seen that the research on xylitol crystallization process is not much, which is probably because most studies stop at a small scale; equipment for crystallization experiments is incomplete.
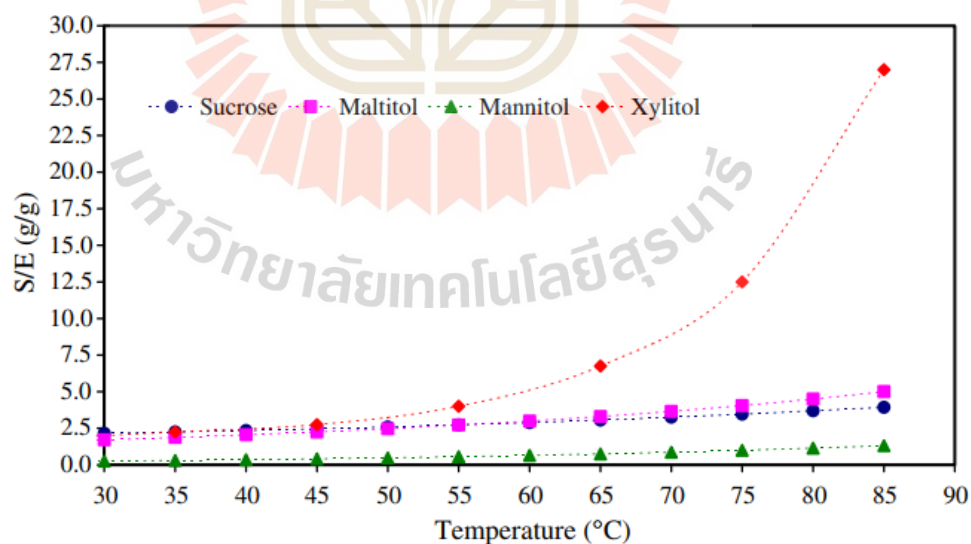
Figure 2.8 Solubility limit expressed as mass ratio of xylitol to water (S/E) (Bensouissi, Roge *et al.* 2010)

Table 2.5. The xylitol purification processes in the fermentation solution before crystallization

Method	Fermentation broth and microorganism	Optimal conditions	Results	References
Activated charcoal	Sugarcane hemicellulosic hydrolyzate by *Candida guilliermondii*	25 g/100ml solution, 80 °C, 100 rpm, 1 h, pH 6.0	19.1% xyl loss	(Gurgel 1995)
	Synthetic media by *Debaryomyces hansenii*	20 g/L solution, 25 °C, magnetic agitation, 1 h, pH 6.0	~0% xyl loss, 69.0% protein removal	(Sampaio, Passos *et al.* 2006)
Ion exchange resin	Sugarcane hemicellulosic hydrolyzate by *C. guilliermondii*	Amberlite 200C cation-exchange and Amberlite 94S anion-exchange resins	21-57% xyl loss	(Gurgel 1995)
	Wheat straw hemicellulosic hydrolyzate by *C. guilliermondii*	A-860S strong base anion-exchange and A-500PS strong base anion-exchange resins	21.1% xyl loss	(Canilha, Carvalho *et al.* 2008)
	Synthetic media by *C. guilliermondii*	A-505 anion-exchange and C-504 cationexchange resins	97.5% removal of soluble byproducts, 15.23% xyl loss	(Martínez, de Almeida e Silva *et al.* 2007)
Evaporation	Hardwood hemicellulose hydrolyzate fermented by *D. hansenii*	30-50 °C, 1.6 x 104 Pa and 45-50 rpm	Xylitol solutions 730 g/L	(Martínez, Canettieri *et al.* 2015)
Liquid-liquid extraction	Synthetic xylose and corn cob hemicellulosic hydrolyzate	1:5 (v/v) of fermentation broth and ethyl acetate	21.72 g/l xyl extracted	(Misra, Gupta *et al.* 2011)
Membrane separation	The synthetic sugar mixtures	Polyethersulfone (PES) membrane with Pluronic	Enhanced xylitol purity from 82% to 93%	(Faneer, Rohani *et al.* 2018)
Precipitation	Synthetic xylose and corn cob hemicellulosic hydrolyzate	Solvent: acetone, 60 min at 4 °C, then centrifugation	76.20% in 50 mL 68.06% in 5 L	(Misra, Gupta *et al.* 2011)

Table 2.5. The xylitol purification processes in the fermentation solution before crystallization (continued)

Method	Fermentation broth and microorganism	Optimal conditions	Results	References
Supercritical CO_2	Sugarcane bagasse and straw hemicellulose by *Scheffersomyces amazonensis*	Ratio of sample/solvent (11/9), extraction time (20 min)	40.51% xylitol recovery, 99.59% xylitol purity	(Silva, Dussán *et al.* 2020)
Precipitation	Synthetic xylose and corn cob hemicellulosic hydrolyzate	1:1 ratio (v/v) fermented broth and acetone	67.44% xyl recovery in aqueous phase	(Misra, Gupta *et al.* 2011)
Combined methods	Sugarcane hemicellulosic hydrolyzate by *C. guilliermondii*	R 120 cation-exchange and IRA 410 anion-exchange resins	60% crystallization yield and 33% total recovery	(Mussatto, Santos *et al.* 2006)
	Sugarcane hemicellulosic hydrolyzate by *C. guilliermondii*	6.5-fold concentrated at 50 °C, maintained at 4 °C for 24 h and supplemented with 400 mg of finely ground standard xyl. pH 7.0 with NaOHA-505 anionexchange, C-504 cation-exchange resins	8.15% xyl loss	(Martínez, de Almeida e Silva *et al.* 2007)
	Oil palm empty fruit bunch (OPEFB) fermented by *Debaromyces hansenii*	UF: TMP 1 bar, flow rate 0.75 m/s EDI: Diluate flow rate 0.5 m/s, concentrate flow rate 0.4 m/s, electrode flow rate 0.8 m/s, current density 22.5 A/m², operation time 270 min	Remove 99% of microorganism and biomass, 99% pigment; 30–50% xyl loss	(Kresnowati, Regina *et al.* 2019)
	Fermentation broth of corncob hydrolysates by *C. tropicalis*	Activated carbon n (1% M-1, 60 °C, 165 rpm), Ion-exchange resins (732 and D301) and vacuum concentration	750 g/L xylitol	(Wei, Yuan *et al.* 2010)

Table 2.6. The crystalline conditions and properties of xylitol crystals obtained from different biological material sources

Fermented media and microorganism	Xylitol concentration (g/L)	Conditions	Results	Reference
Wheat straw hemicellulosic hydrolyzate by *C. guilliermondii*	726.5 g/L	CR = 0.2-0.4 °C min⁻¹ and ST = 50 °C	95.3- 99.9% purity	(Canilha, Carvalho *et al.* 2008)
Corncob hydrolysates by *C. tropicalis*	750 g/L	Adding 1% xylitol crystal seeds, cooled to -20 °C for 48 h	95% purity, crystallization yield 60.2%	(Wei, Yuan *et al.* 2010)
Hemicelluloses of pre-hydrolysis liquor	Xylitol-rich liquid (40 wt%)	72 h at -5 °C	Xylitol purity of 99%	(Fatehi, Catalan *et al.* 2014)
Synthetic broth by *Debaryomyces hansenii*	675 to 911g/L,	-10 °C	96 to 97.8% purity	(Sampaio, Passos *et al.* 2006)
Sugarcane hemicellulosic hydrolyzate by *C. guilliermondii*	935.4 g/L	First crystallization: 0.5 °C min⁻¹ CR; ST = 50 °C	85% purity	(Martínez, de Almeida e Silva *et al.* 2007)
		Second crystallization: add 0.1% xyl seed, CR = 0.1 °C min⁻¹, ST = 30 °C	91.20-94.85% purity	
Semisynthetic medium by *C. guilliermondii*	745.3 g/L	First crystallization: CR = 0.5 °C min⁻¹; ST = 50 °C	95% purity	(Martínez, Giulietti *et al.* 2009)
		Second crystallization: add 0.1% xyl seed, CR = 0.10 °C min⁻¹; ST = 30 °C ST	98.5-99.2% purity	

*CR = cooling rate; ST = saturation temperature; xyl = xylitol.

CHAPTER III

MATERIALS AND METHODS

3.1 Materials

3.1.1 Xylose

In this study, alkaline hydrolysis method was used to hydrolyze bagasse to obtain a hydrolyzed solution containing xylan. Next, we used ethanol mixed with the hydrolysate to precipitate and recover the xylan by centrifugation. The enzyme xylanase (from *Trichoderma reesei*) was used to hydrolyze xylan to obtain xylose for xylitol fermentation.

Figure 3.1 The xylan after recovery by centrifuge

3.1.2 Microorganism

Yeast acts as microorganisms that metabolize the xylose sugar into xylitol products. *Candida guilliermondii* TISTR 5068 was purchased from TISTR (Thailand Institute of Scientific and Technological Research). The prototypes were re-streaked on

YPD (yeast extract, peptone, glucose) supplemented with Agar at 30 °C for 24-48 h. The colonies then grow on the agar plates were used for the further inoculum and fermentation experiments.

Figure 3.2 Original strain and colonies of *Candida guilliermondii* TISTR 5068

3.1.3 Bioreactor

Yeast inoculum was prepared in 100 mL shake flask; a 250 mL shake flask was applied to find environmental factors; nutrition (xylose/glucose ratio), minerals, etc during fermentation.

The fermentation device 5 L (Sartorius stedim, Biostat Bplus) with the working volume of 3.5 L was used on a larger scale (Fig. 3.3). The pH and temperature probe automatical contrlled the fermentor. Oxygen was feeded into the fermentation medium after passing through a filter.

Figure 3.3 A 5 L bioreactor from Sartorius, Germany

The fermentation process was scale up to 50 L fermentation system (Design by Servitech Engineering Co., LTD – Fig. 3.4a with 35 L and 350 L working volumes (Design by BE Marubishi, Thailand, Co., LTD - Figure 3.4b). An active volume of 350 L is used to obtain a large amount of fermentation broth in preparation for the next downstream processes. The fermentation systems can automatically control the temperature, pH, autosampler system. Steam sterilization and CIP (Clean-In-Place) are possible.

During the fermentation process, samples were analyzed criteria such as biomass development; glucose, xylose content; the content of finished xylitol sugar.

(A)   (B)
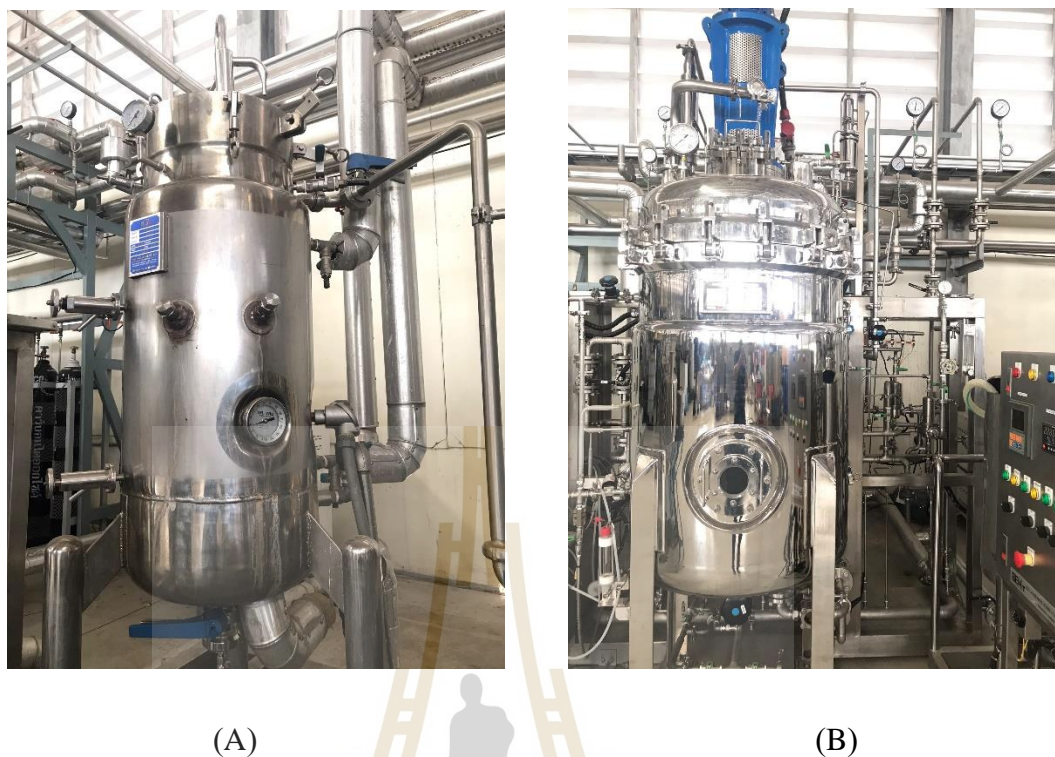
Figure 3.4 Fermentation system of 50 L (A) and 500 L (B)

3.1.4   Membrane filtration system

The membrane system is responsible for separating microorganisms, proteins and non-passing components. The two membrane systems which were used are microfiltration and nanofiltration made from polyamide and polysulfone materials with sizes of 0.1 microns (MF) and 300 Da (NF). The membranes are placed in cylindrical stainless steel tubes, with separate pumping systems and containers of raw materials and products (Fig. 3.5). Membrane systems are supplied by LPE., Thailand (Liquid Purification Engineering International Co., LTD).

A   B

Figure 3.5 Microfiltration (A) and Ultrafiltration + Nanofiltration (B) systems

3.1.5   Electrodialysis membrane

After removing cells and polymers, the fermentation broth was removed from the polar components with Electrodialysis DW-Lab unit (Japan). The effective surface area of each membrane was 30 cm^2/piece. The anode and cathode are made of Platinum and stainless steel that will connect to the negative electrode and the positive electrode of direct current. Between the two electrodes, there are ion exchange films (anion exchange and cation exchange membrane) that separate ions from different solutions. The properties and structure of the DW-Lab unit are shown in Table 3.1 and Fig. 3.6, respectively.

Table 3.1 Characteristic of the DW-Lab equipment

	Specification
Membrane size	80×130 mm
Cell pairs	5
Size	$W300 \times D220 \times H400$
Weight	10 kg
Rectifier input	220 V
Rectifier output	DC 30 V/3A

A	B
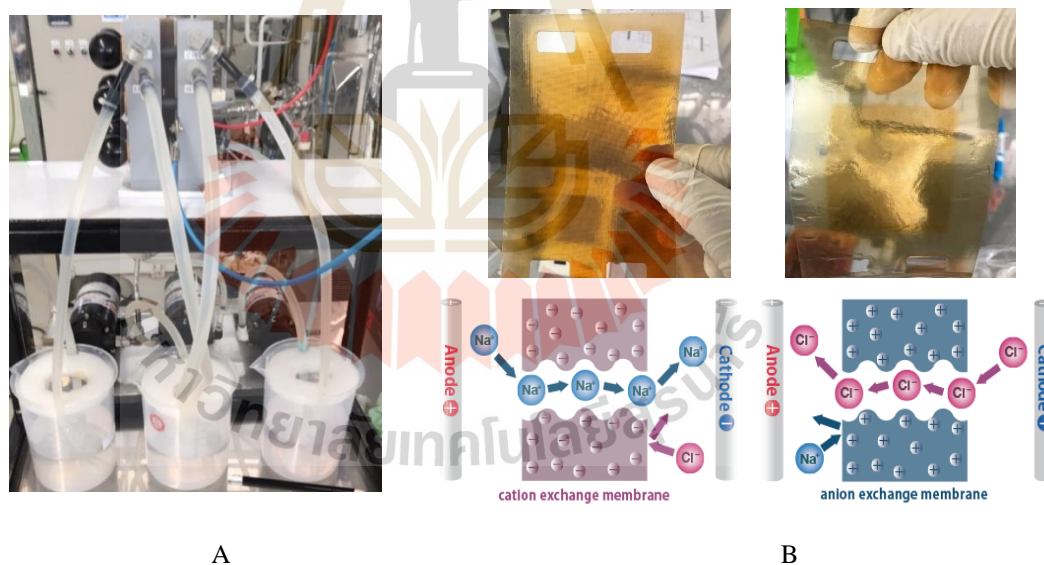
Figure 3.6 Electrodialyer Selemion DW-Lab (A) and ion exchange membrane (B)

3.1.6 Falling film vacuum e**vaporation system**

The evaporation system under vacuum was applied to evaporate the water containing in the solution after removing the salt and polar components. Under vacuum

conditions, the boiling temperature of the water will drop below 100 ºC and evaporate, condensing to form a liquid. Meanwhile, the volume of the mother solution will decrease and the xylitol concentration was increased. The low evaporation temperature of the water will prevent caramelized sugar.

The evaporation system with vacuum pump using a thermal agent is diesel oil with forced circulation pump as shown in Fig. 3.7.

Figure 3.7 Falling film vacuum evaporation system

3.1.7 Crystallization reactor

A glass reactor with two stirrers attached were used for the xylitol crystallization test. Jacket water helped regulate the temperature of the xylitol solution after vacuum concentration. The cooling rate was controlled by water bath and pumped into the water jacket. Different crystalline methods were investigated such as: crystallization by cooling with ethanol; freezing temperatures in ethanol; low temperature in ethylene glycol.

In addition, the reactor has a tube to attach the probe to observe the crystallization process using FBRM (Focused Beam Reflectance Measurement), Raman spectroscopy and PVM (Particles Vision Measurement), (Fig. 3.8, Fig. 3.9).

Figure 3.8 Crystallization reactor
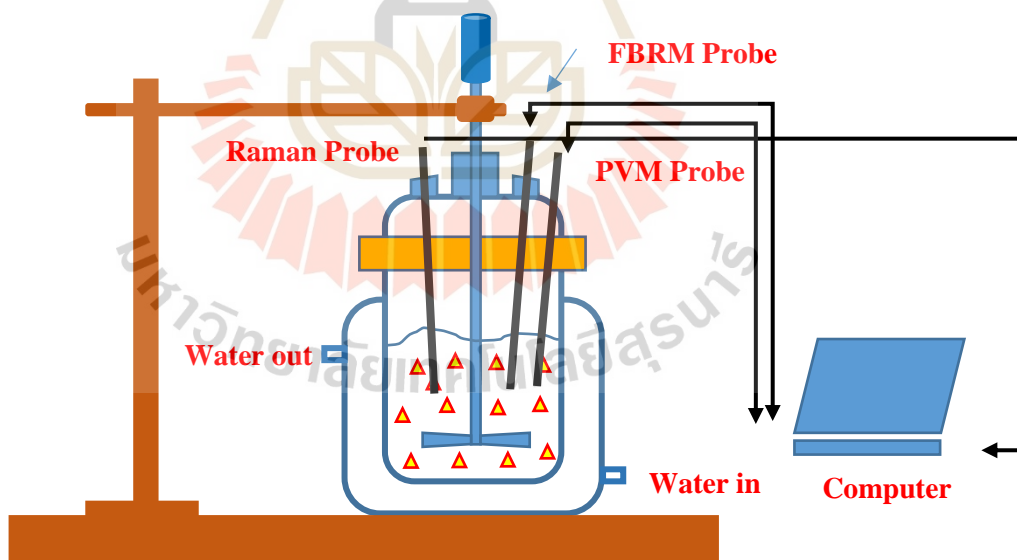
Figure 3.9 Setup crystallization experiment to monitoring using FBRM, Raman and PVM

3.2 Methods

3.2.1 Ethanol fermentation

The xylose mixture after hydrolysis with the enzyme xylanase, contains a large amount of glucose. The xylose mixture was diluted 4 times with RO water and added with nitrogen (WCN-07 Plus, 0.3% (w/v), including DAP, yeast extract. etc*),* *Saccharomyces cerevisiae* (WCY 05, 0.15% (w/v)) for ethanol fermentation. Ethanol fermentation was aimed at removing glucose from the mixture. This process was performed at 30 ºC, stirring 200 rpm for 48 h. After the fermentation process, the fermentation broth is filtered using a microfiltration system to separate yeast cells. The solution is then evaporated using the falling film evaporator to increase the xylose concentration and recover the ethanol.

3.2.2 Xylitol fermentaion process

1. Inoculum preparation

From a single colony of *C. guilliermondii* TISTR 5068 strain, the inoculum was prepared in 100 mL glass shake flasks with a volume of 20 mL YPD broth media, adjusted pH 5.5 by 5N HCl, and incubated at 200 rpm, 30 ºC for 24 h using a rotary incubator (New Brunswick Scientific, USA) (Vaz de Arruda, dos Santos *et al.* 2017). This inoculum was used for further experiments. The composition of YPD broth media as followed: yeast extract 10 g/L, peptone 20g/L, glucose 20 g/L.

2. Batch xylitol fermentation process

The research sequence was carried out in the order: finding the optimal fermentation conditions in a 250 mL shake flask; then keep the same conditions and scale up the 5 L and 500 L bioreactor.

Shake flask 250 mL fermentation

A 250 mL shake flask with a volume of 100 mL was used to examine the factors that affects the xylitol formation. After 24 h, the inoculum was transferred into the fermentation medium at a rate of 10% (v/v). The environmental components and fixed fermentation conditions are: pH 5.5; temperature 30 ºC; stirring speed of 200 rpm; nutritional supplements $CaCl_2.2H_2O$ (0.1 g/L) (Martínez, Silva *et al.* 2003, Vaz de Arruda, dos Santos *et al.* 2017); nitrogen source is $(NH_4)_2SO_4$ (2.0 g/L), peptone (3.0 g/L), commercial yeast extract (5.0 g/L). The amount of glucose and xylose initially influencing the fermentation performance was studied (Dominguez, Gong *et al.* 1997, Ko, Kim *et al.* 2011, Prakash, Varma *et al.* 2011, Tamburini, Costa *et al.* 2015, Zhang, Zhang *et al.* 2016).

Effect of initial xylose concentration: 10; 20; 30; 40; 50 g/L

Effect of initial glucose concentration: 2.0; 4.0; 6.0; 8.0; 10 g/L

The first experiment: Effect of initial glucose concentration on fermentation. The experiment was arranged with a constant initial xylose concentration of 30 g/L; the initial glucose concentration is altered according to different concentrations: 2; 4; 6; 8; 10 g/L. The appropriate glucose concentration was used for the next experiment.

The second experiment: Effect of initial xylose concentration on fermentation. It was carried out to maintain the fermentation environment conditions and initial glucose concentration according to experiment results 1; the initial xylose concentration was changed in turn: 10; 20; 30; 40; 50 g/L.

The third experiment: changing carbon source from commercial xylose to xylose hemicellulosic hydrolysate from bagasse. The nitrogen source was also

compared between synthetic nitrogen source ($(NH_4)_2SO_4$ (2.0 g/L), peptone (3.0 g/L), commercial yeast extract (5.0 g/L)) and commercial nitrogen source (WCN-07 Plus, 3 g/L).

All experiments will end when xylitol concentration reached its maximum value and tend to decrease. The monitored indicators are dry biomass development (CDW), glucose and xylose consumption, xylitol products (g/L); volumetric productivity of xylitol (g/L.h); xylitol yield (g xylitol/g xylose)

Bioreactor 5 L fermentation

The bench bioreactor used was Sartorius stedim, Biostat Bpus (5.0 L total volume, the working volume of 3.5 L). The device was equipped with filters, probes for measuring temperature, pH, DO (dissolved oxygen) and an aeration unit during fermentation. After 48 h, inoculum (YPD broth media) was transferred into the medium for the fermentation process with the ratio of 10% (v/v) of the fermentation working volume.

Ingredients per liter of media include: xylose and glucose (determined after experiments 3, 4 in Shake flask 250 mL fermentation); $(NH_4)_2SO_4$ (2.0 g/L) and $CaCl_2.2H_2O$ (0.1 g/L). The medium was adjusted to pH 5.5, sterilized, cooled and fermented. During fermentation, the pH was automatically adjusted as required. Other conditions of fermentation were temperature 30 ^{o}C, stirring speed 200 rpm.

The third experiment: change the air conditions (no use air after log phase; DO >20%; DO <1%) to find the most optimal of dissolved oxygen for yeast in 5 L bioreactor.

All experiments will end when xylitol concentration reached its maximum value and tend to decrease. The monitored indicators are dry biomass

development (CDW), glucose and xylose consumption, xylitol products (g/L); average
volumetric productivity of xylitol (g/L.h); xylitol yield (g xylitol/g xylose).

Bioreactor 500 L fermentation

A fermentation device of 500 L (B.E. Marubishi, Thailand) with a
working volume of 350 L was used for a pilot scale from 5 L to 500 L. Inoculum (10%
v/v) was prepared according to the fourth experimental results. The fermentation
conditions will be implemented in the same way as the 5 L fermentation device. Two
experiments are DO >20% and DO<1% were used to find the optimal DO for yeast in
500 L bioreactor.

The fermentation process was when the xylitol concentration reaches
its maximum value and tends to decrease. The monitored indicators are dry biomass
development (CDW), glucose and xylose consumption, xylitol products (g/L); average
volumetric productivity of xylitol (g/L.h); xylitol yield ($g_{xylitol}/g_{xylose}$).

3.2.3 Downstreams processing

1. Purification of xylitol from fermentation broth by using microfiltration,
ultrafiltration and nanofiltration

Microfiltration is defined as a membrane separation process using
membranes with a pore size of approximately 0.03 to 10 micron (1 micron = 0.0001
millimeters), a molecular weight cut-off (MWCO) of greater than 1000,000 daltons.
Materials removed by MF include sand, clays, algae, and some bacterial species.

Ultrafiltration has a pore size of approximately 0.002 to 0.1 microns,
an MWCO of approximately 10,000 to 100,000 dalton. UF will remove all
microbiological species removed by MF (partial removal of bacteria), as well as some

viruses (but not an absolute barrier to viruses)

Nanofiltration membranes have a nominal pore size of approximately 0.001 microns and an MWCO of 100 to 1000 daltons. Pushing water through these smaller membrane pores requires a higher operating pressure than either MF or UF. NF systems can remove virtually all cysts, bacteria, viruses.

After finishing fermentation in 500 L equipment, the fermentation broth was removed from the debris bag filter yeast before microfiltration system. Next, the fermentation fluid was passed through the nanofiltration system to remove protein and other with high molecular weight components.

Membrane filtration processes were carried out by microfiltration, ultrafiltration, and nanofiltration systems provided by LPE, Thailand. Parameters such as flux, pressure, time was recorded during filtration. The concentration of xylitol before and after filtration was also considered (Faneer, Rohani *et al.* 2017).

2. Purification of xylitol from fermentaion broth by using electrodialysis *(*remove salt*)*

The electrodialyzer DW-Lab from Japan was used to remove salt and other charged components from the solution to increase the purification of xylitol. System layout diagram is made as shown in Fig. 3.10. Accordingly, the electrolyte solution used is 3% Na_2SO_4, 0.1% NaCl dilute salt solution is used to evaluate the salt content removed from fermentation broth. Conditions such as amperage and membrane voltage; flow; temperature changes, pH were investigated.
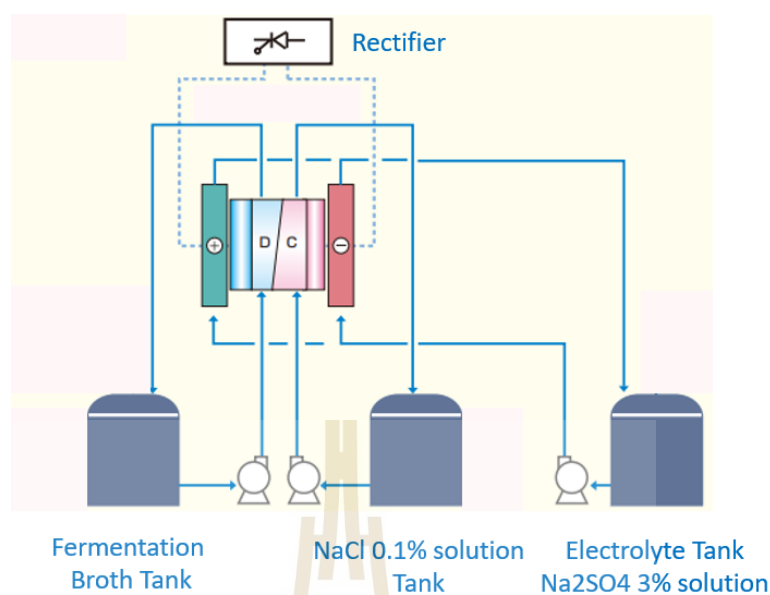
Figure 3.10 Setup electrodialysis system

The monitored indicators include: conductivity of fermentation broth and concentration solution over time; volume of fermentation broth before and after desalination; xylitol concentration of fermented solution.

Next, the DW permeate was concentrated by using a rotaty evaporator under the vacuum effect, 50-60 °C until the brix of solution reached maximum value (approximately > 70). This concentrate xylitol solution was subsequently used in crystallization experiments.

3. Purification of xylitol from fermentation broth by using Ion exchange
resin.

To comparing with ED, high conductivity xylitol solution was pumped from bottom to top into column A containing resin DOWEX 66 (weak base anion), after going through column A, the solution was entered into column A containing resin

DOWEX 88 (strong acid cation). A and B are fabricated steel columns 120 cm long and 6 cm diameter. The flow rate is 4 L/h (equal to 2 times the resin volume in the column). After leaving the cation column, the solution returns to the container and continues the second cycle. The process repeated until the measured conductivity value is constant.

4. Purification of xylitol from fermentation broth by using crystallization

Methods of xylitol crystallization after concentration were investigated to compare and select the most effective method. The basic principle was based on the supersaturated state of xylitol at different temperatures and the solubility of xylitol in water and seeding.

The crystallization process was carried out in a 500 mL reactor with two glass jacket. Temperature and cooling rate can be adjusted as required. After vacuum, concentration reached > 650 g/L (Bx 70, 75 and 80), high-concentration xylitol was put into the reactor, stirring 200 rpm at 60 $^{\circ}$C for 30 minutes. Then, the solution was cooled down to 1 $^{\circ}$C with a cooling rate of 2 $^{\circ}$C/min. When the required temperature is reached (40 $^{\circ}$C), add crystals (1% w/v) to make nucleations. The commercial xylitol was also dissolved and adjusted Bx to crystalline for comparison purpose. After crystallization, xylitol crystals were recovered by vacuum filtration, drying and analysis (Canilha, Carvalho *et al.* 2008)

3.3. Analytical methods

3.3.1 Fermentation broth

The parameters to analyze in fermentation broth over time were: cell concentration; residual xylose and xylitol content, efficiency and yield xylitol forming.

1. Cells concentration

Yeast growth was determined by optical density (OD) measurement at 600 nm. For cell dry weight, the broth culture was centrifuged (10.000 rpm, 10 min, 4 °C) to recover the cells. The cells were washed twice with deionized water, recovered and dried at 105 °C for 24 h (Wannawilai, Lee *et al.* 2017).

2. Sugar analysis

After centrifuged to recover the cells, the supernatant was filled by membrane filter 0.22 µm pore size and analyzed sugars. The sugars (glucose, xylose, xylitol) were determined by HPLC [Bio-Rad Aminex HPX-87H column (300×7.8 mm)] with a RI detector at 45 °C with 0.008 N sulfuric acid as the eluent at a flow rate of 0.6 mL/min with 20 µL injection volume (Vaz de Arruda, dos Santos *et al.* 2017).

The concentration of xylitol, and xylose were calculated from the standard curve. A diagram of changes in xylose and xylitol concentrations over time were also generated.

The Xylitol yield (g/g)

Xylitol yield and productivity were determined according to the following equations (Kumar, Krishania *et al.* 2018)

$$Y_x = \frac{\text{Xylitol produced (g)}}{\text{Xylose consumed (g)}}$$

Xylitol productivity (g/L.h)

$$P_x = \frac{\text{Maximum xylitol concentration } (\frac{g}{L})}{\text{Fermntation time (h)}}$$

Determination of colorant of xylitol fermentation broth

The colorant was determined by measuring the optical density (OD) at 420 nm using an UV-vis spectrophotometer. The decolorization ratio was calculated using equaition:

$$C\% = \frac{A0 - A1}{AO} \times 100\%$$

C, the decolorization ratio; AO, the IU (ICUMSA Units) color index of the fermentation broth before treatment; A1, the IU color index of the fermentation broth after treatment (Wei, Yuan *et al.* 2010)

3.3.2 Microfiltration, ultralfiltration, and nanofiltration analysis

Permeate flux (L/m².h)

$$\text{Flux} = \frac{\text{Permeate volume (L)}}{\text{Membrane effective area (m}^2\text{)x nanofiltration time (h)}}$$

Xylitol lost (%)

$$L = \frac{\text{Total xylitol in feed (g)} - \text{Total xylitol in permeate (g)}}{\text{Total xylitol in feed (g)}} \times 100$$

3.3.3   Electrodialysis and Ion exchange resin analysis

Conductivity of solution before and after treat by ED and ion exchange resin were measured by conductivity meter M400, Mettler Toledo. Ion removal was calculated to show the decrease of ions in the feed solution using the following equation:

$$\beta = \frac{G_0 - G_1}{G_0} \times 100\%$$

Therein:

β: is the removal of total ion; G_0: the conductivity of the fermentation broth before desalination (μS/cm); G_1: the conductivity of the fermentation broth after desalination (μS/cm); (Wei, Yuan *et al.* 2010)

3.3.4 Crystallization analysis

Particle size and particle size distribution (PSD) which were observed real time use the focused beam reflectance measurement technique (FBRM) (Model G600, Mettler Toledo)

The structure and characteristics of xylitol crystals were determined by Raman spectroscopy (ReactRaman 785, Mettler Toledo).

The shapes of the xylitol crystals were viewed in real-time with an in situ PVM probe (Model EV400, Mettler Toledo)

Xylitol crystal morphology was determined by Scanning Electron Microscopy (SEM, JSM-6010LV).

The xylitol purity (%) was calculated using Eq.

$$PD = \frac{m}{C.V} \times 100\%$$

Therein: PD, the purity degree of xylitol; m, the mass of xylitol crystal (g); V, the volume of dissolving xylitol crystals (L); C, the concentration of dissolving xylitol crystals (g/L) (Wei, Yuan *et al.* 2010)

Crystallization productivity (%)

$$\alpha = \frac{\text{Amount of xylitol crystal}}{\text{Amount of xylitol in initial solution}} \times 100\%$$

CHAPTER IV

RESULTS AND DISCUSSION

Research diagram of xylitol production from hemicellulosic hydrolysate of sugarcane bagasse.
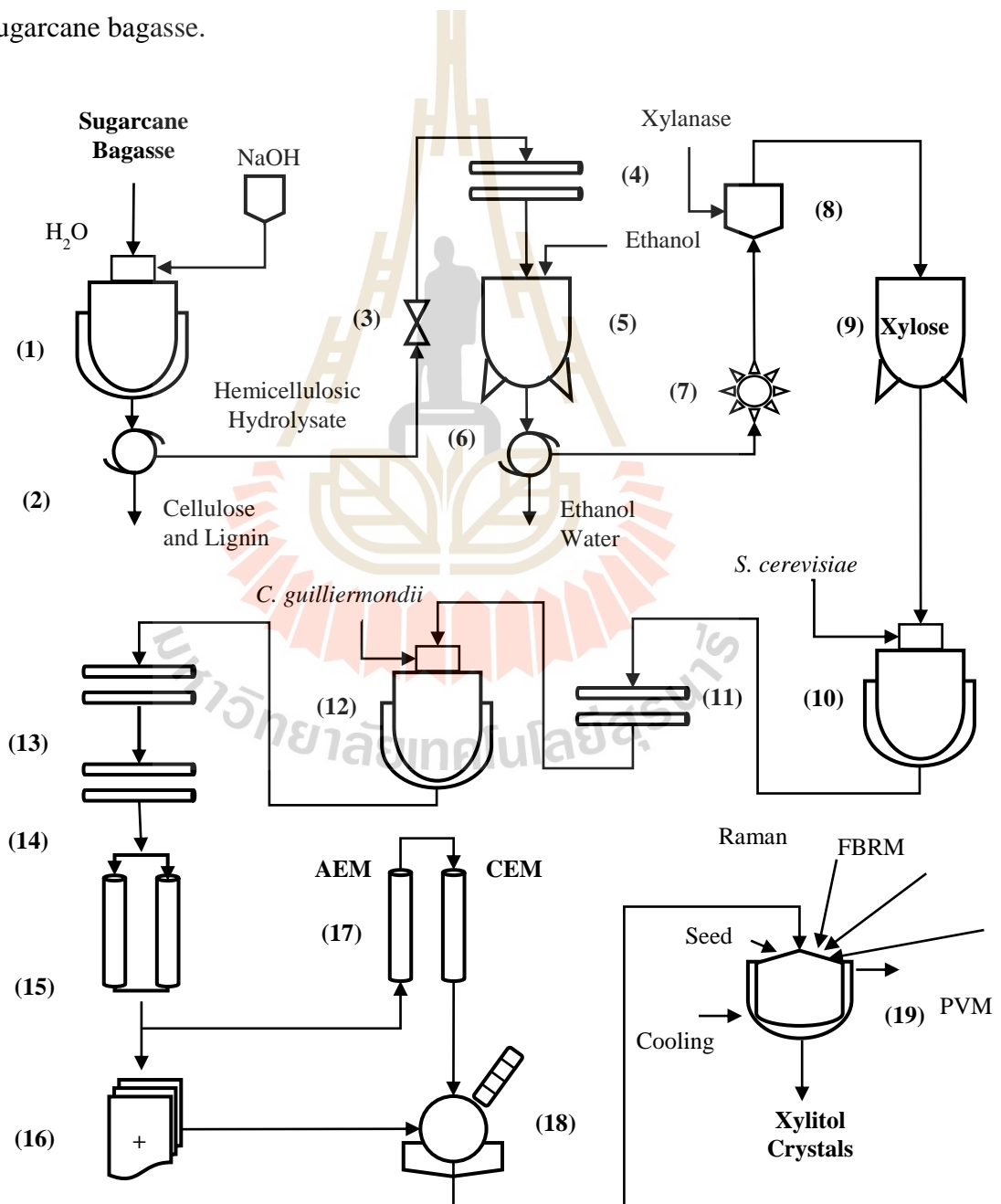
1. 1000 L alkaline hydrolysis reactor; 2. Turbo sieve; 3. Bag filter; 4. Microfiltration; 5. Xylan precipitation reactor; 6. Centrifuge; 7. Dryer; 8. Xylose emzyme hydrolysis reactor; 9. Xylose container; 10. 1000 L ethanol fermentation bioreactor; 11. Microfiltration; 12. 1000 L xylitol fermentation bioreactor; 13. Microfiltration; 14. Ultrafitration; 15. Nanofiltration; 16. Electrolyzer; 17. Ion exchange resin; 18. Rotary evaporator; 19. Crystallization reactor

4.1 Sugarcane bagasse pre-treatment

The pre-treatment of bagasse (Fig.41a) and preparation of xylose syrup were shown in Fig. 4.2. Sugarcane bagasse (from Mitr Phol company) has the basic ingredients: hemicellulose (27%), Cellulose (46%), Lignin (23%) has been brought to the Pilot plant for hydrolysis with dilute alkali (4%). This process's parameters are hydrolysis temperature 60 $^{\circ}$C, hydrolysis time 24 h, alkali/bagasse ratio is 15: 1 (v/w). At the end of the hydrolysis, the mixture was neutralized to pH 8-9 with hydrochloric acid. Next, the mixture was fed into a high-speed centrifuge to separate the residue. The liquid fraction with small solid particles was put into a pocket filter with a pore size of 0.5 µm. After that, the hydrolysis solution was added to the membrane filter to remove solid particles completely.

Xylan obtained after hydrolysis and filtration was precipitated by ethanol because of its ethanol insoluble properties. Then, the xylan recovery was performed by centrifugation under 3000 rpm/10 mins. Raw xylan after centrifugation was dried (Fig 4.1b) and transferred to Milr Phol company to perform the enzymatic hydrolysis process.

The xylan hydrolysis to obtain xylose and other sugars has been performed using the enzyme xylanase. This was performed under the following conditions: temperature

40-50 °C, stirring speed 150 rpm for 24 h; substrate concentration (xylan) 70 g/L; enzyme concentration 1.5 µg/mL). Sugar mixture after hydrolysis has been concentrated to preserve and use as raw materials for the next process.

Figure 4.1 Xylan precipitation, xylane centrifugation, wet xylane
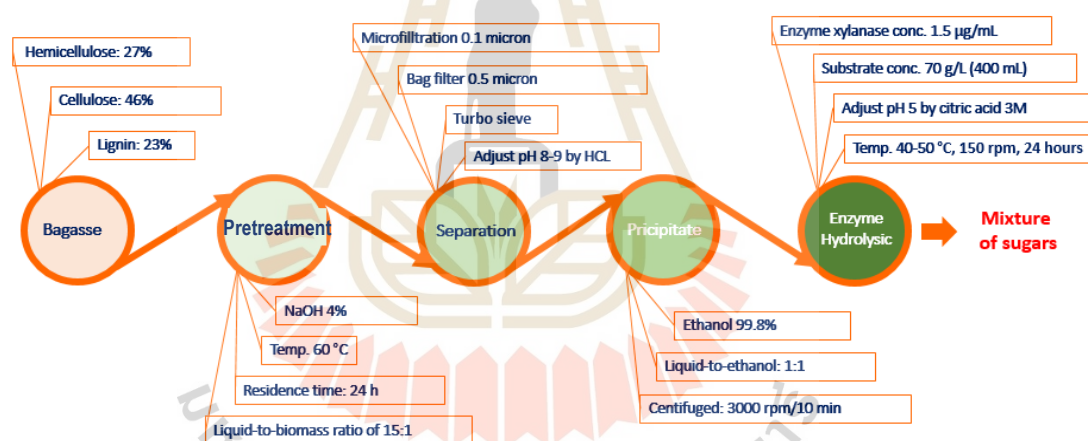
Figure 4.2 Pretreatment sugarcane bagass to obtain xylose

Fig. 4.3 and Table 4.1 are the HPLC results showing the sugar mixture content in the syrup after concentration. As shown in Fig. 4.2 and Table 4.1, in addition to xylose (retention time is 9.37) also has a large content of glucose (retention time is 8.74) 3 times higher than xylose. This makes xylitol fermentation difficult, so we have to remove the glucose before the xylitol fermentation. We have done the method to use yeast to ferment it to form ethanol (section 4.2.1).

In addition to the sugars above, there are different ions in the syrup mixture (Table 4.1.) That has been formed in the previous process, especially those using alkaline hydrolysis and acids to neutralize. These ions will also influence the fermentation and subsequent purification of xylitol.
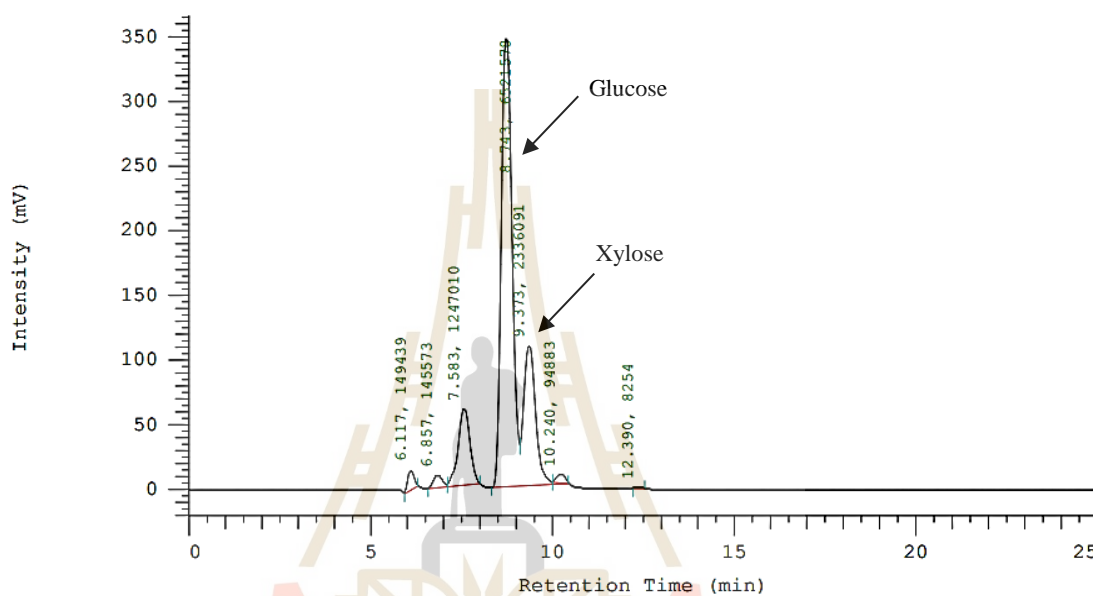
Figure 4.3 HPLC peak analysis of mixture sugar after hydrolysis

Table 4.1 Mixed composition of syrup after concentration

Glucose (g/L)	Xylose (g/L)	pH	Conductivity (mS/cm)
562.88	129.64	6.5	17.45

The results of using alkali to pre-treat bagasse were also done by some authors before. In 2016, Liu et al., hydrolyzed bagasse by NaOH combined with ultrasound, the results showed that the metabolism of glucan and xylan reached 99.51% and 92.76% after 72 h of hydrolysis (Liu, Xu *et al.* 2016); In 2017, Wunna et al. used NaOH

concentration 2 (wt%), solid to liquid ratio of 1:20 (wt), treatment temperature 120 °C for 1 h. The results showed that 83.7% of lignin was removed and recovered 37.3 and 33.2% glucan and xylan, respectively (Kyaw Wunna 2017). Roni Maryana et al. (2014) used 1N NaOH for 30 minutes to treat bagasse, the result of lignin removal reached 92.87% (Maryana, Ma'rifatun *et al.* 2014)

4.2 Xylose syrup preparation

4.2.1 Ethanol fermentation

As mentioned above, it is necessary to remove the glucose from the syrup before xylitol fermentation. The removal of glucose was performed using commercial yeast *Saccharomycea cerevisiae* (WCY 05, 0.15% (w/v)); with a synthetic carbon source (WCN-07 Plus, 0.3% (w/v)) including DAP, yeast extract...The syrup mixture was diluted with water at syrup ratio to water for 1: 3 (v/v) with a total volume 800 L; fermentation temperature 30 °C, stirring speed 120 rpm. Fermentation time 48 h, every 3 h, take samples to analyze the content of sugar and ethanol to determine the end time of the fermentation process.

The results of the changes in the concentration of sugars and the formation of ethanol are shown in Fig. 4.4 and Fig. 4.5. The glucose concentration decreased gradually with fermentation time (from 140.72 g/L to 0.00 g/L), along with a decrease in the Bx value (20 to 8.94). This suggests that the yeast effectively utilized glucose to grow biomass and form various products of the fermentation process. The amount of ethanol formed slowly in the first 12 h (>1.55%), then increased rapidly and the maximum value after 42 h (6.82%) then decreased (6.52%) when the glucose was consumed. What is surprising in ethanol fermentation is that besides the formation of ethanol, desirable

sugars xylose is also increased (from 32.41 g/L to 42.89 g/L) and xylitol was also formed
(0.85 g/L) after 48 h. That can be seen when observing the analysis results by HPLC after
42 h in Fig. 4.5 and comparing with the results in Fig. 4.3. At 8.73 min of retention time,
the glucose peak almost disappears; the peak of xylose is highest (RT 9.37 min) and a
peak of xylitol occurs (RT 10.75 min). This could be explained that besides the main
product of ethanol, other byproducts of metabolism (such as xylose and xylitol) are also
produced. In this step, we have selected the time to finish of 42 h. The aim is to retain
some of the glucose presents in the solution to facilitate xylitol fermentation.
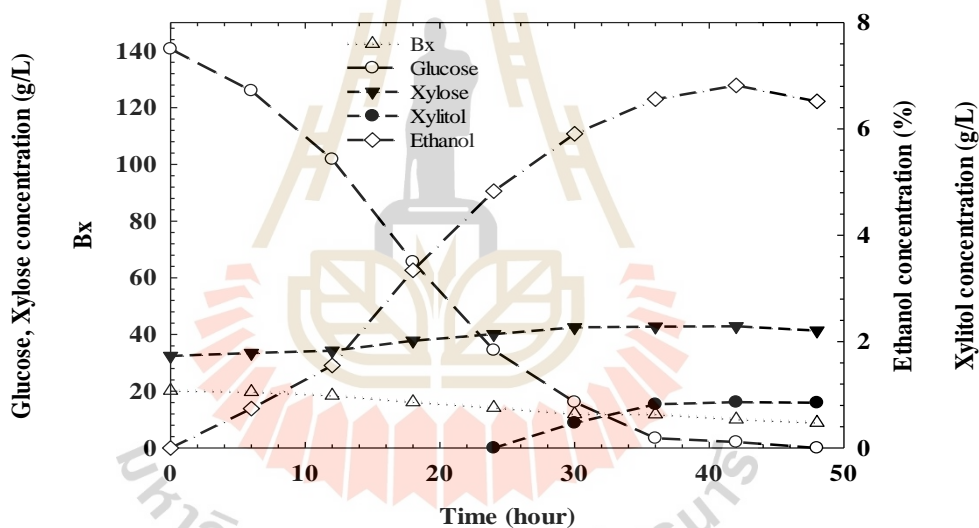
Figure 4.4 Change in the sugars and formation of ethanol
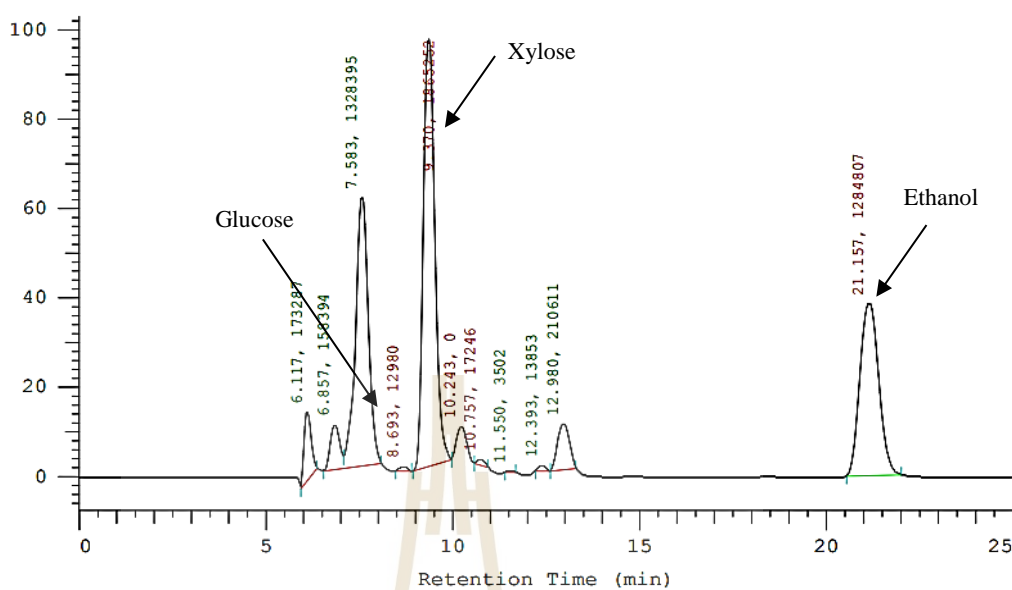
Figure 4.5 HPLC peak of fermentation broth after 42h ethanol fermentation

Unrean (2018) used *S. cerevisiae* and *C. tropicalis* for co-production of ethanol and xylitol from sugarcane bagasse hydrolyzate. As a result, 56.1 g/L at 44% of yield, 0.53 g/L.h yield was formed (Unrean and Ketsub 2018).

4.2.2 Preparation of xylose solution

At the end of the ethanol fermentation (after 42 h), the fermentation broth was sterilized at 90 ºC for 15 minutes to suspend the yeast activity. Then, the solution was cooled to 30 °C to perform microfiltration. The purpose of microfiltration is to separate the yeast cells from the solution. The membrane filtration system is used with 4 columns, using a high-pressure pump (6 bar). Before filtration, the membranes were cleaned with NaOH (1%) for 30 minutes, HCl (2%) for 30 minutes. Then rinsed with water for 1 h, finally, rinsed with RO water for 15 minutes. During the filtration process,

the membranes are cooled with water. The change of permeate flux and sugars

concentration in solution is shown in Fig. 4.6.
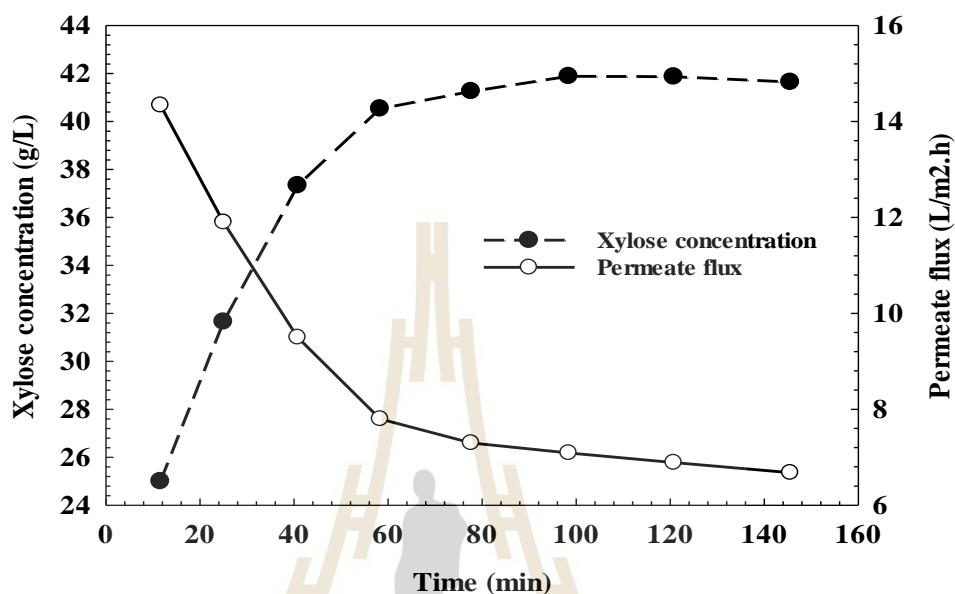
Figure 4.6 Change in the permeate flux and xylose concentration during the MF

At the first time, the membrane system still has some RO water, so at this

time the membrane is in contact with RO water before it is in contact with the real

solution. At this time, the cell density was low because of dilution, the permeate flux

reaches 14.34 L/m^2.h. After that, the change gradually decreases with increasing yeast

cell density and reaches a steady state. Towards the end of the process, the throughput

decreases due to increased membrane resistance. The initial xylose concentration of

permeate was low because it was diluted with water inside the microfiltration system.

Then increase gradually and stabilize with values from 40.54 - 41.65 g/L. This suggests

that xylose can effectively pass through the membrane to remove the cell. Discussions

on membrane properties and their applications in xylitol purification will be discussed in

more detail later. The total fermentation volume was 800 L. However, to recover the

sugar and reduce the loss (some sugar in the retentate), 150 L of RO water is added at the end of the filtration to obtain the total permeate volume of 900 L. Sugar loss after microfiltration is 12.13% of the initial total sugar.

After filtration, the solution was condensed by a vacuum falling film system, condensation temperature 50-60 ℃, the vacuum pressure of 0.05 bar. Concentration increased the concentration of xylose from 41.65 g/L to 393.7 g/L. This xylose syrup was refrigerated for follow-up research.

Figure 4.7 Picture showing evidence of the removed cells by the MF process

4.3   Xylitol fermentation process by using *C. guilliermondii* TISTR 5068.

Among the yeasts, *Candida* sp. are known to be the most potent and widely used (Ikeuchi 1999). Among them, *C. guilliermondii* is an easy-to-cultivate strain with a high conversion yield of xylose to xylitol. In this part, experiments have clarified the growth characteristics of *C. guilliermondii* 5068 in PDA; xylitol metabolism using commercial xylose sources and xylose hydrolyzed from bagasse. Effects of nitrogen source and

oxygen concentration on fermentation performance are also mentioned. The experiments were conducted from laboratory scale to pilot scale.

4.3.1   Growth curve of *C. guilliermondii* TISTR 5068

In the PDA media, the yeast growth curve has three main stages: the lag phase, the exponential phase and the stationary phase. The growth curve of *C. guilliermondii* TISTR 5068 at 30 °C, 200 rpm was shown in Fig. 4.8. It can be seen in the YPD medium, *C. guilliermondii* TISTR 5068 has a lag phase in the period of 0-15 h, with the value OD_{600} 0.15-0.55. During this period, the number of cells is stable, biochemical activities still occurred but the rate of the division was slow, also known as the period of adaptation to the environment to prepare for the next stage. The exponential phase of *C. guilliermondii* TISTR 5068 for the period 18-42 h with OD_{600} values 5.81-14.9, respectively. In this stage, cell density grows exponentially to grow biomass. This showed that YPD medium and the factors of temperature, pH, stirring speed were suitable for the yeast biomass development. The stationary phase of *C. guilliermondii* TISTR 5068 in the time after 42 h. During this period the metabolic rate and cell division rate slowed down, xylitol were formed. Optical density is a widely used method for estimating the number of cells in a culture medium, the optical density was proportional to the number of cells (within the optical density <1). According to the growth curve, the inoculum was selected at 24 h with the OD_{600} value of 8.41.
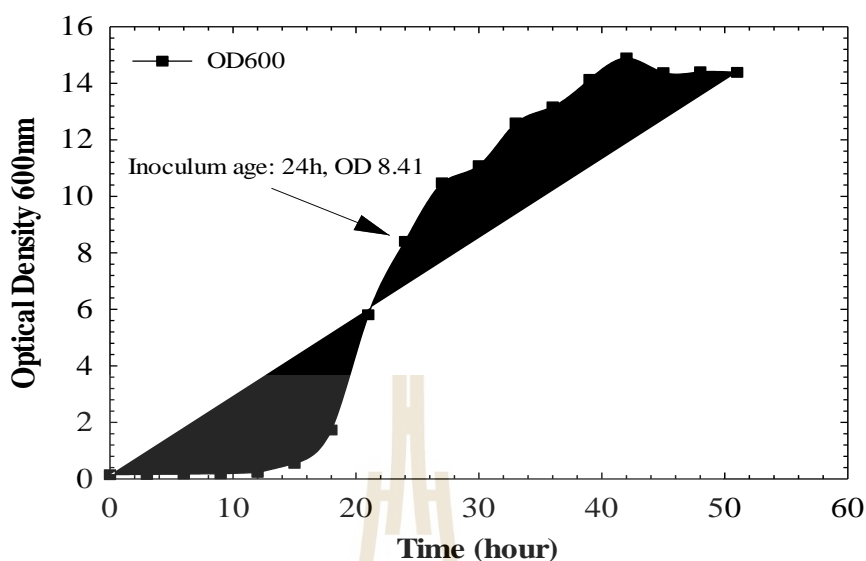
Figure 4.8 Growth curve of *C. guilliermondii* TISTR 5068

4.3.2 Shake flask 250 mL xylitol fermentation from commercial xylose

1. Effect of initial glucose on xylitol fermentation

To determine the effect of initial glucose concentration, 10% (v/v) inoculum after 24 h culture was added to Erlenmeyer 250 mL containing 100 mL of fermentation medium with nitrogen ((NH_4)$_2$SO$_4$ (2.0 g/L), peptone (3.0 g/L), commercial yeast extract (5.0 g/L)) and 30 g/L xylose concentration. The initial glucose concentrations were 2, 4, 6, 8, and 10 g/L glucose, respectively. The effect of glucose on the biomass development, glucose and xylose consumption, the forming xylitol concentration is shown in Fig. 4.9. Xylitol yield and xylitol productivity of each respective experiment are shown in Table 4.2.

Fig. 4.9a showed the growth ability of *C. guilliermondii* TISTR 5068 at different glucose concentrations. During the first 12 h of fermentation, biomass growth rates in experiments in the first 12 h were faster than in YPD media (Fig. 4.8), both of

which could be explained by the initial cell density in the media. The fermentation field is higher than the initial cell density in inoculum. Next, in the log phase, the higher the glucose concentration experiment, the greater the growth rate and the higher cell density, suggesting that glucose was the necessary and preferred carbon source for biomass development at the initial stage. The OD_{600} value evidenced this in Fig. 4.9a and the glucose consumption in Fig. 4.9b. In Fig 4.9b, glucose was completely consumed after 12 h at low concentrations (2 g/L and 4 g/L), after which, the yeast continues to use xylose for biomass development in the next stage and form the product. The lower glucose concentration explained it, the xylitol induction point earlier than the high glucose (Fig. 4.9d). In parallel with the use of glucose, yeast also used xylose at the beginning to develop biomass; however, the speed of using xylose was slower than glucose (Fig. 4.9c). After the yeast has used up glucose and entered a stable phase, the amount of xylose is consumed faster to form xylitol. The consumption of xylose in Fig. 4.9c shows the relationship between the initial glucose and xylose content. While xylose was completely consumed after 120 h and 132 h in the experiment of supplementing with low glucose concentration (2 and 4 g/L), at higher glucose concentrations, xylose was consumed completely later (144 and 156 h). This suggests that the presence of high glucose concentration competes and prevents the cell's xylose absorption, synonymous with low product xylitol content. The highest xylitol concentration was reached 25.84 g/L after 132 h of fermentation at 2 g/L glucose concentration (glucose: xylose 1:10), corresponding to xylitol yield 0.86 g/g, and xylitol productivity 0.20 g/L.h (Fig. 4.9d, Table 4.2). Simutaneously, the lowest xylitol concentration when supplemented with glucose 10 g/L reached 10.20 g/L, corresponding to Y_{xyt} 0.44 g/g and P_{xyt} 0.08 g/L.h.

Figure 4.9 The effect of initial glucose concentration to xylitol fermentation. A) Optical

density at 600 nm; B) Glucose consumption; C) Xylose consumption; D)
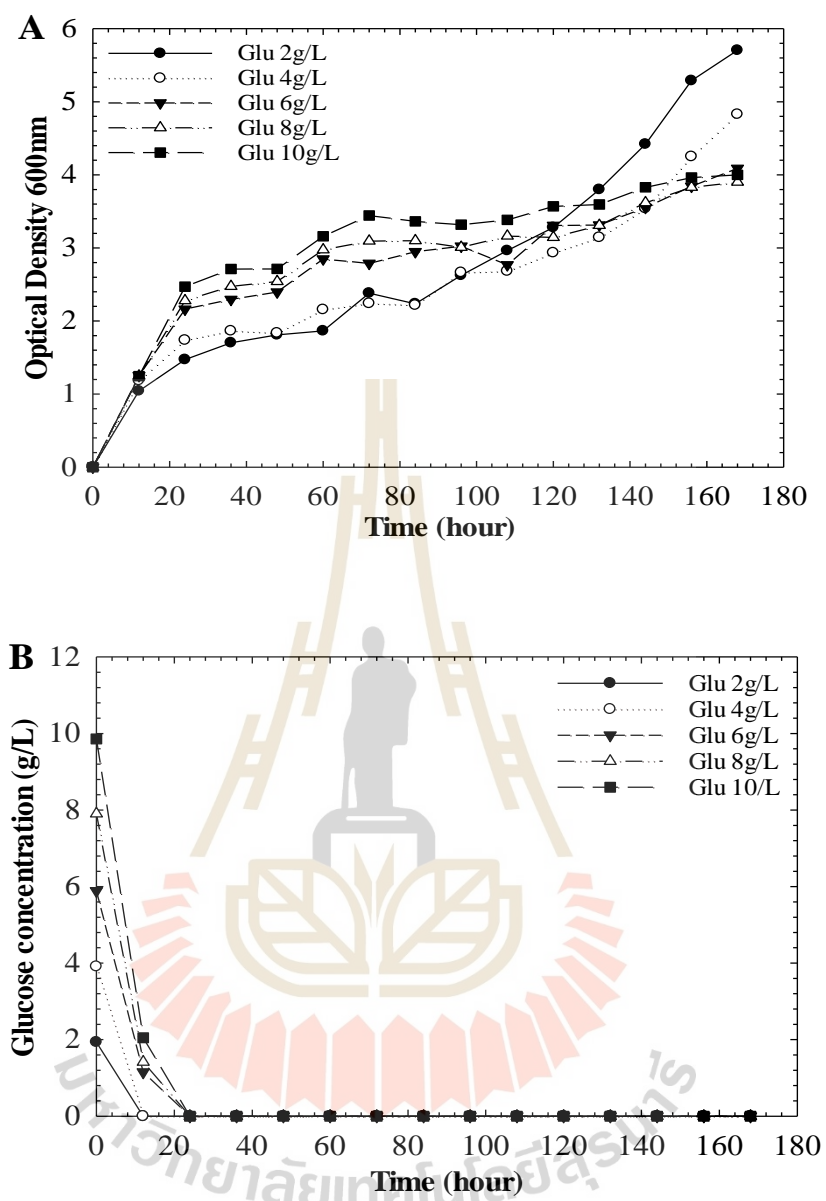
Xylitol production

Figure 4.9 The effect of initial glucose concentration to xylitol fermentation. A) Optical

density at 600 nm; B) Glucose consumption; C) Xylose consumption; D)

Xylitol production (Continued)

Table 4.2 Effect of initial glucose to xylitol production

Experiment	Xylitol Concentration (g/L)	Y_{xlt} (g/g)	P_{xyl} (g/L.h)
Glu 2g/L	25.84	0.86	0.20
Glu 4g/L	18.47	0.64	0.14
Glu 6g/L	13.01	0.51	0.10
Glu 8g/L	10.77	0.46	0.08
Glu 10g/L	10.20	0.44	0.08

For yeast, xylose was diffused into cells and reduced to xylitol by the enzyme xylose reductase (XR) with an intermediate NADPH effect. NADPH is converted to $NADP^+$ and regenerated from glucose-6-phosphate (G6P) through the action of glucose-6-phosphate dehydrogenase (G6PD) in pentose phosphate (PPP) or hexose monophosphate (HMP) pathways. Here, the role of glucose has been shown when making direct contributions to the production of G6P and NADPH. Therefore, it could be said that the presence of glucose via the pentose phosphate pathway can enhance xylitol production by mediating the activity of xylose reductase (XR). Tochampa *et al.* (2005) demonstrated that supplementing with 3 g/L glucose, the ratio of glucose:xylose 1:10 is the optimal condition for xylitol fermentation by *C. mogii* (Tochampa, Sirisansaneeyakul *et al.* 2005). The study of Wannawilai *et al.* (2017) with *C. magnoliae* TISTR 5663 also demonstrated that the initial glucose concentration of 3 g/L in fermentation medium containing 30 g/L xylose gave the highest xylitol production efficiency (Wannawilai, Lee *et al.* 2017). However, the study of Felipe *et al.* (2006) showed that the *C. guilliermondii* strain was more effective when supplementing with 9

g/L glucose at a glucose: xylose 1: 5 ratio compared to a medium containing only xylose (da Silva and de Almeida Felipe 2006).

2. Effect of initiate xylose on xylitol fermentation

To determine the effect of initial xylose concentration, 10% (v/v) inoculum after 24 h of culture were added to Erlenmeyer 250 mL containing 100 mL of fermentation medium with nitrogen, and 2 g/L glucose available. Initial xylose concentrations were 10, 20, 30, 40, and 50 g/L, respectively. The effects of xylose on biomass development, glucose and xylose consumption, and xylitol concentration are shown in Fig. 4.10. Xylitol yield and xylitol productivity of each respective experiment are shown in Table 4.3.

Initial xylose concentration had a great influence on the biomass development during fermentation. During the first 24 h, a high initial concentration of syrup (40-50 g/L) had a cell growth effect. However, along with the depletion of glucose, the growth rate slowed down, OD_{600} was lower than the smaller xylose concentrations (10-30 g/L) (Fig. 4.10a, 4.10b). This showed that after the lag phase is finished, high xylose concentration will inhibit the growth of *C. guilliermondii* TISTR 5068 is finished, high xylose concentration will inhibit the growth of *C. guilliermondii* TISTR 5068.

Figure 4.10 The effect of initial xylose concentration to xylitol fermentation. A) Optical

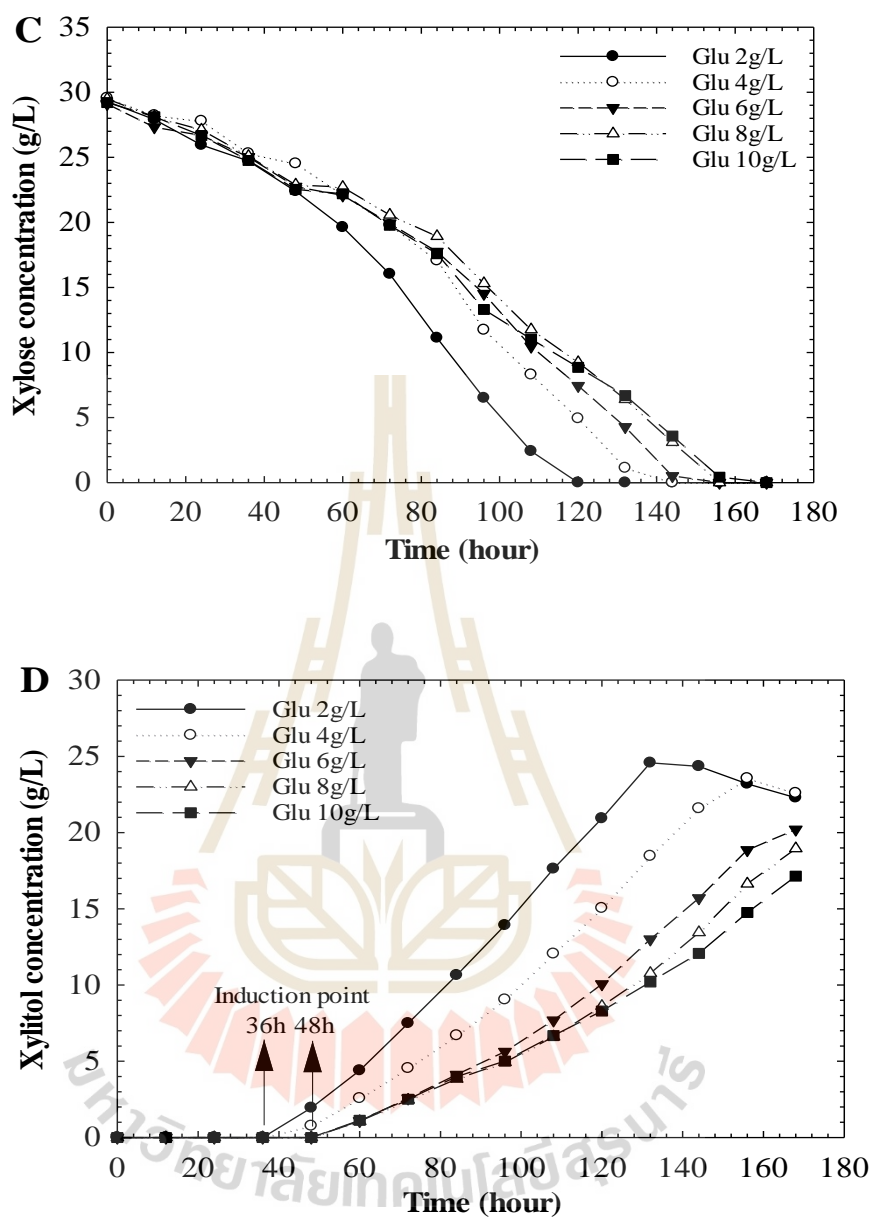density at 600 nm; B) Glucose consumption; C) Xylose consumption; D)

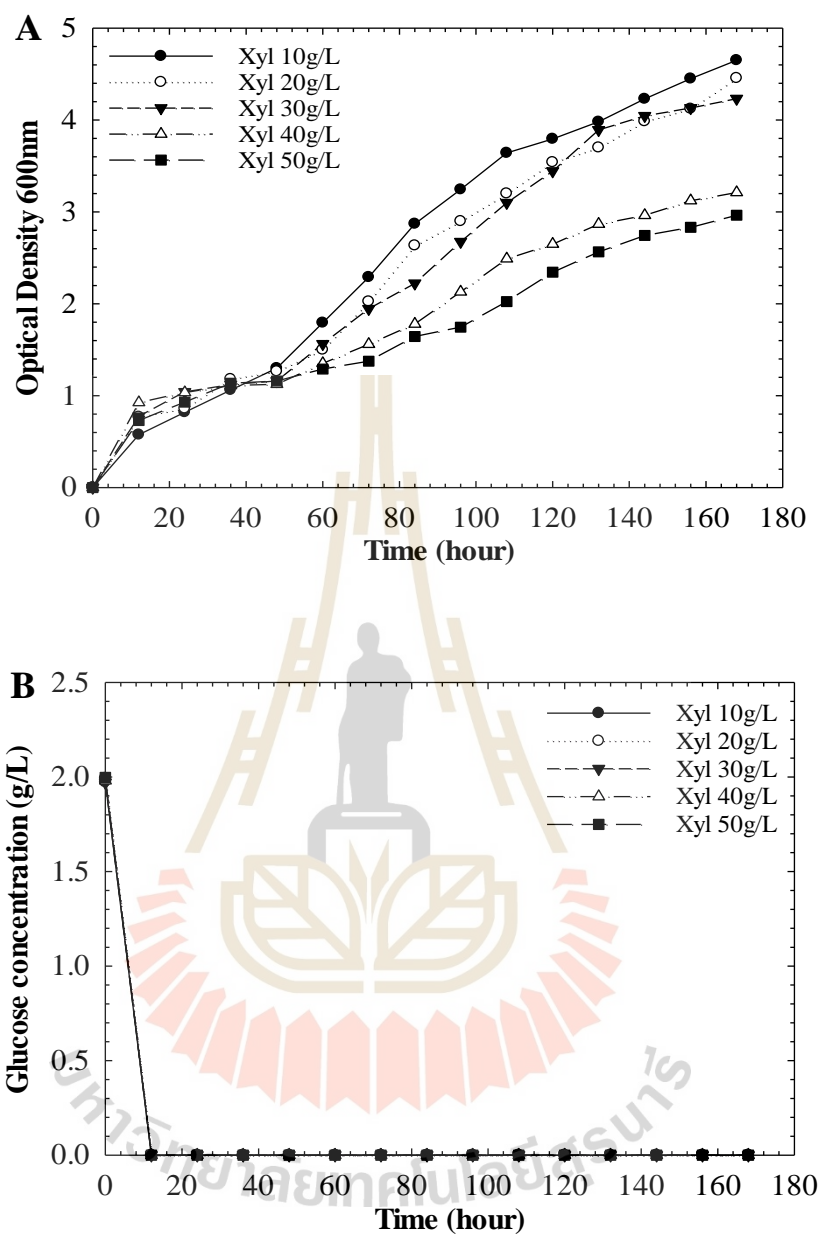Xylitol production.
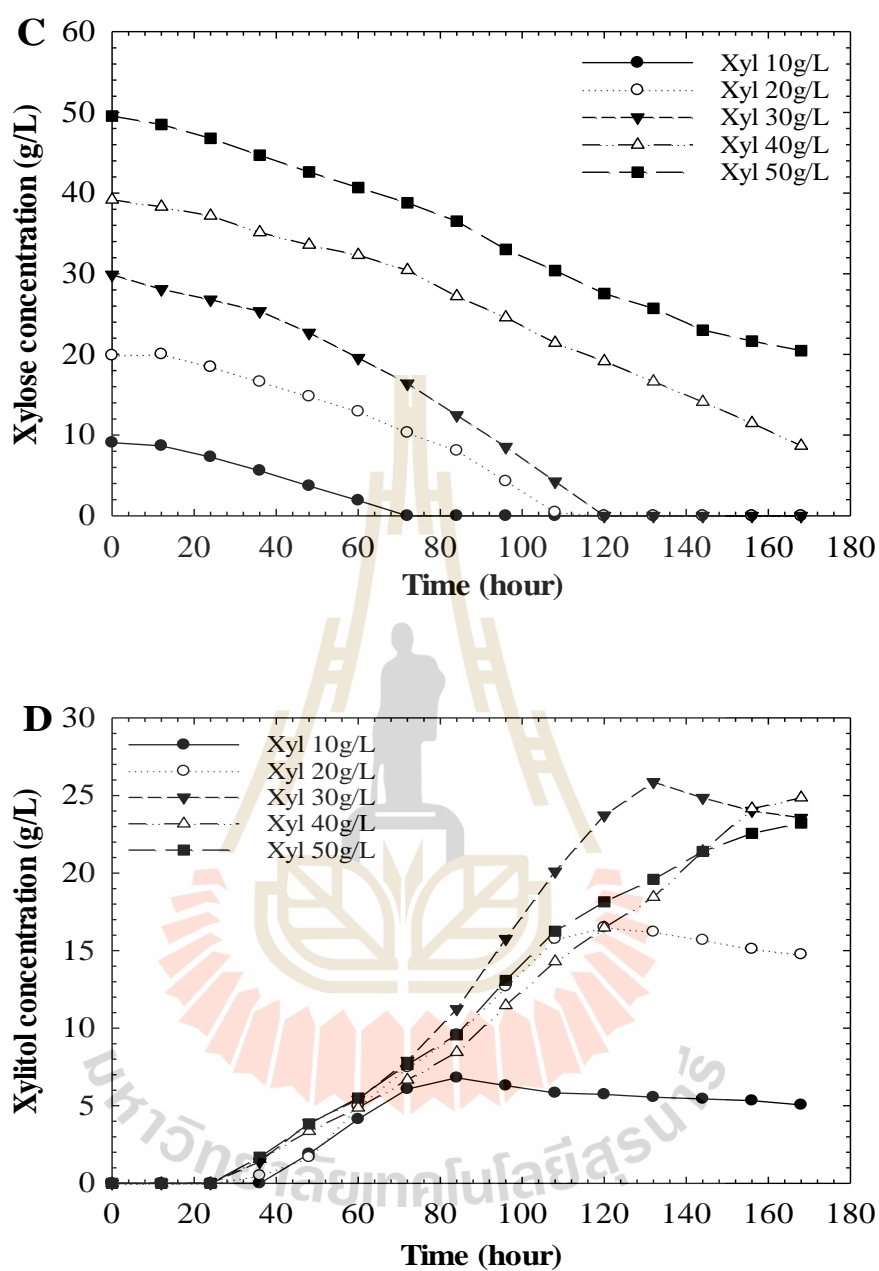
Figure 4.10 The effect of initial xylose concentration to xylitol fermentation. A) Optical

density at 600 nm; B) Glucose consumption; C) Xylose consumption; D)

Xylitol production (Continued)

Table 4.3 Effect of xylose to xylitol production

Experiment	Xylitol Concentration (g/L)	Y_{xlt} (g/g)	P_{xlt} (g/L.h)
Xyl 10 g/L	5.55	0.55	0.04
Xyl 20 g/L	16.21	0.81	0.12
Xyl 30 g/L	25.87	0.86	0.20
Xyl 40 g/L	18.45	0.79	0.14
Xyl 50 g/L	19.43	0.77	0.15

The xylose consumption of *C. guilliermondii* TISTR 5068 is shown in Fig. 4.10c. At 10 g/L, xylose was consumed quickly and completely after 72 h. At this concentration, xylose was only sufficient for biomass development, the production of xylitol was reduced resulting in low xylitol concentration. The maximum xylitol concentration reached 6.3 g/L after 96 h and then gradually decreased over time. After 132 h of fermentation, the values of Y_{xlt} and P_{xlt} were 0.55 g/g, and 0.04 g/L.h, respectively (Fig. 4.10d, Table 4.3). The xylose concentration of 40-50 g/L indicated incomplete xylose consumption after 168h, the remaining xylose concentration in the medium is 8.67 and 20.46 g/L, respectively. This indicated that high xylose concentration leads to high osmotic pressure in the environment, which was detrimental to the growth of *C. guilliermondii* TISTR 5068. Initial xylose concentration of 30 g/L has been shown to be the optimal condition and the best for xylitol fermentation. The xylitol concentration has reached a maximum of 25.87 g/L after 132 h with Y_{xlt} and P_{xlt} reaching 0.86 g/g and 0.2 g/L.h, respectively. At this concentration, a quantity of xylose has been used to

continue the growth of biomass and the rest was absorbed and converted into xylitol. Xylitol was formed and accumulated continuously in cells, facilitating diffusion into the environment. The relatively high xylitol concentration showed that at this concentration. At the initial xylose concentrations of 10, 20, 40, 50 g/L, after 132 h, the xylitol concentrations reached 5.55, 16.21, 18.45, and 19.43 g/L, respectively.

In the study of Kim *et al*. (2002) with *C. tropicalis* strains fermented in a synthetic medium, the optimal initial xylose concentration was 50 g/L. At the end of the fermentation, xylitol yield reached 0.59 g/L (Kim, Han *et al.* 2002). In the study of Tamburini *et al*. (2010) with *C. tropicalis* showed that maximum xylitol yield (0.38-0.42 g/g) in the initial xylose concentration range was 50-70 g/L, respectively (Tamburini, Bianchini *et al.* 2010). However, also for this strain, the optimal initially xylose concentration was raised to 60-80 g/L with Y_{xlt} reaching 0.84 g/g after controlling oxygen, temperature, and pH values during the fermentation (Tamburini, Costa *et al.* 2015). In 2018, Linlin *et al*. used *Candida tropicalis* 31949 to ferment xylitol from sugarcane bagasse hydrolysate. The results showed that the initial optimal xylose concentration is 100 g/L, and the xylitol concentration is 62.98 g/L (Xu, Liu *et al.* 2018).

Effects of glucose and xylose initially on the conversion efficiency of xylitol from commercial xylose used to study the fermentation potential of xylose hydrolyzed from bagasse.

4.3.3 Shake flask 250 mL xylitol fermentation from xylose hydrolyzate

The commercial xylose concentration and fermentation conditions in section 4.3.2 were applied to investigate the effects of xylose from bagasse (XBS-sugarcane bagasse hemicellulosic hydrolysate). In this test the mixed nitrogen source

prepared as above ((NH$_4$)$_2$SO$_4$ 2.0 g/L), peptone (3.0 g L), commercial yeast extract (5.0 g/L)) were compared with commercial nitrogen source WCN-07 Plus (3 g/L). The Effects of XBS and alternative nitrogen sources are shown in the graph in Fig. 4.11.
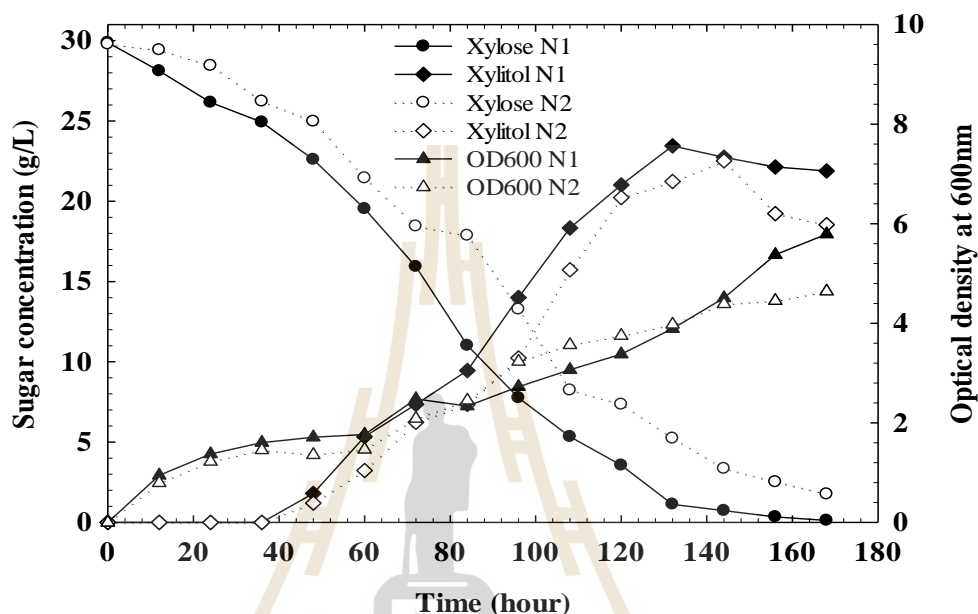
Figure 4.11 Effect of nitrogen sources on xylitol fermentation. N$_1$ - mixed nitrogen source; N$_2$ - alternative nitrogen source WCN 07-Plus

In media containing XBS with a mixed or alternative nitrogen source, the yeast *C. guilliermondii* TISTR 5068 showed good growth. OD$_{600}$ from 2 experiments N$_1$ and N$_2$ was equivalent to commercial xylose source. It has been shown that although XBS solution contains many different ingredients, it was still favorable for the yeast to grow. Alternative nitrogen source WCN-07 Plus has a maximum OD$_{600}$ of 4.65, which is lower than mixed nitrogen source with OD$_{600}$ value of 5.79.

The xylose consumption and xylitol formation were also compared and compared with commercial xylose. When replacing the carbon source with XBS, xylose showed incomplete consumption after the end of fermentation (0.12 g/L in the N$_1$ test

and 1.76 g/L in the N_2 test after 132 h and 144 h, respectively). Meanwhile, xylose was consumed after 120 h of fermentation for commercial xylose. It is shown that although XBS is suitable for yeast growth, it is demonstrated by the high OD_{600} value, however, the solution still contains substances that inhibit the growth and consumption of xylose to produce into xylitol. One of the factors that inhibit fermentation is the concentration of sugar-free substances dissolved in the media, especially the Na^+ and Cl^- ions formed after the hydrolysis of bagasse. It is shown at the conductivity value of the high fermentation medium (16-17 mS/cm), which creates high osmotic pressure in the medium, making it difficult for yeast growth and conversion to xylose into xylitol. On the other hand, this is also a hindrance to the xylitol purification process later.

The xylitol concentration formed in the experiment N_2 was lower than in the experiment N_1, and lower than that of the commercial xylose, reaching 22.52 g/L after 144 h compared with 23.45 g/L (132 h) and 25.87 g/L (132h), respectively. However, the deviation is not too big and is acceptable. One of the reasons we can choose an alternative nitrogen medium (WCN-07 Plus) is the high fermentation yield (0.85 g/g) and the low nitrogen mass (3 g/L compared to 10 g/L of mixed nitrogen source). This is very significant because the purity of xylitol in the fermentation medium was high, which is favorable for the purification and recovery of xylitol.

Silva et al. (2006) used *C. guilliermondii* FTI 20037 to ferment xylose from bagasse hemicellulosic hydrolysate (xylose 46 g/L, glucose 1.8 g/L), the results showed that the concentration of xylitol formed reached 27.80 g/L with yield 59% and productivity 0.53 g/ L.h after 48 h of fermentation (da Silva and de Almeida Felipe 2006). Xu et al. fermented xylose from sugarcane bagasse hydrolysate with *C. tropicalis* 31949, medium containing 100 g/L xylose after detoxification, with 10% inoculum, inoculum

age 26h. Results showed that 62.98 g/L xylitol was formed after 54 h (Xu, Liu *et al.* 2018). Kumar et al. 2014 simultaneously fermented xylitol and ethanol from bagasse hemicellulosic hydrolysate rich in glucose and xylose. As a result, xylitol conversion yield reached 61% and ethanol 43% respectively (Kumar, Dheeran *et al.* 2015). In 2019, *C. tropicalis* JA2 strain was used by Junior to ferment xylose from sugarcane bagasse hydrolysate with an initial concentration of 177 g/L, supplemented with 2.0 g/L yeast extract, 4.0 g/L urea. 109.5 g/L xylitol was formulated with 86% of yield (Morais Junior, Pacheco *et al.* 2019).

We have used alternative nitrogen source (WCN-07 Plus) for further studied on a larger scale through the results obtained in the above experiments. Experiments were performed in 5 L and 500 L bioreactor.

4.3.4   5 L bioreactor xylitol fermentation from XBS

Dissolved oxygen concentration in the fermentation medium significantly affects the yeast growth and xylitol conversion efficiency. In the 250 mL flask, oxygen was not added to the fermentation medium because of the small volume of solution. In the 5 L fermentation equipment, with a working volume of 3.5 L, dissolved oxygen was investigated to find the most appropriate concentration. Other fermentation conditions were maintained.

Experiment 1 investigated the necessity of adding dissolved oxygen to the fermentation medium by arranging 2 Duran bottles at the same time. Duran 1 (D_1) replenished air during the fermentation period; Duran 2 (D_2) stopped providing air after 48 h of inoculum. Experiment 2 used a 5 L bioreactor with an oxygen probe to find the exact dissolved oxygen concentration suitable for the fermentation.
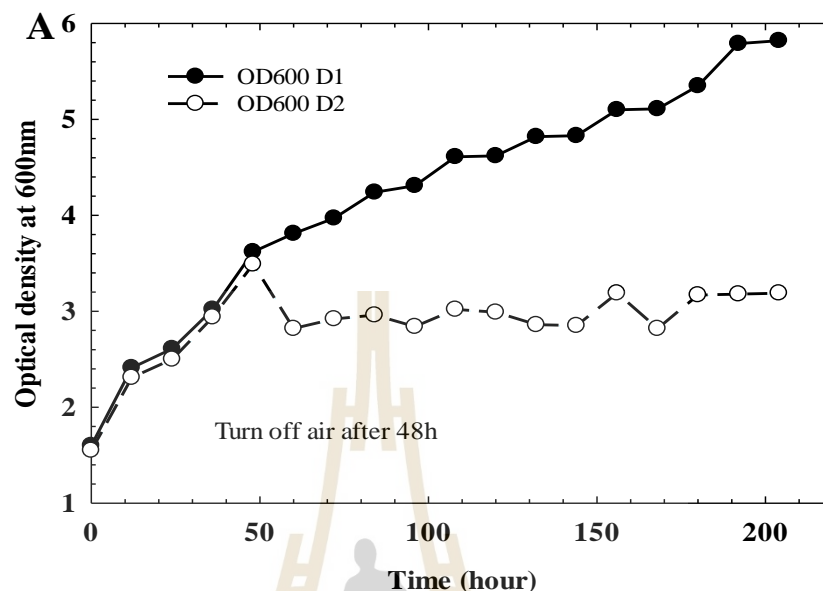
Figure 4.12 The optical density at 600nm of diferent air conditions. D1-full air condition; D2-turn off air after 48h inoculum

The growth of *C. guilliermondii* TISTR 5068 under two different conditions was shown on the graph in Fig. 4.12. Looking at the graph we can see that at the first 48 h, the OD_{600} values under both conditions are similar. However, the difference was evident under hypoxia (D2), the OD_{600} decreased from 3.49 to 2.88 after stopping air supply (48 h to 60 h). Meanwhile, under sufficient oxygen (D_1), the OD_{600} increased from 3.62 to 3.81 and continued to increase throughout the fermentation period, reaching 5.79 at the end. This indicates that oxygen is essential for the growth of the yeast *C. guilliermondii* TISTR 5068.
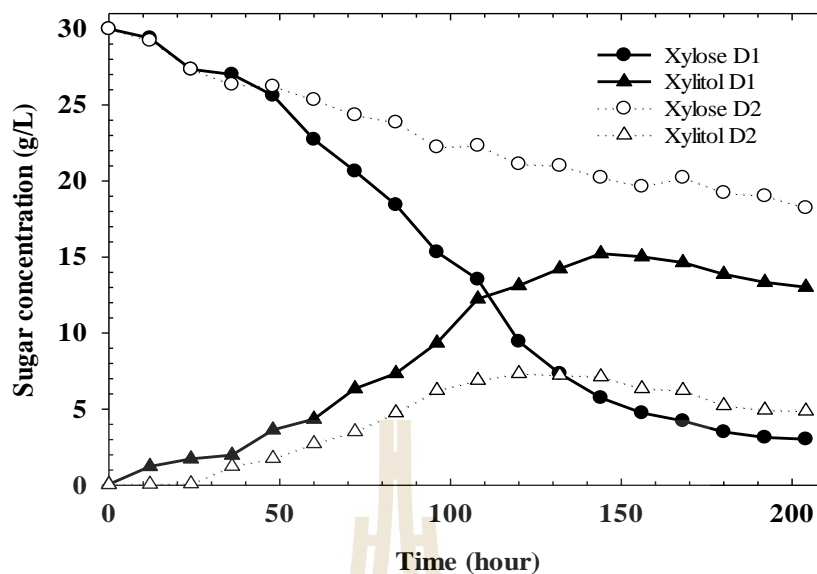
Figure 4.13 Effects of different oxygen conditions on xylitol in 5 L duran fermentation

bottle

The xylose consumption in D_2 was faster than D_1 and achieved the lowest

value of 3.02 g/L compared with 18.24 g/L (6 times lower), corresponding to 89.9% and

39.2% of xylose consumed compared with the initial. However, the amount of xylose

remaining in D1 was still 25 times higher than the amount of xylose in a 250 mL flask.

The xylitol concentration increased in both fermentation conditions with an increase in

OD. This shows that along with the growth of biomass, xylitol is also formed at low

concentrations initially. Under the D_1 conditions, the highest xylitol concentration was

15.23 g/L after 144 h, twice as high as the xylitol concentration under the D_2 condition

7.34 g/L after 132 h. After reaching the maximum value, the xylitol concentration

decreased with time under both fermentation conditions (13.01 g/L and 4.87 g/L

respectively), although xylose remained in the fermentation medium. The fermentation

efficiency and yield under the two conditions reached 0.62 g/g, 0.1 g/L.h and 82.69 g/L,

0.05 g/L.h, respectively. Although the xylitol concentration and fermentation yield under

D_1 were higher than that of D_2 but lower than the fermentation results in the flask. This shows that under hypoxia or too much oxygen does not yield a high fermentation efficiency. This is explained because oxygen plays a very important role in the fermentation process. Yeasts cannot convert xylose to xylitol under anaerobic conditions due to the redox imbalance between NAD^+ and NADH. Under low oxygen conditions, NADH is not completely oxidized, the increasing xylitol digestion. At too high oxygen concentration, an imbalance occurs when the NAD^+/NADH couple has a larger ratio than $NADP^+$/NADPH, which will lead to the xylitol-to-xylulose oxidation occurring more strongly, consuming much more desired products.

The 5 L bioreactor with an oxygen probe was used to determine the most suitable dissolved oxygen concentration for xylitol fermentation. The air was supplied into the environment through a bacterial filtration system and flow regulation. Dissolved oxygen concentration was displayed on the main screen. Bioreactor with motor and agitator, probes to determine pH values, temperature. In the experiments with duran, when the air flow is too large, yeast biomass development was preferred. Therefore, in this experiment, the dissolved oxygen concentration was adjusted at 1% to consider the fermentation efficiency. Results are shown on the graph in Fig. 4.14.
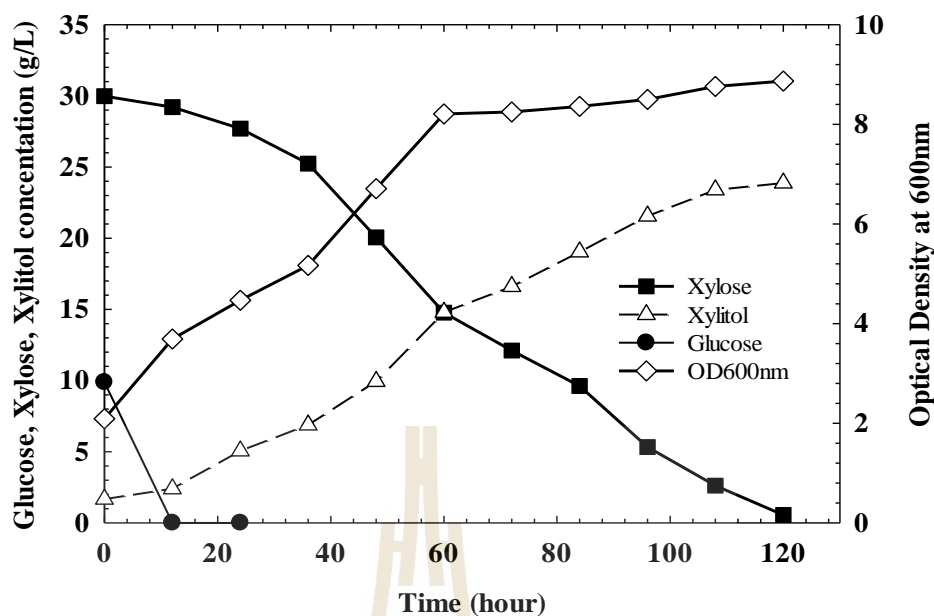
Figure 4.14 The change of sugars during fermentation of sugarcane bagasse hemicellulosic hydrolysate by *C. guilliermondii* TISTR 5068 in 5 L bioreactor with 1% dissolved oxygen

The glucose provided for the first time to develop biomass was consumed entirely after the first 12 h. Along with that, the OD_{600} increased continuously from 0 to 60 h of fermentation and reached the maximum value of 8.21, then maintained until the end of fermentation. Xylose was consumed slowly at the first 24 h, then decreased rapidly after the number of cells in the medium increased and the demand for nutrients was great, glucose was consumed. At the end of fermentation, 98.13% of the xylose was consumed as compared to the initial xylose. The xylitol concentration increased during fermentation and reached the maximum value 23.88 g/L after 120 h of fermentation. This corresponds to an efficiency of 81.18% and a productivity of 0.199 g/L.h. The above results showed that at a concentration of 1% dissolved oxygen, it is very favorable for yeast to grow and metabolize xylitol. Although the yield was 81.18% lower than 250 mL flask, the

productivity was as high as 0.199 g/L.h because of the short fermentation time (120 h).

Faria et al. (2002) evaluated the behavior of *C. guilliermondii* during fermentation performed at different oxygen concentrations (0.5-30% saturation). Research has shown that oxygen concentration as the key variable governing xylitol secretion must be controlled to increase xylitol production. At concentrations of O_2 greater than 25%, cells thrived, not found xylitol was excreted into the environment. Thereafter, xylitol was formed when the oxygen attachment was stopped. Oxygen absorption 13-30 mg O_2/g cells showed the highest xylitol excretion yield (Faria LF 2002). In 1997, Kim et al. also demonstrated DO value has an effect on xylitol fermentation. At high DO values, the cell concentration and activity of the enzyme xylitol dehydrogenase increases, and the xylitol formed is converted to xylulose and used by the cell. At DO value of 0.7% showed that the activity of xylose reductase was maximized. At concentrations of DO from 0.8 to 1.2%, xylitol conversion yield reached the highest of 210 g/L after 66 h of fermentation from a medium containing 300 g/L xylose (Kim 1997). At 18 L fermentation volume, Vaz de Arruda (2017) showed that at the aeration rate of 0.7 vvm, the fermentation yield was 0.66 g/g, the productivity was 0.29 g/L.h (Vaz de Arruda, dos Santos *et al.* 2017). Tamburini et al. (2015) used *C. Tropicalis* DSM 7524 to ferment xylitol from a synthetic medium. The parameters were studied in which of temperature, pH, initial xylose concentration and DO. The results showed that with DO <1%, *C. Tropicalis* DSM 7524 can form xylitol with a concentration of 71.34 g/L from 80 g/L of initial xylose, yield 0.86 g/g (Tamburini, Costa *et al.* 2015).

4.3.5   500 L bioreactor xylitol fermentation from hydrolyzate xylose

Pilot scale fermentation is the essential basis for adoption on an industrial scale. Therefore, we expand the scale for 500 L bioreactor capable (350 L media) of automatically controlling the parameters of temperature, pH, foam breakage, and stirring speed. Although it has been demonstrated in the 5 L fermenter that a 1% DO concentration is adequate for xylitol metabolism, the yeast behavior in the 500 L is likely to change. Therefore, in the 500 L device we have attached a saturated oxygen probe for verification. Experiment 1 was performed with concentrations of DO >20%, experiment 2 was done with concentrations of DO <1%. The fermentation conditions were similar to fermentation experiments at the 5 L bioreactor.

Fig. 4.15 shows the results of xylitol fermentation in 500 L bioreactor under DO >20%.

Figure 4.15 The change of sugars during fermentation of sugarcane bagasse hemicellulosic hydrolysate by *C. guilliermondii* TISTR 5068 in 500 L bioreactor with DO >20%

OD value increased suddenly and reached a maximum of 37.8 (7 times higher than normal) after 72 h, proving that a high DO concentration is very suitable for biomass development. Along with the growth of biomass is the consumption of xylose in the environment. At the first 24 h, the concentration of xylose decreased from 29.89 to 15.82 g/L, then decreased to 0 after 72 h. Glucose in previous experiments was completely consumed after the first 12 h. In this experiment, all glucose was consumed after the first 36 h. This suggests that at high DO levels, yeasts tend to favor xylose. Xylitol was formed and reached the highest 6.35 g/L after 36 h (yield 0.28 g/g), but then quickly reduced to 0 g/L after 72 h. This showed that under highly saturated oxygen conditions, yeasts can use both xylose and xylitol to grow biomass.
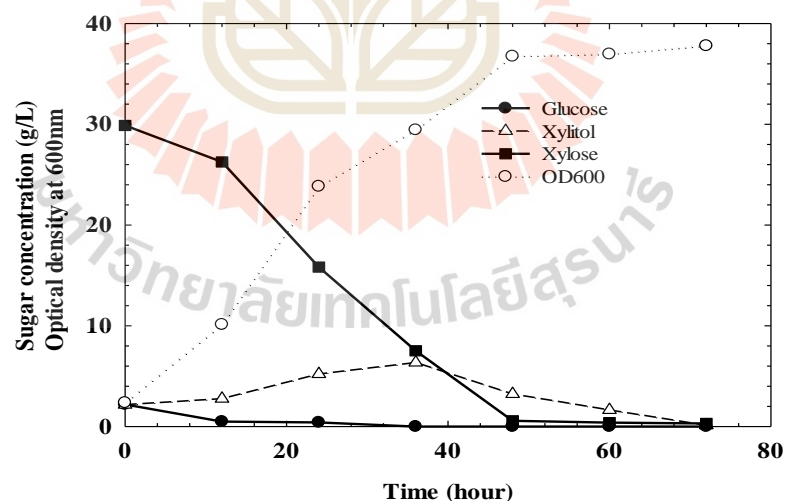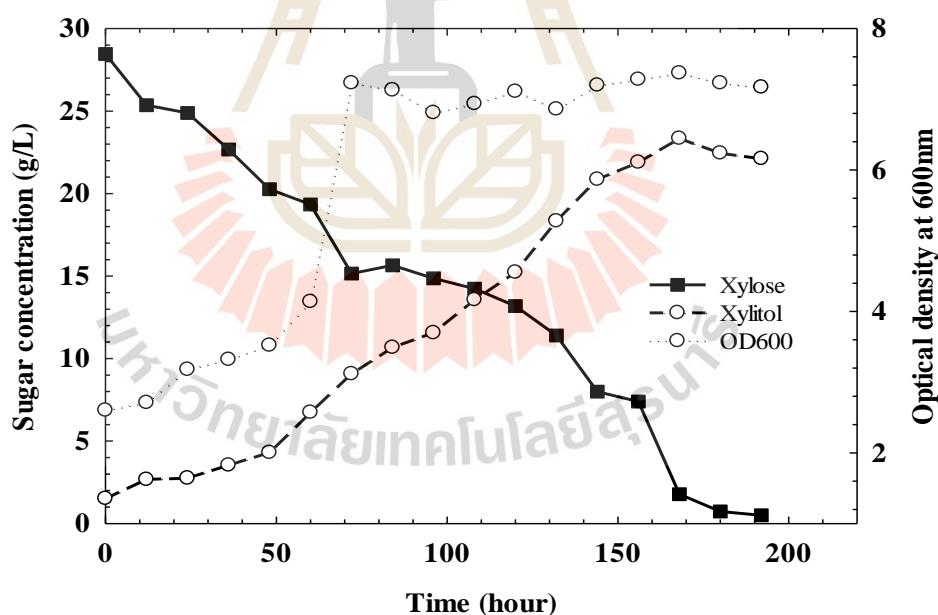

Figure 4.16 The change of sugars during fermentation of sugarcane bagasse hemicellulosic hydrolysate by *C. guilliermondii* TISTR 5068 in 500 L bioreactor with DO <1%

In the condition of DO <1%, the value of OD_{600} and the change of the lines are shown on the graph in Fig. 4.16. The OD_{600} increases over the first 72 h and reaches 7.23, followed by the stationary phase. That showed that when increasing fermentation volume from 5 L to 500 L, the yeast's growth remained the same. Xylose was used for biomass development and xylitol formation, the xylose concentration decreased from 28.46 g/L to 0.50 g/L after 192 h (consumption 98.24%). Along with the consumption of xylose is the formation of xylitol in the medium. The xylitol concentration increased during the fermentation period was about 0 to 168h, reaching 23.34 g/L with a yield of 0.87 g/g and productivity 0.14 g/L.h, respectively. Then decreased to 22.12 g/L, although the amount of xylose was still in the medium. This can be explained that yeast can absorb a part of xylitol in the medium to convert to xylulose, providing raw materials for the cell.

There is little publication of xylitol fermentation on a pilot scale, most of it on laboratory scale with triangular flasks or 5 L bioreactor. This can be explained by the high investment and operating costs of the equipment. In 2017, Arruda fermented xylitol in a 125 L bioreactor, resulting in xylitol conversion yield of 0.55 g/g, 17% lower than a 5 L (0.66 g/g) bioreactor, which yielded 0.31 g/L.h (Vaz de Arruda, dos Santos *et al.* 2017). Because of the shorter fermentation time (84h vs 168h), the productivity was higher than our study (0.31 g/L.h vs 0.14 g/L.h), but lower xylitol yield (0.55 g/g vs 0.87 g/g).

Table 4.4. Xylitol concentration, xylitol yield and productivity of different conditions

Experiments	Carbon source	Nitrogene source	Xylitol concentration (g/L)	Yield (g/g)	Productivity (g/L.h)
250 mL, no air	Commercial sugar (30 g/L xylose, 2 g/L glucose)	Yeast extract (5.0 g/L), peptone (3.0 g/L), $(NH_4)_2SO_4$ (2.0 g/L)	25.84	0.86	0.2
250 mL, no air	Sugars from bagasse (30 g/L xylose, 2 g/L glucose)	Yeast extract (5.0 g/L), peptone (3.0 g/L), $(NH_4)_2SO_4$ (2.0 g/L)	23.45	0.81	0.17
250 mL, no air	Sugars from bagasse (30 g/L xylose, 2 g/L glucose)	WCN-07 Plus (3 g/L)	22.52	0.85	0.16
5 L, turn off air after 48h	Sugars from bagasse (30 g/L xylose, 2 g/L glucose)	WCN-07 Plus (3 g/L)	7.34	0.82	0.05
5 L, high oxygen concentration	Sugars from bagasse (30 g/L xylose, 2 g/L glucose)	WCN-07 Plus (3 g/L)	15.23	0.62	0.10
5 L, 1% oxygen	Sugars from bagasse (30 g/L xylose, 2 g/L glucose)	WCN-07 Plus (3 g/L)	23.88	0.81	0.19
500 L, >20 oxygen	Sugars from bagasse (30 g/L xylose, 2 g/L glucose)	WCN-07 Plus (3 g/L)	6.35	0.28	0.17
500 L, 1% oxygen	Sugars from bagasse (30 g/L xylose, 2 g/L glucose)	WCN-07 Plus (3 g/L)	23.34	0.87	0.14

When replacing the commercial xylose with XBS in a 250 mL flask, we noticed a decrease in xylitol concentration, yield and productivity. The concentration of xylitol formed decreased from 25.84 to 23.45 g/L; yield decreased from 0.86 g/g to 0.81 g/g, productivity decreased from 0.2 g/L.h to 0.17 g/L.h. This has been explained above because the XBS contains inhibitors, which cause high osmotic pressure. Even so, that decline was acceptable to replace low-cost carbon sources to protect the environment.

When the fermentation volume was expanded from the 250 mL flask to 500 L bioreactor, using alternative nitrogen sources and 1% DO, xylitol concentration and yield decreased. Specifically, the xylitol and productivity decreased from 23.88 g/L, 0.19 g/L.h at 5 L bioreactor to 23.34 g/L, 0.14 g/L.h at 500 L bioreactor. However, xylitol yield increased from 0.81 g/g to 0.87 g/g. This makes economic and technological implications. In economic terms, a high yield will improve the amount of recovered products, reducing product costs. In terms of technology, high yield means fewer impurities ratio, downstream purification process was done more smoothly. Thereby we can conclude that scale up xylitol fermentation was successful at pilot scale.

4.4 Purification of xylitol from fermentation broth

At the end of the fermentation, the fermentation broth was pasteurized at 90°C for 15 minutes to suspend the yeast activity. The purification process then begins with the use of a membrane filtration system to remove cells and polymeric compounds. The membrane system includes microfiltration, ultrafiltration, and nanofiltration. After that, the fermentation broth was purified by removing ions with electrodialysis, resin, and short path distillation before concentration to crystallize xylitol crystals.

4.4.1 Purification of fermentation broth by membrane filtration

To separate cells, and polymeric compounds from fermentation broth, we can use centrifugation or filtration method. In this work, membrane filtration technique was employed to clean fermentation broth because the device can operates continuously, is easy to operate and has the ability to remove cells thoroughly. In this process, fermentation broth was passed through three membrane filtration systems: microfiltration (MF), ultrafiltration (UF) and nanofiltration, respectively. The MF and UF systems are operated by high-pressure pumps, maintaining a steady inlet pressure at 6 bar. The 4 columns filters are divided into 2 groups working at the same time, the total working area of the filter is 36.2 m². The UF system is operated by two high-pressure pumps, the working pressure is maintained at 8 bar, the membrane area was the same with MF. The NF system is operated by two high-pressure pumps. The first pump pressurizes the flow up to 8 bar, and the second pumps the flow pressure to 25 bar before entering the membrane system. The change of sugar concentration, pH, conductivity as well as the change of permeate flux is shown in the graph in Fig. 4.18.

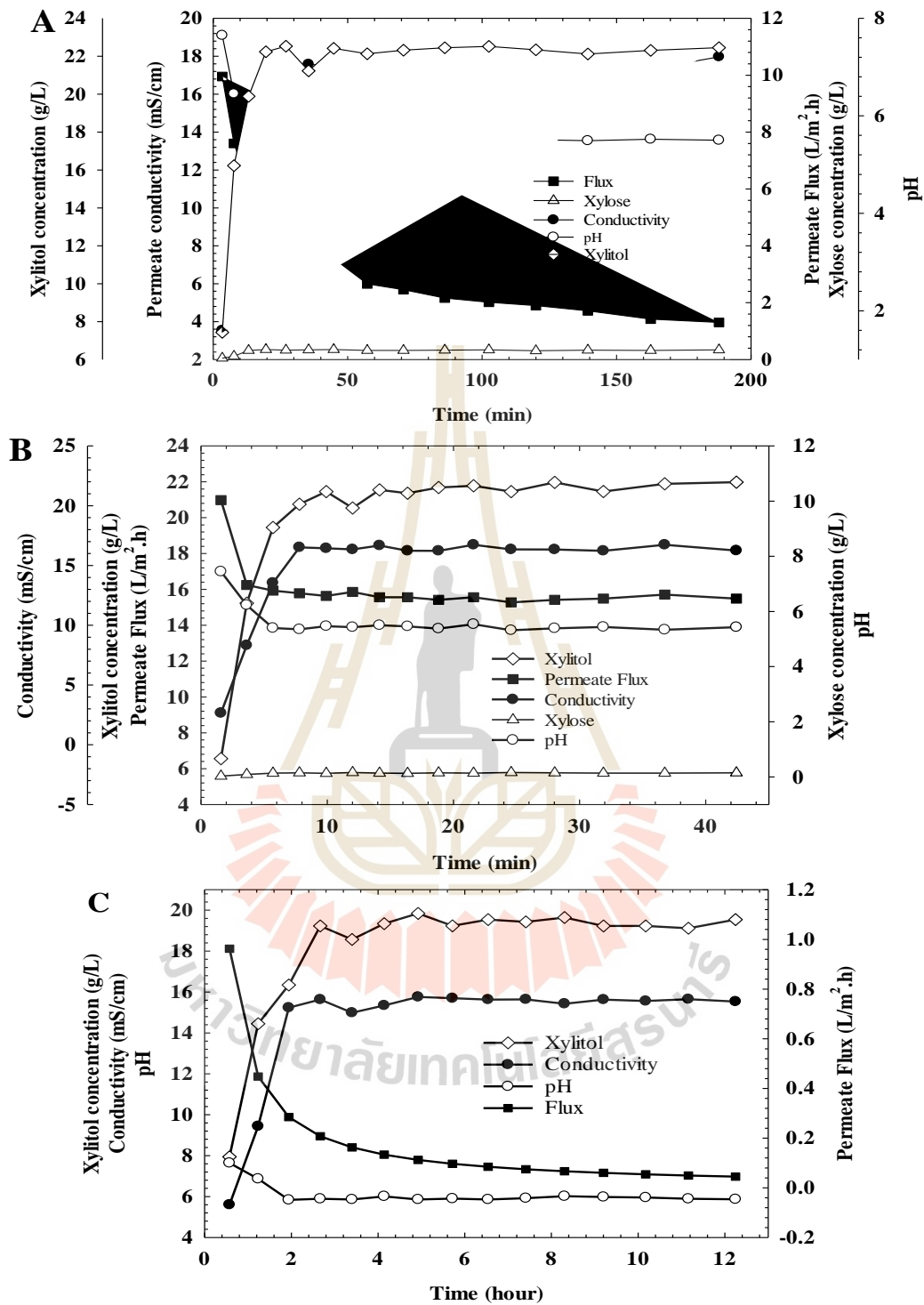**Figure 4.17** The MF, UF and NF experiments to purify the fermentation broth

Figure 4.18 Change in the flux, sugar concentration, conductivity and pH of permeate

during the MF, UF, NF (A-Microfiltration, B-Ultrafiltration, C-Nanofiltration)

We must ensure that the membrane temperature is less than 35 °C to avoid damaging the membrane life. Therefore, the cooling system has been used to reduce the temperature of the system when the pump is running for a long time, especially with NF. Total usage times (for 300 L of permeate) of MF, UF, and NF were 190 minutes, 42 minutes and 734.4 minutes, respectively. All 3 systems MF, UF, NF showed low initial sugar concentration, conductivity, then increased and stabilized after 2-3 sampling times (40-60 liters of permeate). Specifically, the concentration of xylose increased from 0.05 g/L to 0.32 g/L after 13.13 minutes, 0.03 g/L to 0.17 g/L after 5.7 minutes in MF and UF systems. Xylitol concentration increased from 7.43 g/L to 22.24 g/L; 6.56 g/L to 20.75 g/L; 7.94 to 19.23 in MF, UF, and NF maintained during filtration. The low initial sugar concentration was explained because in the early stages there is still a certain amount of RO water in the membrane after the cleaning process. Therefore, fermentation broth has been diluted with water, at this time the membrane has not come into full contact with fermentation broth. After stable operation, the membrane is in full contact with the real solution, then the sugar concentration in the permeate increases. This law also holds true for conductivity when at first time, conductivity value was low, then increases rapidly to equilibrium with fermentation broth. Specifically, conductivity increased from 3.54, 2.65, 5.6 mS/cm to 17.97, 16.25, 15.53 mS/cm in MF, UF, NF respectively. Although conductivity decreases through MF, UF, and NF processes, it decreased not too much. This can be explained because the solution is diluted with water after each entry into the above systems. The above results also showed that the ions cannot be eliminated through the membrane filtration systems. Therefore, to purify xylitol we need to use additional techniques. The quantity used to evaluate the film efficiency is flux, expressed as 1 volume unit of permeate passing through the membrane per 1 m^2 surface for 1 h. This

value depends on the pore size, operating pressure...When the above quantities were fixed, the flux depends on the concentration and molecular weight of substances contained in the retentate. On the graph in Fig. 4.18 we see that in MF and NF, permeate flux decreases with time. With MF, the flux was initially 9.95 $L/m^2.h$ but then gradually decreased with time. After 120 minutes, the flux dropped to 1.89 $L/m^2.h$ and continued to decrease for the next time. With NF, despite the high inlet pressure (25 bar) but the flux permeate is very low (starting with 0.96 $L/m^2.h$), long filtration time (more than 12 h) and ending with flux 0.045 $L/m^2.h$. The reason for the small flux value, the long filtration time is because the membrane pore size in NF is very small, passing through only molecules smaller than 700 Da. In addition, as the process progresses, the high concentrations of polymers in the retentate cause a blockage on the membrane surface, reducing the membrane performance. As mentioned above, during operation, the temperature of the solution should be maintained below 35 ^{o}C to avoid damaging the membrane. However, for the NF experiment, we maintained the solution and membrane temperature less than 15 °C to limit xylitol loss by microorganisms. Shorter UF time (42 min for 300 L) showed high flux permeate, starting at 20.89 $L/m^2.h$ then decreased and maintained at 15 $L/m^2.h$ until the end. The filtration time of UF is short because then fermentation broth has passed through MF and the UF membrane size is large (> 3000 Da), most compounds can pass through UF except for color compounds with large molecular weight. It is also demonstrated through the decreased IU color index after passing through the UF system.

There are many methods of single or combination removal and purification of xylitol. For example, cation exchange resins were used to separate xylitol by interacting with weak acidic hydroxyl groups and cations such as calcium, followed

by a low-temperature crystallization of the xylitol-rich solution (Jandera 1974). However, impurities such as proteins, carbohydrates, microorganisms, and low levels of xylitol in the broth is a big challenge to the purification. At that time, using membranes was considered energy efficient and of high purity. The membrane technique can be used to purify xylitol in fermented broth with nanofilm with cross-flow, reverse osmosis membranes. Cross-flow filtration allows the liquid to flow parallel to the membrane in order to limit the fouling of the membrane surface. Accordingly, the polysulfone (10 kDa) membrane proved to be the most effective for separating and recovering xylitol. The membrane allows 82.2-90.3% xylitol in fermentation broth to pass through and retain 49.2-53.6% of impurities such as peptides and oligopeptides. The permeate obtained after concentration has been crystallized to form crystals of 90.3% purity (Affleck 2000).

Operating pressure can also affect the filtration process as the molecular weights of the components to be separated are nearly equal. The low operating pressure allowed smaller molecules such as xylose and arabinose to pass through the membrane, while the xylitol was retained. Faneer et al. (2017) operated the filter at high pressure so that the xylitol had to pass through the membrane along with other sugars. Accordingly, the operating pressure from 4-10 bar used with different xylitol concentrations from 19.0-88.0 g/L. Accordingly, high operating pressure can clog membranes, resulting in reduced filtration efficiency. Therefore, a 4 bar operating pressure was chosen to purify xylitol out of the mixture (Faneer, Rohani *et al.* 2017). In this study, we adjusted the operating pressure of MF, UF, NF to 6, 8, and 25 bar respectively to ensure the efficiency of filtering impurities while maintaining permeate flux at an acceptable level. Desiriani (2017) demonstrated that the combination of 2 phases UF and NF has brought great promise in downstream processing xylitol from fermentation. Accordingly, UF has

removed 99% of biomass cells (microscopic analysis showed no cells). NF shows a high (90%) xylitol retention at a low 1.5 bar operating pressure. Although the high pressure produces a higher permeate flux, however, the flow rate of the permeate flux decreases over time due to due to concentration polarization and fouling obstruction in the UF and NF membranes (Desiriani, Made Tri Ari Penia Kresnowati *et al.* 2017).

To increase xylitol yield during fermentation, membrane techniques including UF, NF were performed for xylose purification after hemicellulose hydrolysis. Guirimand et al. (2016) have been successful in purifying hydrolysates from straw. The hydrolyzate increased the xylose concentration to 59.3 g/L, glucose 48.7 g/L and decreased the concentration of inhibitors such as acetate (7.23 mM), furfural (0.23 mM) and 5-HMF (0.11 mM). The mixture was then used to ferment to form xylitol (Guirimand, Sasaki *et al.* 2016).

Cerceau et al. (2021) fermented xylitol from bagasse hydrolysis, then selected 4 nanofiltration membranes for xylitol purification. The membrane material used is NF (polypiperazine amide), NF90 (fully aromatic polyamide), and NP010 and NP030 (polyethersulfones). As a result, NF had the lowest fouling tendency, the highest xylitol/protein cleavage coefficient, and the color parameter a* improved significantly[1]. The best operating pressures were 40 bar, 40 °C, and pH 5.4. The result with a xylitol purification factor of 3.3, protein separation factor of 8.4, and color removal of 96.0% were achieved. This study concludes that nanofiltration can be used as an effective step to purify xylitol obtained from sugarcane bagasse hydrolysate (Cerceau Alves *et al.* 2021).

Our results as well as other publications have shown the effectiveness of using the membrane in the purification of xylitol. However, after the application of the

membrane system, there is still a major challenge that is the high salt concentration in the solution. That leads to the need to apply other techniques to obtain purer xylitol. The methods we use next are electrodialysis and resin absorption.

4.4.2 Purification of fermentation broth by electrodialysis

Electrodialysis (ED) is a membrane separation process based on ion exchange (IE) membranes. Ionic compounds are transported from one solution to another under the influence of an applied potential difference. An ED cell consisting of an anion exchange membrane (AEM) and a cation exchange membrane (CEM) is alternately arranged between the positive and negative electrodes. Diluents and concentrates move between the two membranes. When an electrical current field is applied, cations move towards the cathode, traverse CEM but are blocked by AEM. Similarly, the anions travel back to the anode, pass through AEM but are blocked by CEM. As a result, the ions are concentrated in the concentrated stream, the dilution current is reduced ionic compounds. ED was widely used in water treatment, softening, and food processing (Wang, Jiang *et al.* 2019).

The electrodialyzer DW-Lab from Japan was used to remove salt and other charged components from the solution to increase the purification of xylitol. When the ED system is active, the amperage is the driving force that determines the speed of ions transport across the membrane. However, too high amperage will lead to water splitting into H^+, OH^- ions. Limiting current density (LCD) is called the amperage suitable for ED operations. The electrodialyzer needs to be operated at this amperage. LCD value is found through the relationship between current and voltage across the membrane when running with real solution.
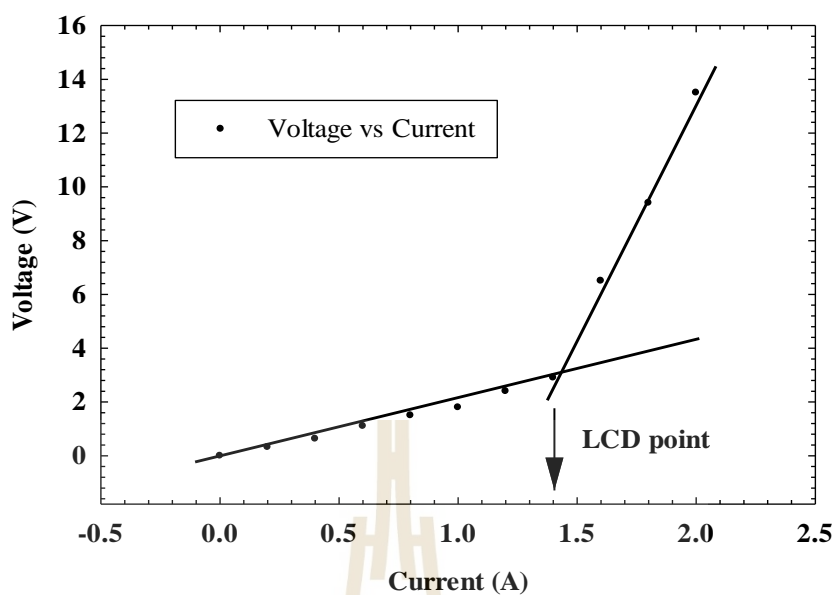
Figure 4.19 Characteristic of current - voltage density in ED membrane

Through Fig. 4.19, LCD determined by slowly increasing the current from 0 to 2 A/m^2. Then, use a voltmeter to record the voltage across the membrane. When current increases, two regions are formed with different rates of voltage rise. The voltage increases gradually in the first region (when the current increases from 1-1.4 A/m^2, the voltage increases from 0-2.3 V) and increases faster in the 2nd region (when the voltage increases from 1.4-2 A/m^2, the voltage increased from 2.3 to 14 V). Based on the graph, we can determine the LCD value for active ED is 1.4 A/m^2, then the transport of ions will prevail. In addition, the LCD value is also recommended by the manufacturer for the membrane to have a longer service life.
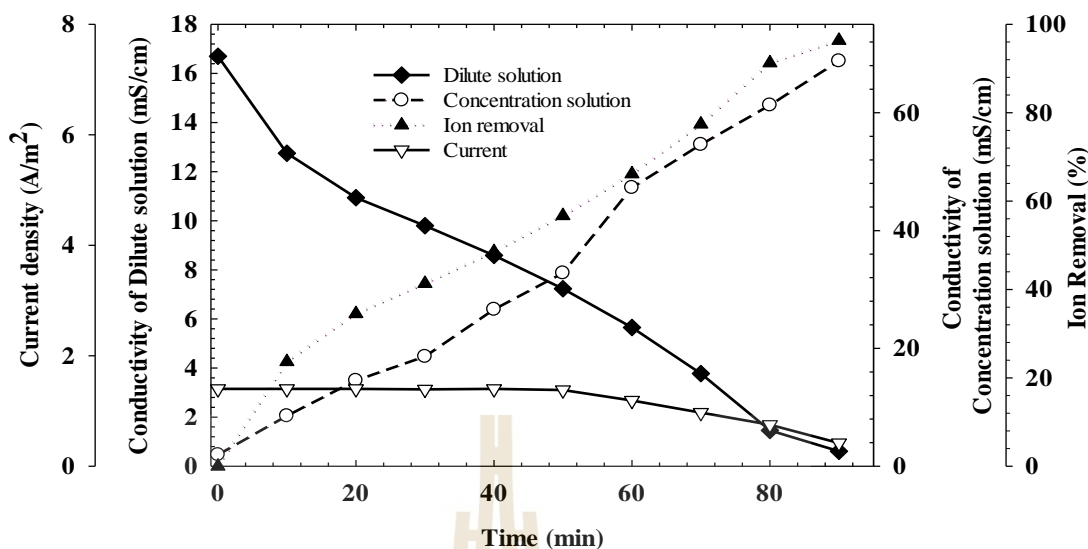
Figure 4.20 Ion concentration profile of fermentation broth by ED

The method of hydrolysis of bagasse by NaOH then neutralization with HCl generates a large amount of salt in the solution, causing high conductivity of fermentation broth. In which, mainly the existence of ions Na^+ and Cl^-. The change of conductivity and ion removal is shown in Fig. 4.20. Under the effect of electric current, dilute solution conductivity (after membrane filtration) decreased overtime after 90 minutes from 16.7 mS/cm to 0.61 mS/cm. Meanwhile, concentrate solution conductivity (NaCl solution) increased from 1.95 mS/cm to 68.8 mS/cm. This shows that ions have moved from solution after filtration to NaCl solution and reduce conductivity. After 90 activities, ion removal reaches 96.34%, the conductivity of dilute solution is 0.61 mS/cm, compared with normal water is 0.35 mS/cm. During operation, current decreased gradually with the decrease of conductivity of dilute solution, current decreased from 1.4 A/m^2 to 0.42 A/m^2.

The use of membrane combination UF and EDI (electrodeionization) was reported by Kresnowati (2019) in the purification of xylitol from fermentation. After the

UF, the fermentation solution was entered into the EDI system with optimal parameters current 22.5 A/m^2 respectively, concentration and dilution flow rates 0.4 and 0.5 m/s. This UF-EDI technique has removed 99% of biomass, 99% of pigmentation, > 46% xylose, > 99 ions, respectively. Xylitol losses was about 30-50%. The report confirmed that the UF-EDI technique performed better than other xylitol purification methods (Kresnowati, Regina *et al.* 2019).

In this study, although the solution obtained after ED has relatively low conductivity (0.61 mS/cm), however with low xylitol concentration (~ 20 g/L), it is necessary to concentrate to perform crystal. That also makes conductivity increase again and make it difficult for xylitol crystallization. In addition, ED is not an effective method of color separation (compared to EDI), so the syrup after concentration has a dark color, demonstrating more color impurities. We concentrated xylitol after ED with rotary evaporator to Bx 70, then crystallized by adding ethanol and maintained temperature of -20 ^{o}C overnight. As a result, the number of crystals formed is very small, dark in color, and has a salty taste (Fig. 4.21). Since then, we have experimented with the ion resin absorption technique to compare the xylitol purification efficiency.

Figure 4.21 Xylitol crystallization from syrup after ED

4.4.3 Purification of fermentation broth by ion exchange resin absorption

The operation diagram of the ion exchange resin system is arranged as in Fig. 4.22. In which, high conductivity xylitol solution was pumped from bottom to top into column A containing resin DOWEX 66 (weak base anion), after going through column A, solution was entered into column A containing resin DOWEX 88 (strong acid cation). A and B are fabricated steel columns 120 cm long and 6 cm diameter. The flow rate is 4 L/h (equal to 2 times the volume of resin in the column: flow rate = 2BV). After leaving the cation column, the solution returns to the container and continues the second cycle. The process repeated until the measured conductivity value is constant.
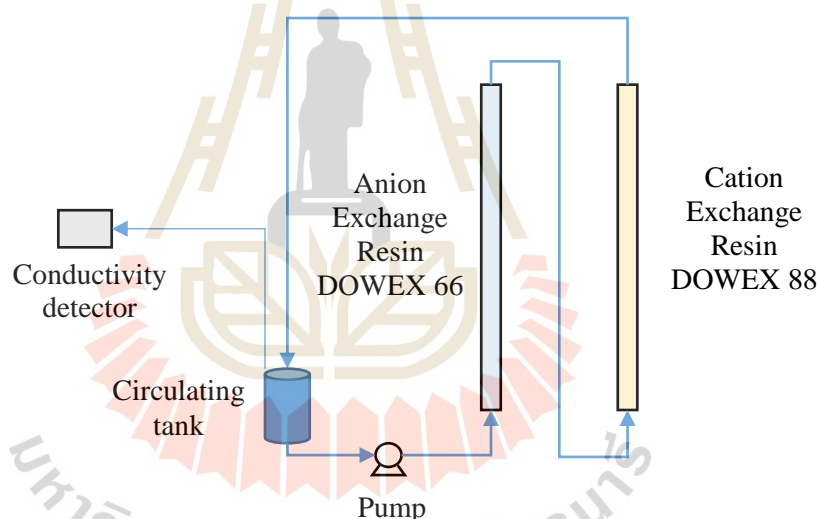

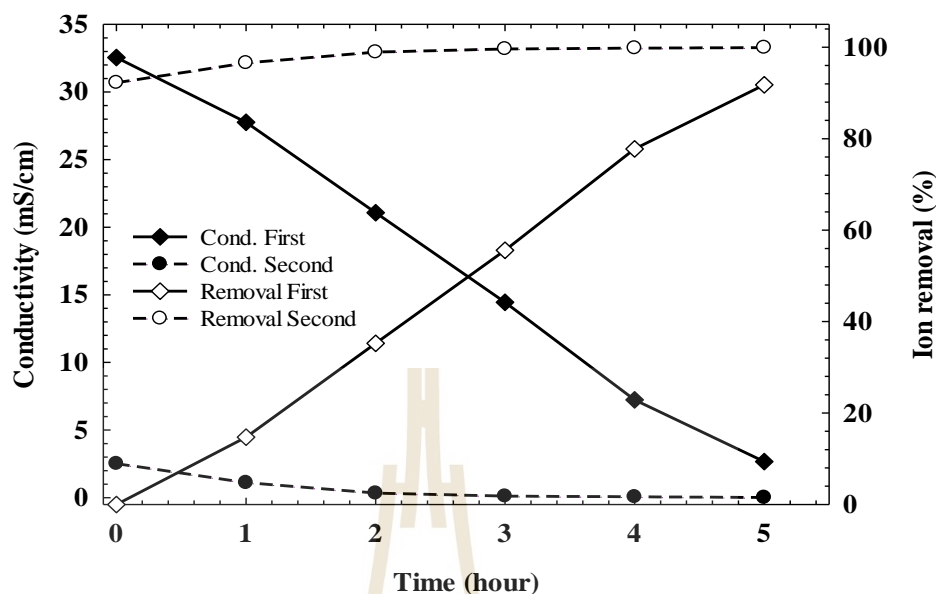**Figure 4.22** Diagram of ion exchange resin experiment

Figure 4.23 Ion concentration profile of fermentation broth by ion exchange resin

It is necessary to treat the solution with 2 times the resin to achieve the desired effect because the salt concentration in the solution is high. Between 2 treatments, the resin is regeneration with NaOH (4%) and HCl (2%) then rinsed with RO water. When processing resin for the first time, conductivity decreased from 32.55 to 2.67 mS/cm, reaching 91.79% efficiency. The second resin decreased conductivity from 2.52 to 0.017 mS/cm, reaching 99.94% efficiency. This is a very low conductivity value when compared to RO water (conductivity 0.008-0.012 mS/cm). It has been shown that exchange resin ions are very effective in removing salt from xylitol solution. In addition, with the pore-shaped structure, the resins are also able to absorb color compounds effectively (the results of the change in the color index will be discussed later).

The ion exchange resin is widely used to purify hemicellulose hydrolysates to remove inhibitors, increase the xylose concentration to perform the fermentation process. In addition, ion exchange resin is also used in xylitol purification

in fermentation broth to increase purity. Canihal (2008) used two types of anion exchange resins A-860S and A-500PS to clean hydrolyzate from wheat straw. As a result, 95% of the abrasive compounds, acetic acid, and lignin derivatives are removed. After fermentation, removing the cells, the fermentation broth was concentrated 40 times (726 g/L) and crystallized by cooling with ethanol combined with addition of crystal germ. Crystallization efficiency is 43.5% (Canilha, Carvalho *et al.* 2008).

Martínez et al. (2007) tested a combined treatment with resins and crystallization as processes for xylitol purification and found better results. In that study, xylitol was obtained for fermentation of sugarcane hemicellulosic hydrolysate. Before the crystallization stage, the fermented broth was centrifuged, filtered, treated with cation and anion resins and concentrated. Crystallization was performed twice (initially 10 °C and after 2.5 °C) and pure crystals (92–94%) were obtained (Martínez, de Almeida e Silva *et al.* 2007).

Glass column 50 cm long, 2.5 cm diameter with 30 mL strong cation-exchange resin (FLC-10) chelated Ca^{2+}, flow rate 0.5 mL/min was used for xylitol purification. The Ca^{2+} resin that absorbed xylitol and other sugars were passed through the column. After equilibrium absorption, xylitol was washed with eluate to recover xylitol. Then, resin 732 and D301 was used to desalinate the xylitol solution. The 70% salts were desalted and the decolored ratio reached 98%, and 5.5 BV of the sample was treated. The loss ratio of xylitol could be kept at an acceptable level using the two resins in series, which allowed by-products removal (Wei, Yuan *et al.* 2010).

Although it has been proven that ion exchange resin is highly effective in desalting and removing color compounds, it depends on the resin type. In 1995, Gurgel et al. used a strong cation-exchange resin (Amberlite 200C) and a weak anion-exchange

resin (Amberlite 94S) to purify the xylitol after it was treated with coal. The results showed that, compared with activated carbon, ion exchange resin did not have a negligible effect on xylitol purification process. The xylitol/dry weight ratio was the same before and after the ion exchange treatment (Gurgel 1995).

Comparing with previous publications shows that our results are better with salt removal rate in xylitol solution up to 99.94%. In addition, the results of decolorization are also very positive. This has increased the purity of xylitol, which facilitates the subsequent crystallization process.

The change in color of xylitol solution was also assessed by ICUMSA Color (IU) value measured at 420 nm (Fig. 2.24). The change of ion concentration, decolorization rate, xylitol loss was showed in Table 4.5.
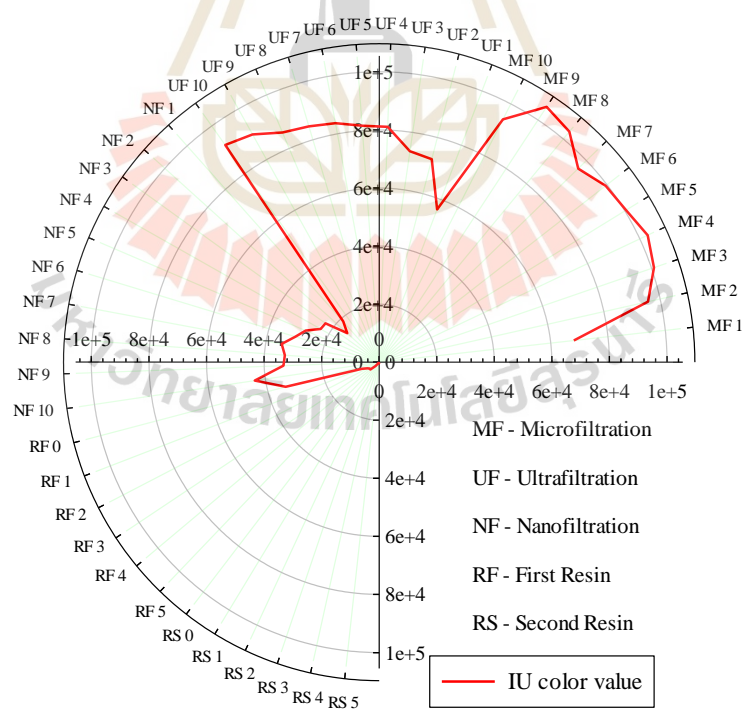

Figure 4.24 The change of IU value during processing

Table 4.5 The change of ions concentration, decolorization rate and xylitol loss during

processing

Experiments	Decolorization rate (%)	Xylitol loss* (%)
MF	3.37	9.33
UF	19.89	4.69
NF	71.75	14.04
Total loss compared with fermentation broth		25.73
First Resin	95.23	4.3
Second Resin	99.63	6.89
Total loss of 2 times Resin		10.9

* Compared with before process

Fig. 4.24 shows the change of IU value through different processes from MF, UF, NF and 2 times of resin. After each treatment, we can clearly see that the lower the IU value and get closer to the center of the graph. Specifically, the average IU value of MF of 96627.04 has decreased to 80110, 28241, 4767, 363 in UF, NF, first resin and second resin respectively. IU value decreased slightly from MF to UF (decolorization rate from 3.37% to 19.89%). However, the decolorization rate increased to 71.75% after NF treatment. This shows that NF is very good at removing color compounds because of the small membrane size. The resin treatment has shown a very high decolorization efficiency with 95.23% at the first resin and 99.62% at the 2nd resin. We can notice the difference in color of xylitol solution through the process is different in Fig. 4.25.

Table 4.5 showed the xylitol losses in the processes. Accordingly, losses of MF, UF, NF processes were 9.33, 4.69, 14.04% respectively compared to the previous process. The total xylitol losses after membrane filtration compared with fermentation broth were 25.73%. After nanofiltration, xylitol is concentrated by a falling film evaporator system. Then desalinate with ion exchange resin. The losses of this submission are assessed individually. The loss of xylitol after resin the first was 4.3%, the second resin is 6.89% compared to the first time. The total xylitol loss of the whole

desalination was 10.9%. In previous publications, xylitol loss rates have also been mentioned. The xylitol loss was 8.15% (Mussatto, Santos *et al.* 2006), 15.23% (Martínez, de Almeida e Silva *et al.* 2007), 21.1% (Canilha, Carvalho *et al.* 2008), 22.56% (Misra, Gupta *et al.* 2011), 30-50% (Kresnowati, Regina *et al.* 2019), 59.49% (Silva, Dussán *et al.* 2020).
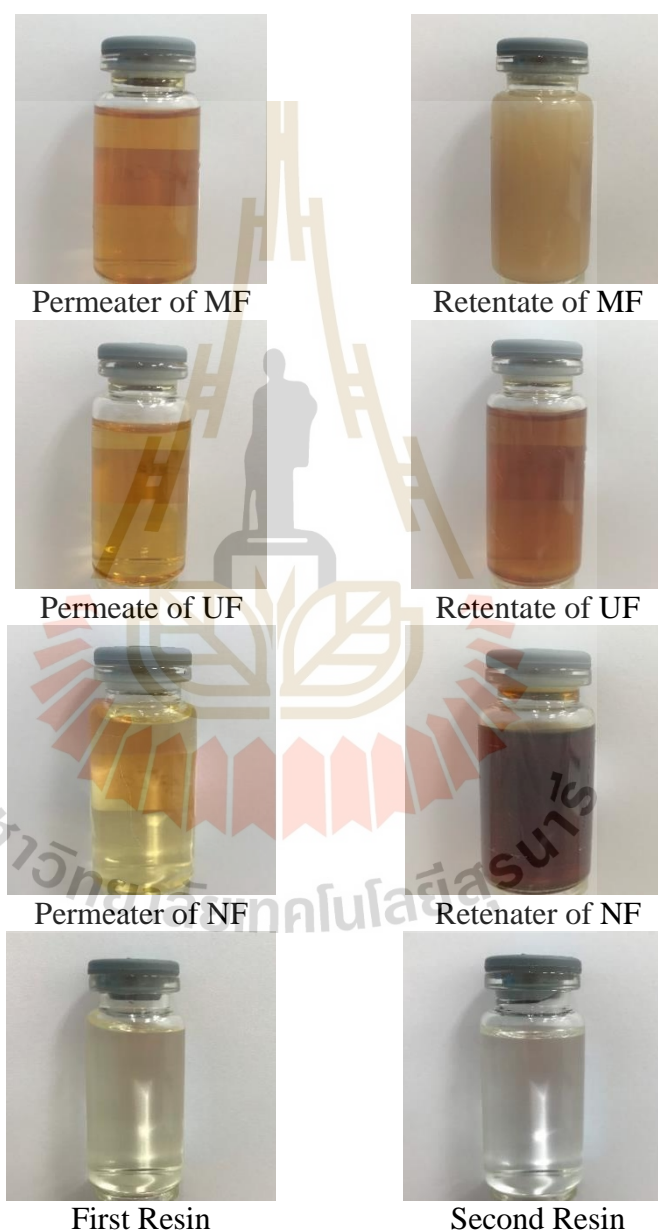

Permeater of MF	Retentate of MF
Permeate of UF	Retentate of UF
Permeater of NF	Retenater of NF
First Resin	Second Resin

Figure 2.25 The change color of xylitol solution during the processing

4.4.5 Purification of xylitol from fermentation broth using crystallization

Crystallization is considered the last and most important step in the downstream processing of xylitol. Crystallization is the process by which molecules link together to form highly organized structures called crystals. This process is only possible when the purity of the solution is high, with few impurities. After crystallization, high purity and solid state make the product easy to preserve and commercialize.

In this study, after desalination and decolorization, xylitol was concentrated into syrups with different Bx to perform the crystallization experiment. Bx values were changed to investigate the crystallization process as Bx 70, 75, 80 (B70, B75, B80), commercial xylitol Bx 70 (C70) was done at the temperature adjustable reactor. 300 mL of syrup was added into the crystallizer. At the beginning of the crystallization process, the temperature was maintained at 60 °C to ensure the solubility of xylitol. Then reduce the temperature at a rate of 2 °C/min to 1 °C. At low temperature, the solubility of xylitol decreases, when it reaches the supersaturation state, xylitol crystals form. The nucleation method used is natural nucleation and artificial nucleation with 1% (w/v) xylitol crystal. During the crystallization process, modern world-class measuring instruments are used to record the data every 10 seconds. Fig. 4.26 depicts the design of xylitol crystallization experiment with Raman spectroscopy, FBRM (Focus Beam Reflectance Measurement), PVM (particle vision and measurement) devices. Raman spectroscopy showed the chemical structure change of xylitol during crystallization, FBRM showed the analysis of crystal particles (number and size), PVM detects the crystalline particles formed, the shape of the crystal. (Muller Molnar, Berghian-Grosan *et al.* 2020).
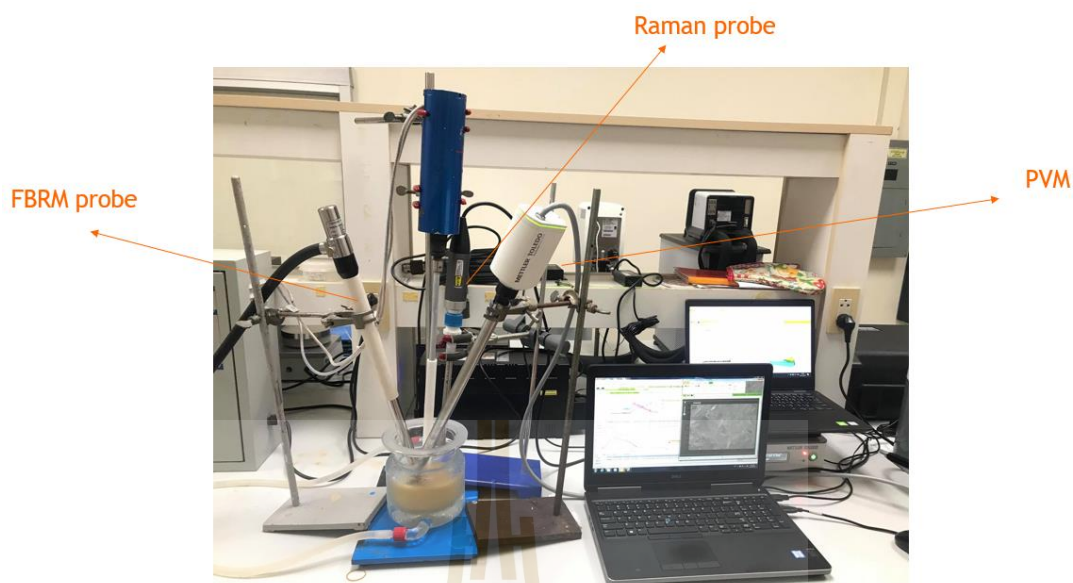
Figure 4.26 Experimental setup for the crystallization process of xylitol crystals in crystallizer using in situ Raman, FBRM and PVM probes

1. Crystallization experiment with xylitol B70, no seeding

The results of xylitol B70 (no seeding) crystallization experiment were shown in Fig. 4.27, table 4.6, Fig. 4.28 and Fig. 4.29, respectively.
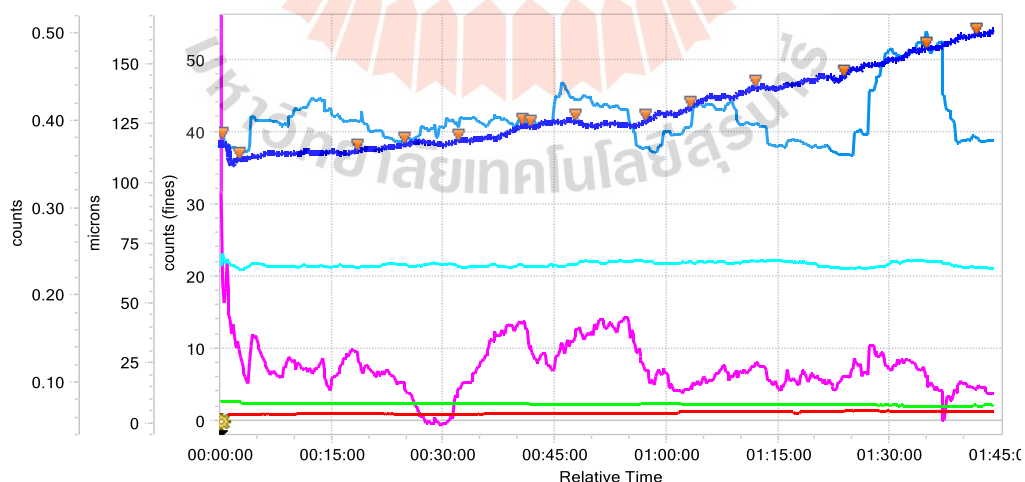

Figure 4.27 Trend of number and crystals size during the crystallization with 70Bx xylitol without seeding.

Table 4.6 Average number and size of crystals during the crystallization with 70Bx

xylitol without seeding

| Trend	Line Color	60 °C 0 min	50 °C 19 mins	40 °C 33 mins	30 °C 48 mins	20 °C 64 mins	10 °C 85 mins	1 °C 102 mins
Counts <50		35.69	37.23	38.72	41.38	43.19	47.47	53.34
Mean <50		8.43	8.03	8.05	7.53	7.64	7.41	7.1
Counts 50-100		0.774	0.895	0.753	0.899	1.07	1.21	1.08
Mean 50-100		65.62	64.99	65.31	66.18	67.41	64.14	65
Counts100-1000		0.152	0.136	0.0928	0.148	0.0919	0.106	0.093
Mean 100-1000		115.13	126.46	123.42	135.43	123.25	112.12	117.41
Counts >1000	-	N/A	N/A	N/A	N/A	N/A	N/A	N/A
Mean >1000	-	N/A	N/A	N/A	N/A	N/A	N/A	N/A
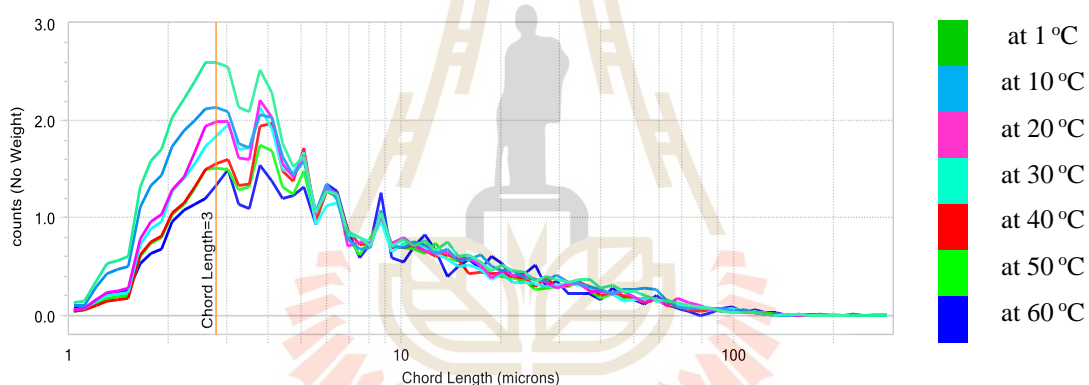
Figure 4.28 Particle size distribution (PSD) of crystals during the crystallization with

70Bx xylitol without seeding

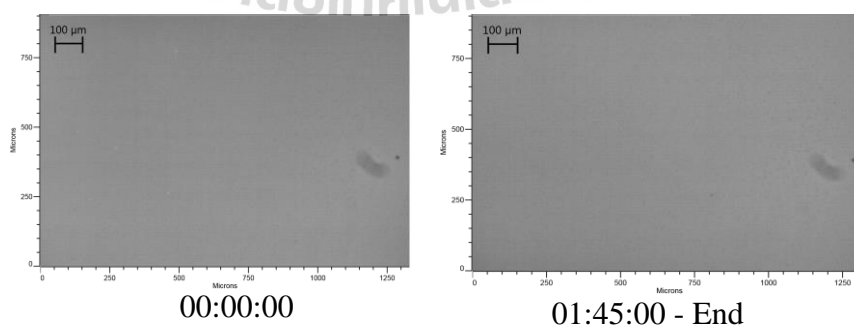00:00:00   01:45:00 - End

Figure 4.29 PVM images taken at different times during the crystallization with 70Bx

xylitol without seeding

Fig. 4.27 showed the growth trend in crystal number and average size (<50 µm, 50-100 µm, 100-1000 µm). When reducing the temperature from 60 ^{o}C to 1 ^{o}C in 1 h 45 minutes, the crystal group <50 µm has 35-53 particles, the average size of 7.1-8.42 µm. The crystals group of 50-100 µm has numbers ranging from 0.7-1.2 particles, average size of 64-67 µm. The crystals group of 100-1000 µm has numbers ranging from 0.09-0.15 particles, the average size is 118-135 µm. Although the presence and increase in the number (very small) of crystals (group <50 µm) were noted, PVM did not record the presence of crystals before and after the experiment. This shows that at xylitol B70 no seeding, the crystallization process did not create xylitol crystals. This can be explained because the solution is not super-saturated to nucleate crystals naturally.

2. Crystallization experiment with xylitol B70, seeding with 1% (w/v) of xylitol crystal

To nucleate new crystal formation, we added xylitol crystals at a ratio of 1% (w/v) at 40 ^{o}C to the crystallizer. This process will motivate the crystallization process at low temperature. The results of xylitol B70 with seeding 1% crystallization experiment were shown in Fig. 4.30, table 4.7, Fig. 4.31 and Fig. 4.32, respectively.
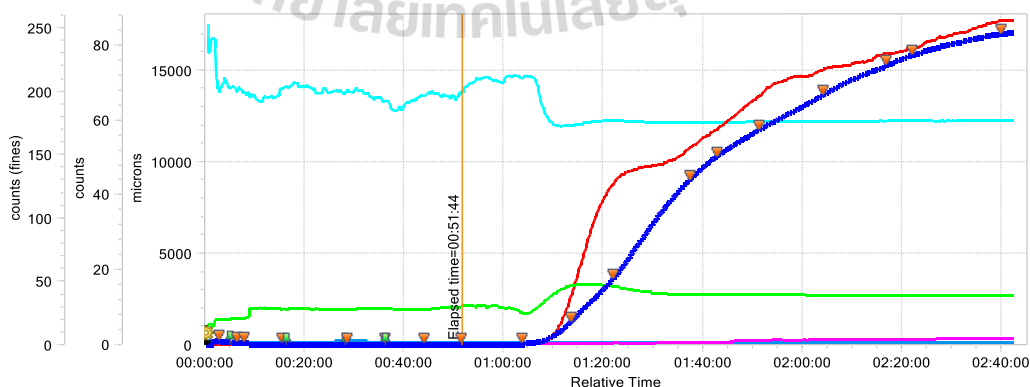

Figure 4.30 Trend of number and crystals size during the crystallization with 70Bx xylitol with seeding 1%

Table 4.7 Average number and size of crystals during the crystallization with 70Bx

xylitol with seeding 1%

Trend	Line Color	60 °C 0 min	50 °C 18 mins	40 °C Seeding 32 mins	30 °C 48 mins	20 °C 63 mins	10 °C 84 mins	1 °C 102 mins	End
Counts <50		66.88	18.86	15.96	3404.54	9827.21	12217.87	15614.75	17351.7
Mean <50		6.66	9.72	10.07	15.86	13.23	13.26	12.89	12.83
Counts 50-100		0.39	0.39	0.41	134.58	159.64	200.91	235.22	261.64
Mean 50-100		58.74	64.89	66.79	59.61	59.04	59.38	59.46	59.99
Counts 100-1000		0	0.17	0.162	0.22	0.97	0.39	2.08	1.08
Mean 100-1000		NaN	153.38	156.03	101.72	108.29	110.62	117.4	105.66
Counts >1000		N/A	N/A	N/A	N/A	N/A	N/A	N/A	N/A
Mean >1000		N/A	N/A	N/A	N/A	N/A	N/A	N/A	N/A

Fig. 4.30 and Table 4.8 show the trend of crystals during crystallization. Before seeding, particles <50 µm with numbers ranging from 15.96-66.88 particles, no crystals recorded at PVM. However, after seeding crystals at 40 °C and reducing the temperature to 30 °C, the number of crystals increased to 3,404.54, then increased to 17,351.71 crystals at the end of the process. It showed stability of crystals after 2 h and 40 minutes when no new formation was noted. The average size increased from 6.66 µm to 15.86 µm. Similar to above, the particles in the 50-100 µm group had numbers 0.39-0.4 (have no crystals), then increased to 134 seeds at 30 °C, ending with 261.64 crystals with an average size of 59.99. This suggests that there is a bond between the small crystal seeds to form large crystals. The results also indicated that there was no formation of crystals 100-1000 µm in size during the crystallization process.
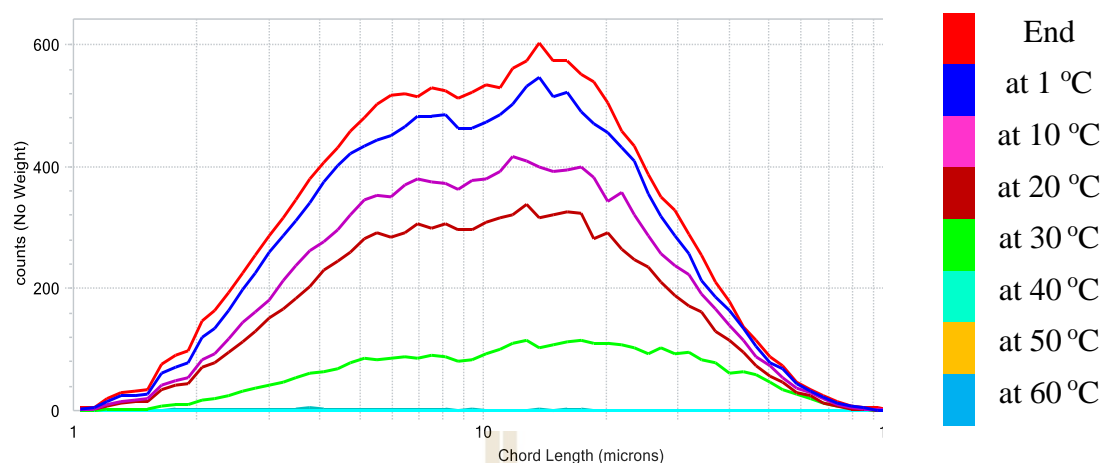
Figure 4.31 Particle size distribution (PSD) of crystals during the crystallization with 70Bx xylitol with seeding 1%
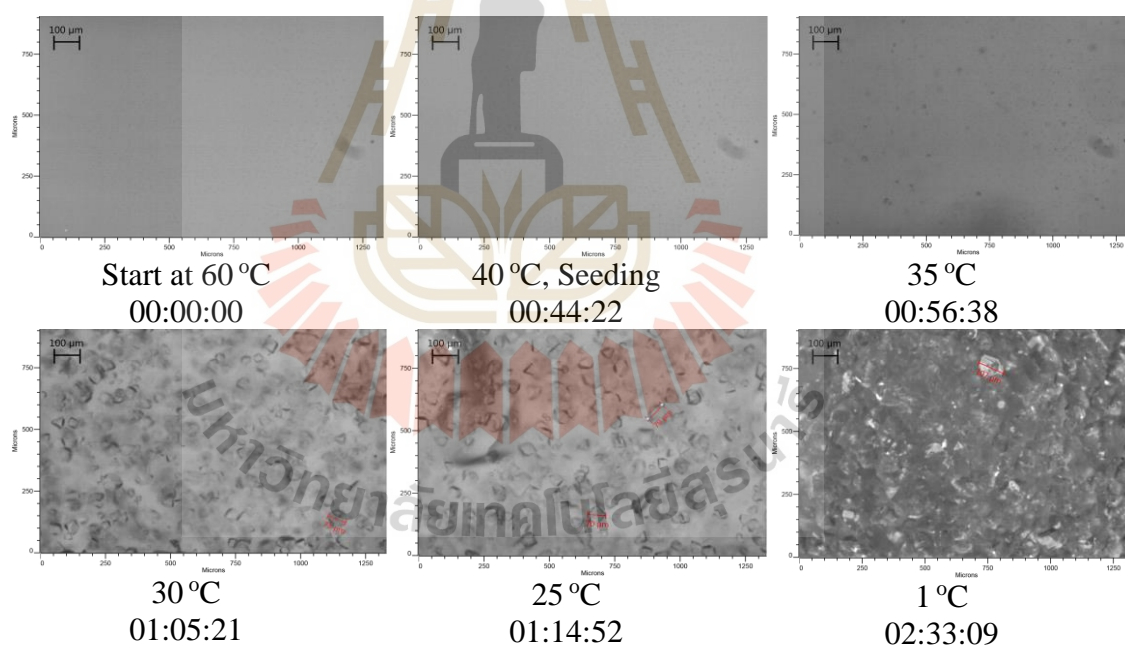

Figure 4.32 PVM images taken at different times during the crystallization with 70Bx xylitol with seeding 1%.

Fig. 4.31 showed the PSD of the crystals during the crystallization process. We can see a change in the PSD line after seeding and reducing the temperature

from 40 °C to 30 °C. At 60-40 °C the SPD line almost touches the horizontal axis (0 µm), but then crystals are formed and rapidly increase in number, especially the group of crystals <50 µm. Fig. 4.42, PVM also clearly shows the crystal formation and its shape. Accordingly, after germination at 40 ºC and the temperature dropped to 30 ºC, small crystals were formed and increased in number and size to reach a steady state. About crystals shape, most crystals are cubes, some are pyramids.

3. Crystallization experiment with xylitol B75, seeding with 1% (w/v) of
   xylitol crystal

   The results of xylitol B75 with seeding 1% crystallization experiment were shown in Fig. 4.33, table 4.8, Fig. 4.34 and Fig. 4.35, respectively.
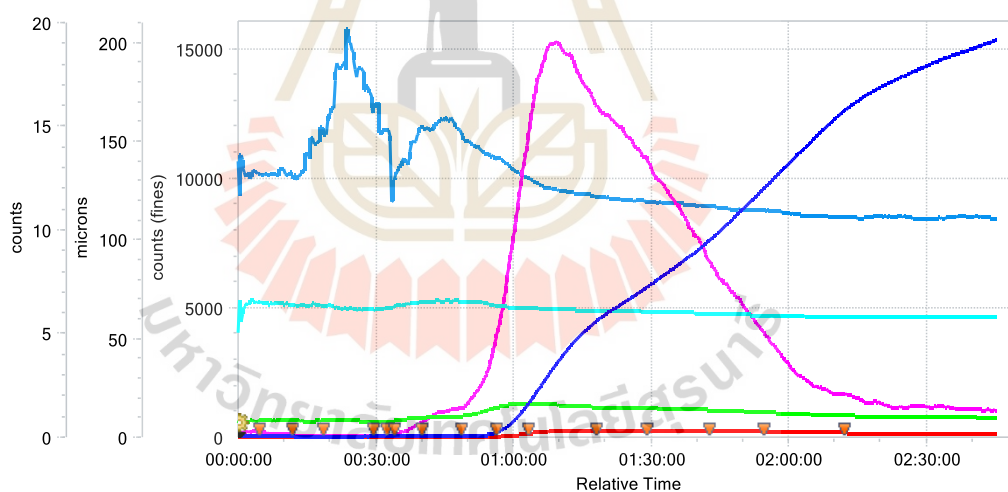

Figure 4.33 Trend of number and crystals size during the crystallization with 75Bx
   xylitol with seeding 1%

Table 4.8 Average number and size of crystals during the crystallization with 75Bx
xylitol with seeding 1%

Trend	Line Color	60 °C 0 min	50 °C 18 mins	40 °C Seeding 35 mins	30 °C 48 mins	20 °C 63 mins	10 °C 84 mins	1 °C 114 mins	End 130 mins
Counts <50		30.33	29.02	32.33	45.78	1551.12	5729.15	9499.33	15324.0
Mean <50		8.05	8.32	8.32	10.56	16.56	14.76	12.6	9.79
Counts 50-100		0.69	0.58	0.85	3.76	153.16	264.77	211.86	132.51
Mean 50-100		64.89	67.23	66.88	69	65.21	63.49	61.77	60.43
Counts 100-1000		0.08	0.08	0.14	1.36	16.05	13.67	5.25	1.33
Mean 100-1000		131.77	150.19	127.53	145.63	128.63	119.33	115.04	110.72
Counts >1000		N/A	N/A	N/A	N/A	N/A	N/A	N/A	N/A
Mean >1000		N/A	N/A	N/A	N/A	N/A	N/A	N/A	N/A

The graph in Fig. 4.33 shows that after seeding and reducing 40°C-30°C the number of crystals <50 µm is still small, but after 20 °C the number has increased to 1,551.2 and reached 15,324.02 with an average size of 9.79 µm. It has been shown that crystal formation at 75B is later than 70B. In the group of 50-100 µm, the largest number increased at 10 °C (264.77 crystals) then decreased towards the end of the process (32 crystals) with the average size unchanged. This trend is also true for the group of crystals 100-1000 µm. This has been shown that during crystallization, the crystals do not grow but dissolved and formed new crystals. It is also shown in Fig. 4.34 when the trend of the PSD lines is to go up and to the left (increase in number but decrease in size). Whereas at 70B, the trend of the PSD lines is upwards and to the right (increasing in both size and number). In addition, the number of crystals in each group of 75B was less than that of other experiments under the same temperature conditions. This can be explained because at different concentrations, under the effect of stirring factors, the rate of cooling...leaded to the formation of crystals with different structures and shapes, thereby

affecting quantity and crystal size. PVM results in Fig. 4.35 show that the crystals form mostly pyramids, some crystals are in the form of cubes, especially with generator towers.
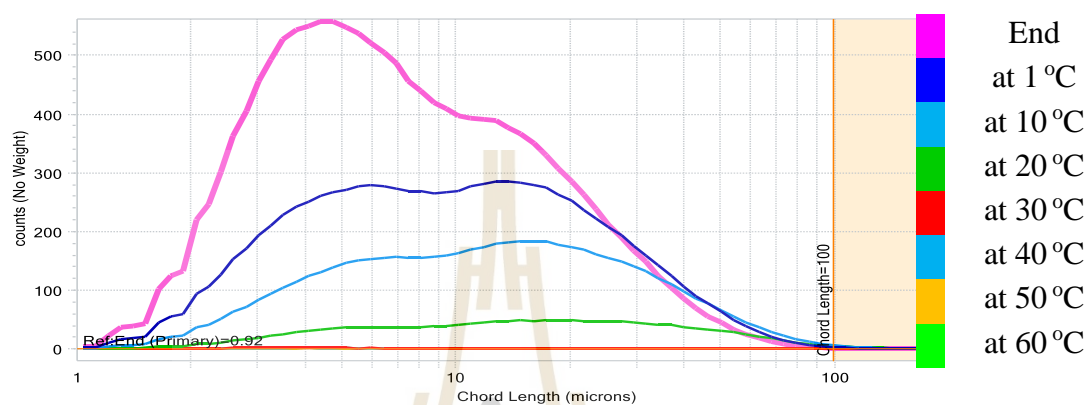

Figure 4.34 Particle size distribution (PSD) of crystals during the crystallization with
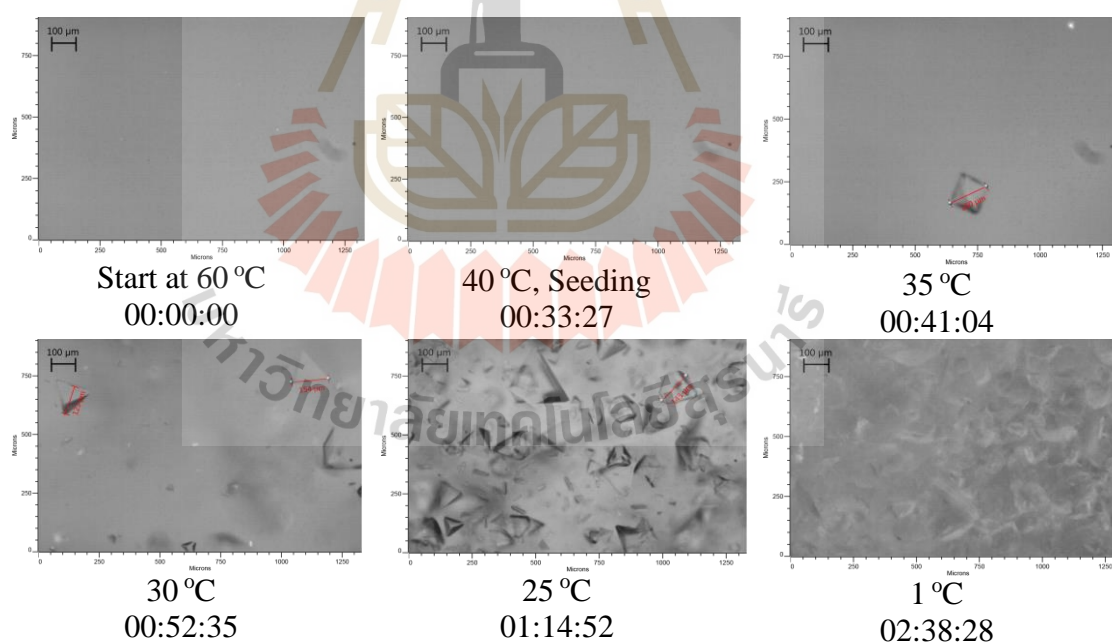
75Bx xylitol with seeding 1%.

Figure 4.35 PVM images taken at different times during the crystallization with 75Bx

xylitol with seeding 1%.

4. Crystallization experiment with xylitol B80

We continued to test crystallization with Bx 80 to monitor the crystallization behavior of xylitol at high concentrations. With a high concentration of xylitol, crystals formed as soon as the temperature began to decrease. The crystal formed very quickly, after 10 seconds (Fig. 4.36) the formed crystals were linked together into a semi-solid state that is difficult to observe by PVM (suitable for suspension). Besides, the results of FBRM were not monitored in time because the crystallization process was too fast. We believe that crystallization of xylitol at high concentrations is not suitable because it is difficult to control the crystallization process as desired.

00:00:10 – Start   00:10:11 – End
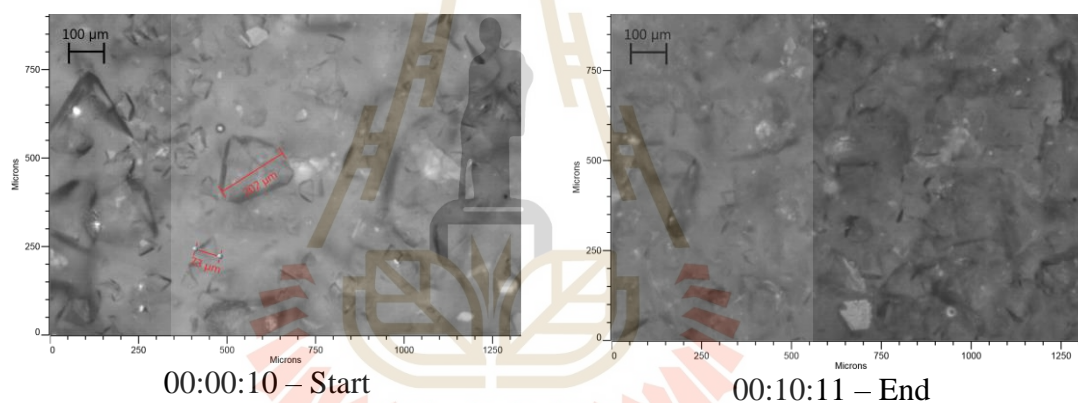
Figure 4.36 PVM images taken at different times during the crystallization with 75Bx xylitol with seeding 1%.

5. Crystallization experiment with commercial xylitol B70, so seeding

To compare xylitol fermentation from XBS, we crystallized commercial xylitol at Bx 70. During the crystallization process, after the temperature dropped to 40 °C, we did not add xylitol crystals for comparison. The results showed that when the temperature dropped to 20 °C, crystals began to form spontaneously.

The results of commercial xylitol B70 crystallization experiment were

shown in Fig. 4.37, table 4.9, Fig. 4.38 and Fig. 4.39, respectively.

Figure 4.37 Trend of number and crystals size during the crystallization with 70Bx

commercial xylitol

Table 4.9 Average number and size of crystals during the crystallization with 70Bx

commercial xylitol

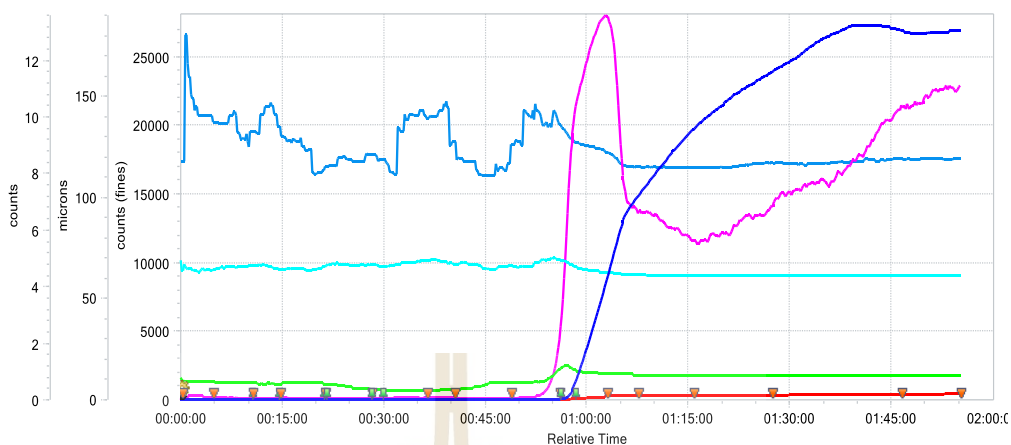| Trend	Line Color	60 °C 0 min	50 °C 11 mins	40 °C 22 mins	30 °C 34 mins	20 °C 49 mins	10 °C 54 mins	1 °C 87 mins	End 95 mins
Counts <50		15.36	15.1	15.39	35.16	14.63	9036.36	23816.24	26886.6
Mean <50		9.13	8.11	8.1	5.3	8.36	13.03	12	12.51
Counts 50-100		0.823	0.597	0.639	0.585	0.739	249.07	322.44	434.73
Mean 50-100		66.68	66.43	64.71	66.82	65.69	63.05	61.22	61.44
Counts 100-1000		0.065	0.0519	0.0635	0.0543	0.0422	13.54	6.82	11.04
Mean 100-1000		117.6	132.66	112.27	121.18	113.34	122.07	117.18	119.06
Counts >1000		N/A	N/A	N/A	N/A	N/A	N/A	N/A	N/A
Mean >1000		N/A	N/A	N/A	N/A	N/A	N/A	N/A	N/A

The results showed that when the temperature decreased from 60 °C to 20 °C, crystals did not form in all size groups, because at this time the solution was not too saturated. When the temperature is lower than 20 °C, crystals have begun to form. Groups <50 µm show a very rapid increase in number when reaching 9,036 crystals.

Finishing crystallization after 1 h 35 minutes reaches 26,886 crystals formed with an average size of 12.51 µm. The 50-100 µm group also recorded an increase in number at the end of the process reaching 434.73 crystals with an average size of 61.44 µm. Significantly, the crystal formation in the 100-1000 µm group, which in previous experiments did not have. The PSD diagram in Figure 4.48 showed higher PSD lines compared to experiments with XBS. That means the number and size of crystals formed at C70 was greater. The growing trend of the crystals, the PSD graph also shows upward and shifting to the right (same as B70), which means there is a simultaneous increase in number and size. Observed results by PVM (Fig. 4.49) showed the time of crystal formation as well as their shape. Through the direct image we see most of the crystals with generator towers.
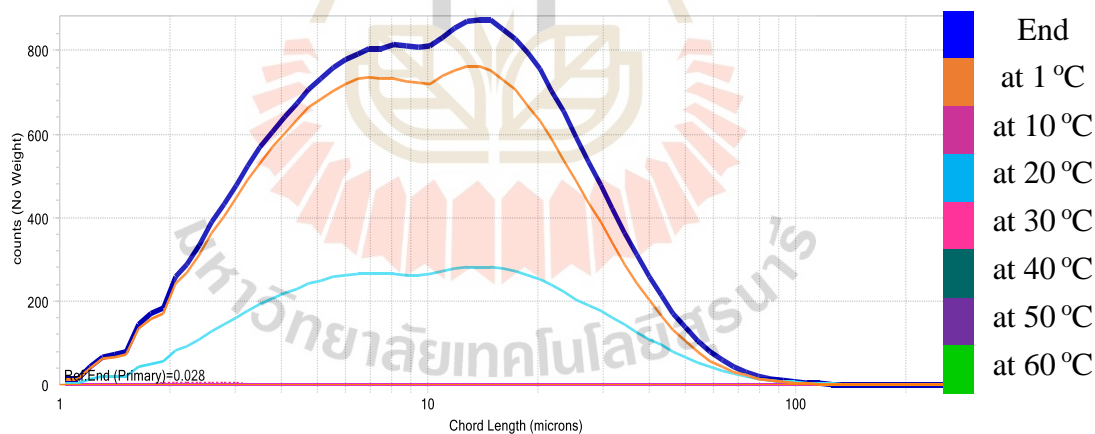
Figure 4.38 Particle size distribution (PSD) of crystals during the crystallization with 70Bx commercial xylitol
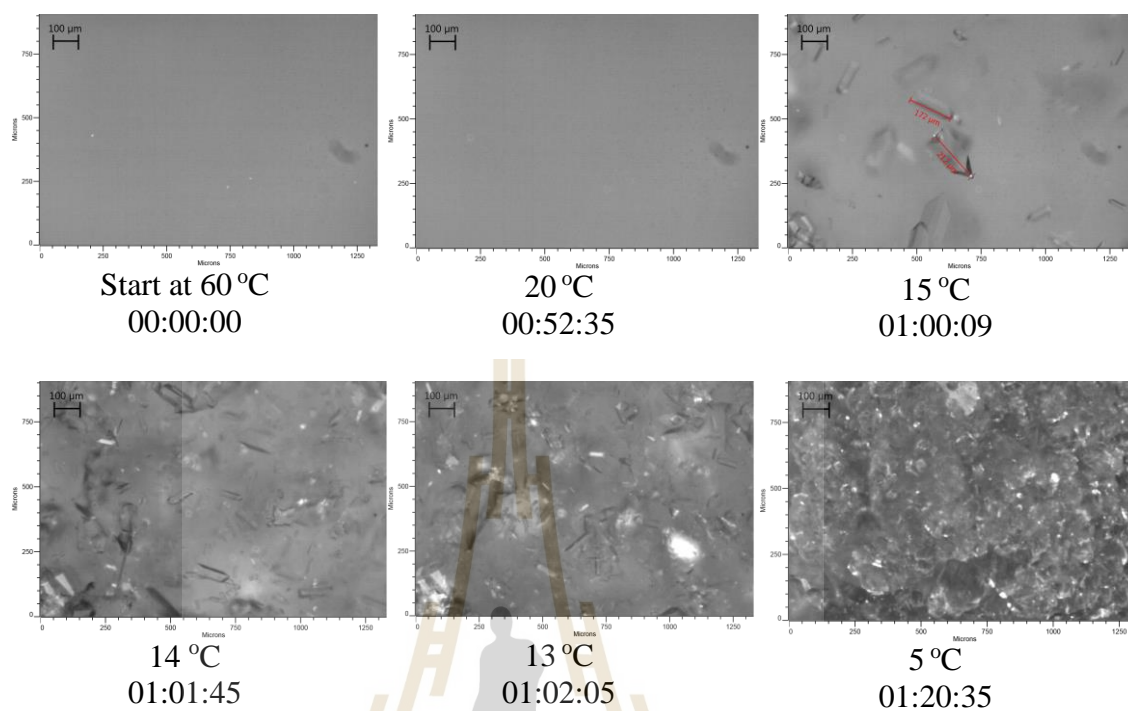
Figure 4.39 PVM images taken at different times during the crystallization with 70Bx commercial xylitol.

Raman spectroscopy is used to evaluate the structural change of xylitol before and after crystal formation. In addition, the Raman spectrum of crystals after recovery and drying was also compared with commercial xylitol to evaluate the uniformity. Results are shown in Fig. 4.40, 4.41. 4.42 and 4.43, respectively.
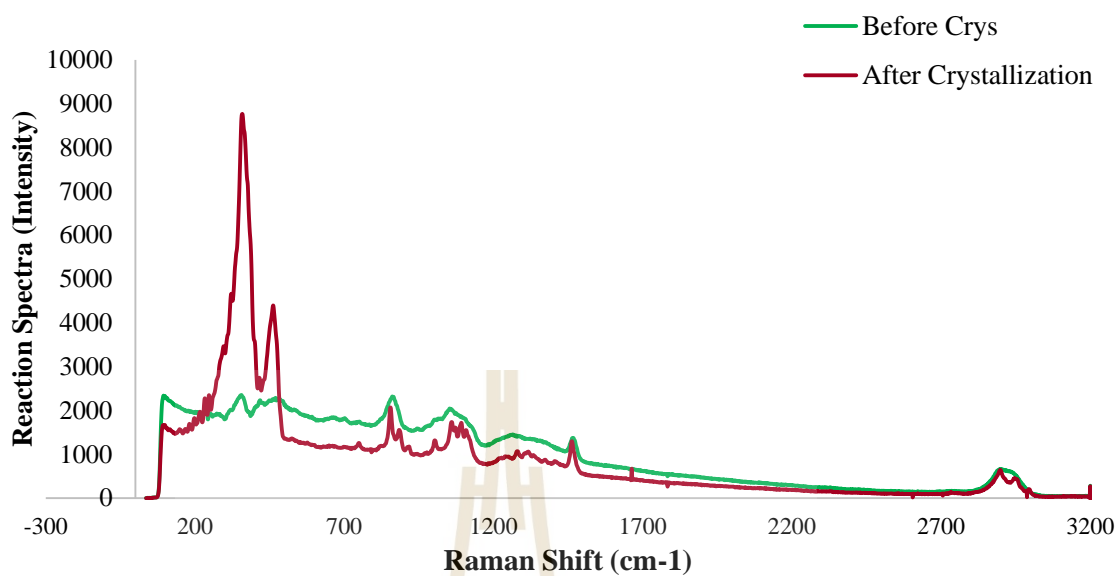
Figure 4.40 Characteristic Raman spectroscopy peaks of xylitol before and after crystallization (inside crystallizer)
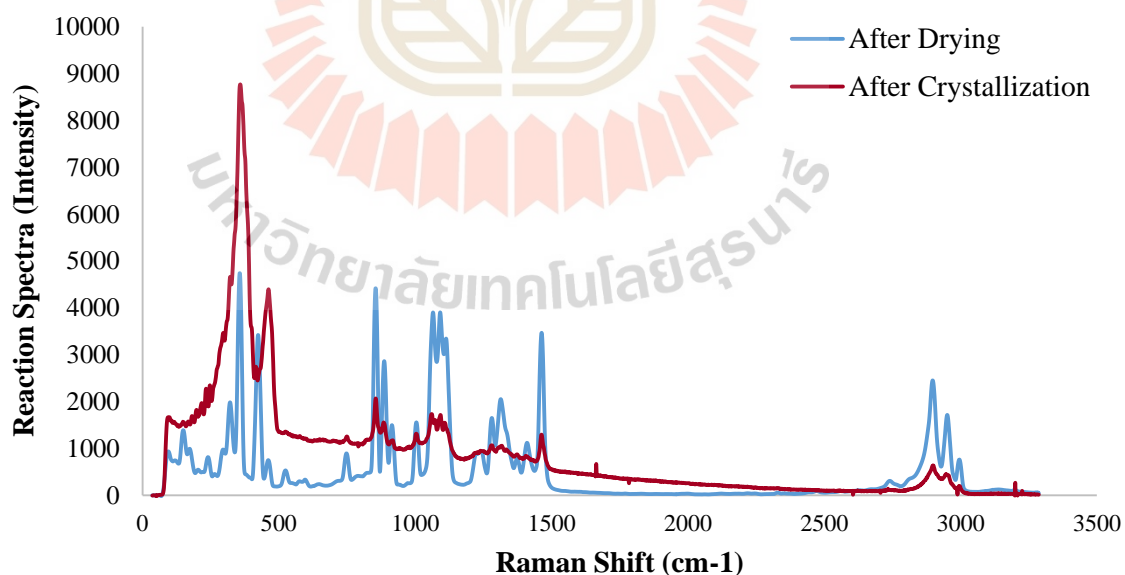
Figure 4.41 Characteristic Raman spectroscopy peaks of xylitol after crystallization (inside crystallizer) and after drying (outside crystallizer)
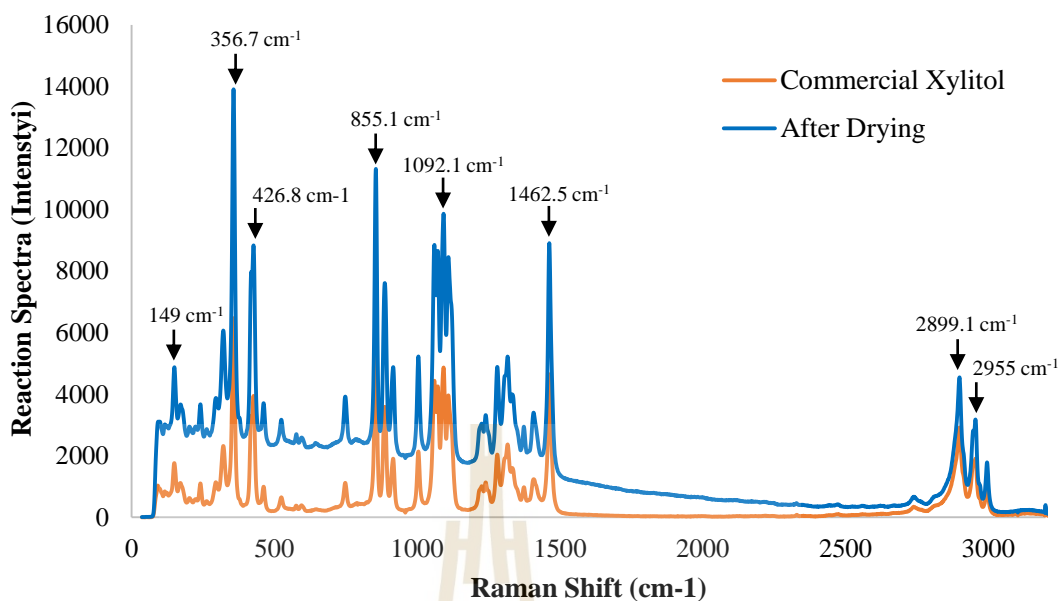
Figure 4.42 Characteristic Raman spectroscopy peaks of xylitol after drying (outside crystallizer) and commercial xylitol.

Figure 4.43 Characteristic Raman spectroscopy peaks of xylitol before, after crysllization; after drying (outside crystallizer) and commercial xylitol.

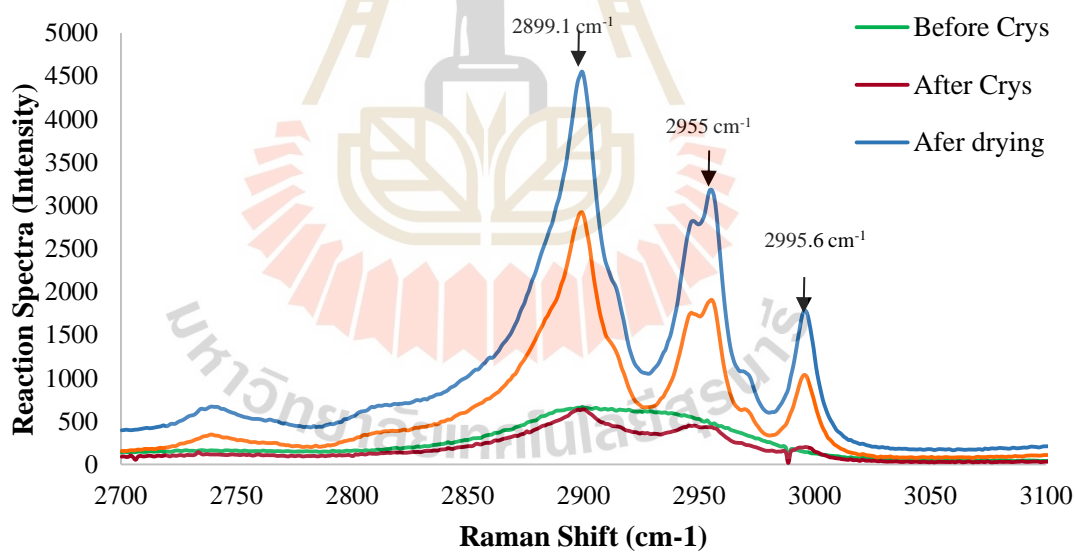The Raman spectrum of xylitol can be divided into 3 different regions. The first region has a peak at 149 to 426.8 cm-1, the second region has a peak at 855.1-

1462.4 cm^{-1}, the third region has a peak at 2899.1-2995.6 cm^{-1}. Fig. 4.50 shows the spectrum of xylitol (before crystallization), although divided into 3 regions but not clear, the low peaks show the connection of xylitol with water. However, after which the characteristic spectral features of crystalline xylitol gradually emerge in the spectra as the xylitol crystallizes. After crystallization, xylitol is filtered to collect crystals, then dried at 35 °C. Fig. 4.41 compares the Raman spectrum of xylitol after crystallization and start drying. On the graph we see, after drying to remove water, the peaks become clearer and almost similar to the spectrum of commercial xylitol (Fig. 4.42). The 748 cm^{-1} peaks did not appear before and after crystallization but did appear after drying, similar to commercial xylitol. Similarly, before crystallization, there is 1 peak at 855 cm-1, but after crystallization, it has divided into vertices 855, 886, 915 cm^{-1}. The Raman shift region from 1230 to 1320 cm^{-1}, before crystallization, had no peaks of the spectrum, then appeared spectral peaks at 1239.9, 1280.5, and 1316.8 cm^{-1}. Fig. 4.43 visually shows the changes in the Raman spectrum of xylitol at different stages. Before crystallization, no spectral peak appeared, but after crystallization, there were 2 peaks formed, but it was not clear. After drying, we clearly see 3 peaks 2899.1, 2955.0, and 2995.6 cm^{-1} on the spectrum. Especially after drying, xylitol has a completely coincidental spectrum with commercial xylitol. The bands' characteristics related to the bonds in the xylitol molecule and its intensity are presented in Table 4.10.

Table 4.10 showed the bonds of xylitol ($C_5H_{12}O_5$) in which Aliphatic chain (C-C-C), C-O, OH bonds are expressed at peaks of Raman spectrum. Besides, the Raman spectrum showed the Lattice Vibration structure, which is the characteristic cubic structure of the crystal.

Table 4.10 Main Raman peak positions of xylitol from XBS and their proposed
assignments

Peak position (cm^{-1})	Intensity	Atomic bond
149.6	Strong	Xmetal-O
	Strong	Aliphatic chain (C-C-C)
170	Strong	Lattice Vibration
207	Strong	Lattice Vibration
356.7	Strong	Xmetal-O
426.8	Strong	Aliphatic chain (C-C-C)
	Strong	Xmetal-O
748.0	Strong	Aliphatic chain (C-C-C)
855.1	Weak	C-O-C
	Strong	Aliphatic chain (C-C-C)
886.0	Weak	C-O-C
	Medium	Aliphatic chain (C-C-C)
915.9	Medium	Aliphatic chain (C-C-C)
	Weak	C-O-C
1408	Weak	Carboxylic acid dimer
	Weak	Methyl -CH$_3$
	Weak	Methylenr –CH$_2$
1060.0	Strong	Aromatic rings
	Strong	Aliphatic chain (C-C-C)
1092.1	Weak	Si-O-C
	Strong	Aromatic rings
	Medium	Aliphatic chain (C-C-C)
1239.9	Medium	Aliphatic chain (C-C-C)
1426.5	Medium	Aromatic rings
2899.1	Strong	C-CH$_3$
	Strong	Aromatic (C-H)
2955.5	Strong	C-CH$_3$
	Strong	Aromatic (C-H)
	Weak	Hydroxyl (OH)
2995.6	Strong	CH=CH
	Strong	Aromatic (C-H)
	Weak	Hydroxyl (OH)

Table 4.11 Crystallization yield and purity degree of difference xylitol crystallization

experiments

Experiments	Crystallization Yield (%)	Purity Degree (%)
XBS xylitol 70Bx, no seeding	-	-
XBS xylitol 70Bx, seeding 1%	85.03	99.64
XBS xylitol 75Bx, seeding 1%	79.74	99.35
Commercial xylitol 70Bx, no seeding	91.32	100*

* Commercial xylitol was considered 100% purity.

When comparing between experiments, the 70B with 1% seeding showed a similar trend with the C70, as the number and size of crystals both increased over time. In addition, the Bx70 value is relatively suitable for a previous treatment when not too much energy is required to concentrate. Thereby, we find that the suitable crystallization method is 70Bx with 1% seeding. The number, size and shape of crystals depend on cooling rate, stirring speed, purity, etc. Table 4.11 showed the crystallization yield and purity of xylitol in different experiments. The experiment with xylitol 70B showed that the crystallization yield reached 85.03%, with the purity reaching 99.64%. Meanwhile, xylitol 75B reached a crystallization yield of 79.74% with a purity of 99.35%. Commercial xylitol C70 has the best results with a crystallization yield of 91.32% at 100% purity. The lower crystallization yield in B75 was also consistent with the results analyzed by FBRM when it shows that the number of crystals formed was less than the other 2 experiments.

In 2002, Favari et al. fermented hemicellulose hydrolyzate with *D. hansenii* (NRRL Y 7426). Then xylitol is purified, concentrated to a concentration of 470

g/L to crystallize at -10 °C. Crystallization yield was 27% with 92% purity, while synthetic xylitol (730 g/L) crystallized at -5 °C has 56% of yield, 100% of purity (De Faveri 2002). Sampaio et al. (2006) used *Debaryomyces hansenii* to ferment synthetic broth, then purified and concentrated to a concentration of 675 to 911 g/L. Xylitol is crystallized at -10 °C, crystallization yield reached 27 to 42%, purity reached 96 to 97.8% (Sampaio, Passos *et al.* 2006). *C. guilliermondii* is used to ferment xylitol from Sugarcane hemicellulosic hydrolyzate. After purification, xylitol is crystallized in 2 phases. Phase 1 at a cooling rate of 0.5 °C/min achieves a purity of 85%. Phase 2 crystallizes at the rate of 0.1 °C/min with 1% added crystals, the purity reaches 91.2-94.85% (Martínez, de Almeida e Silva *et al.* 2007). Then in 2009, the authors had succeeded in increasing purity to 95% in phase 1 and 98.5-99.2% in phase 2 (Martínez, Giulietti *et al.* 2009). A low-temperature crystallization method was also performed by Canilha et al. (2008) with xylitol 726.5 g/L solution (using *C. guilliermondii* fermented from wheat straw hemicellulosic hydrolyzate). The results showed that, with the cooling rate of 0.2-0.4 °C/min, crystal with 95.3-99.9% purity, crystallization yield reached 43.5% (Canilha, Carvalho *et al.* 2008). Meanwhile, Fatehi et al (2014) crystallized xylitol reaching 99% purity after 72 h at -5 °C (Fatehi, Catalan *et al.* 2014).
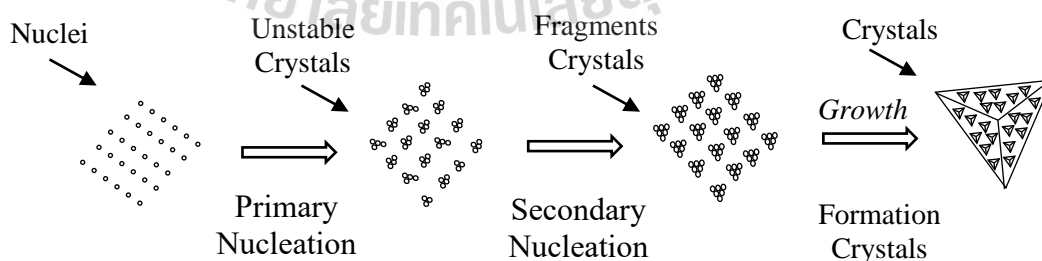

Figure 4.44 Main steps of crystallization process

As mentioned, crystallization is an important process in downstream xylitol processing after fermentation. The motivation of crystallization is the existence of supersaturation of the solute in a liquid (the solute concentration is higher than the solubility limit). The crystallization process is described in Fig. 4.44. Accordingly, the first step of the crystallization process is nucleation. In this stage, it is necessary to create conditions for the molecules to contact, collide with each other to form bonds. That shows the role of mixing (creating the opportunity for contact) and reducing the temperature (reducing solubility and reducing molecular movement). The result of this step will lead to the formation of primary crystals. After the first crystalline seeds are formed, small pieces of these crystals can be changed to form a new nucleus, this step is called secondary nucleation. After that, the crystals begin to grow, increase in size and reach a complete crystal (Antunes, dos Santos *et al.* 2017). The circulation of the solution (mixing), the coefficient of saturation, the temperature and the cooling rate, and the purity affect the growth rate, the size, and final properties of the crystals. In the sugar industry, controlling the number of crystals as needed in order not to form new crystals, focusing only on increasing crystal size is one of the important techniques affecting product quality.
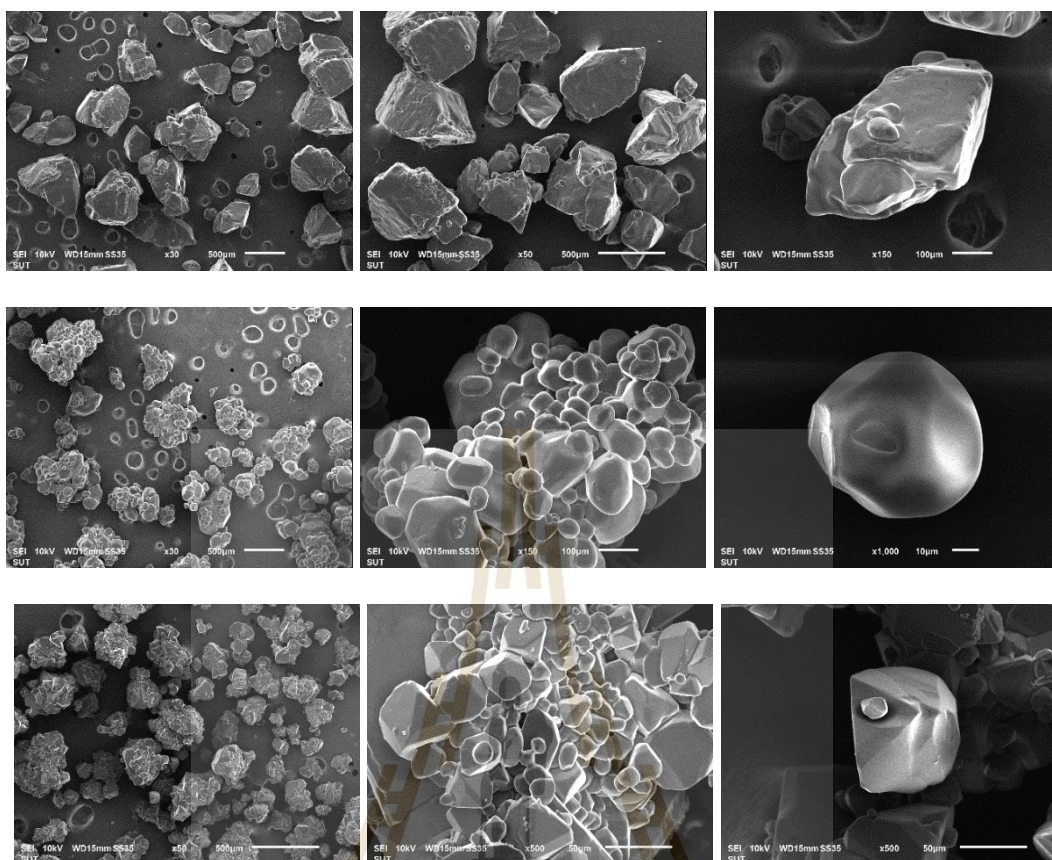
Figure 4.45 SEM images of xylitol crystals. Line 1, commercial xyitol crystals; Line 2, commercial xylitol crystals after crystallization; Line 3, Xylitol crystals from XBS

Fig. 4.45 shows the SEM image of xylitol crystals after crystallization. In the first row, commercial xylitol crystal has a shape of generator towers (corresponding to PVM) with a rather rough surface due to mechanical impact when storing and transporting. In row 2, the xylitol crystal, after recrystallization from commercial xylitol, has the shape of cubes. Row 3, xylitol crystal after crystallization from XBS has the shape of pyramids. We can see that their surface is smooth and there are small crystals on the surface.

In this study, we stop at the successful experiment of crystal formation,

the control of parameters so that the crystals are homogeneous in shape and size will be further studied later. Based on the results obtained in the above experiments, we have proposed the process of producing xylitol from bagasse as shown in the diagram in Fig. 4.47.
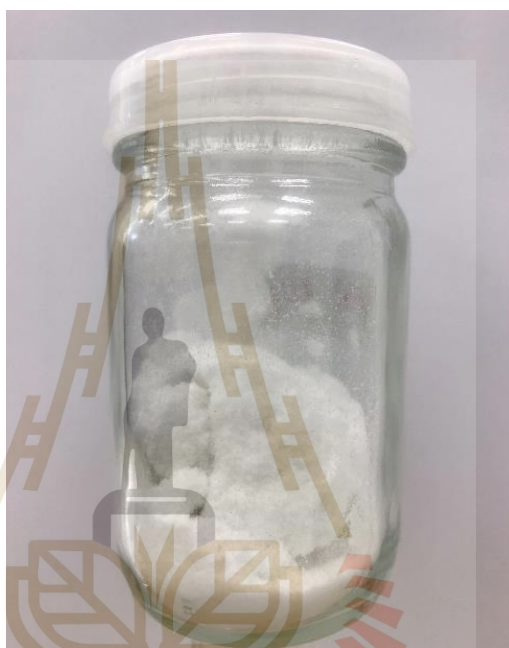
Figure 4.46 Xylitol production from Sugarcane Bagasse
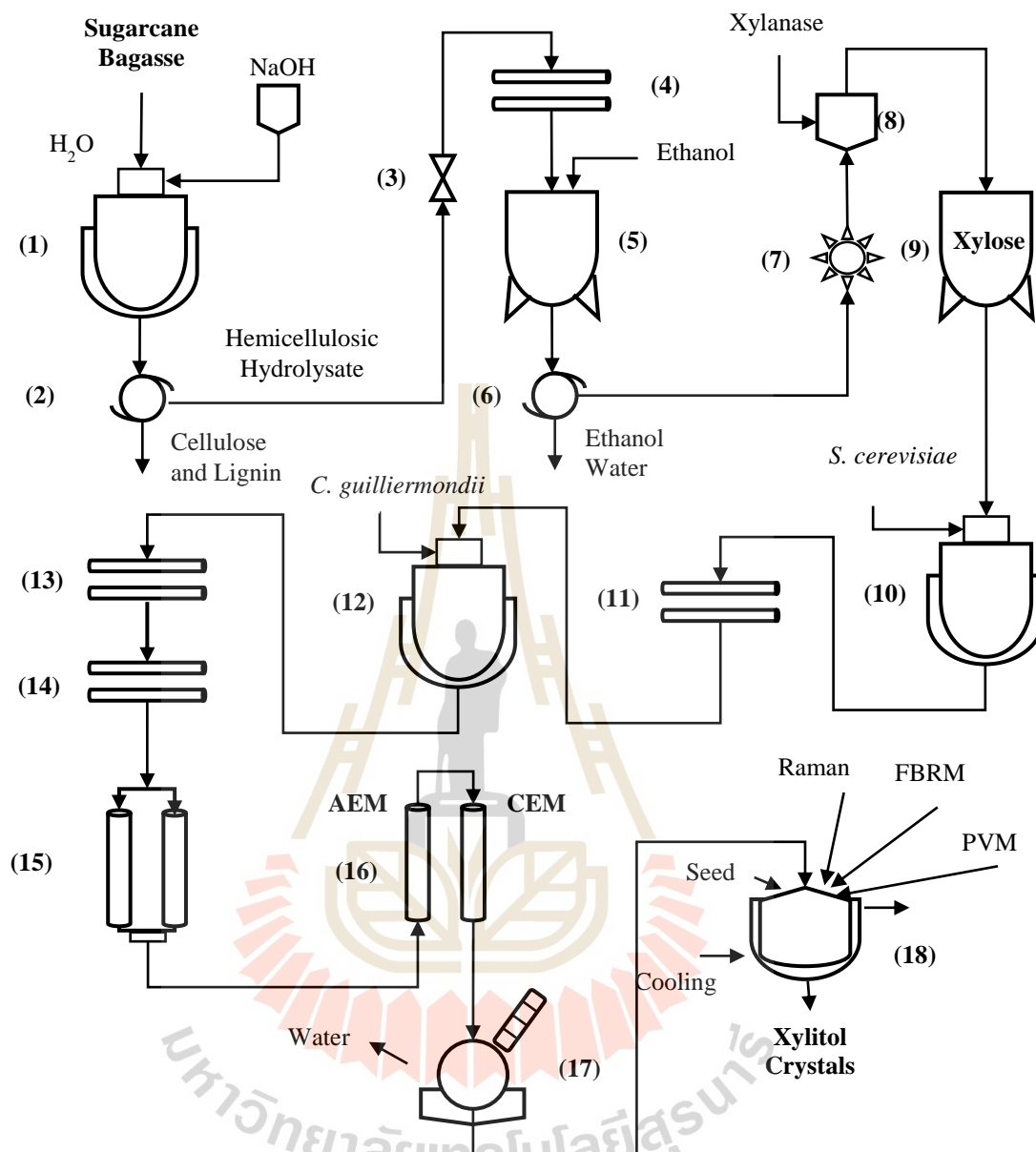
Figure 4.47 Proposed process of producing xylitol from bagasse. 1. 1000 L alkaline

hydrolysis reactor; 2. Turbo sieve; 3. Bag filter; 4. Microfiltration; 5. Xylan

precipitation reactor; 6. Centrifuge; 7. Dryer; 8. Xylose enzyme hydrolysis

reactor; 9. Xylose container; 10. 1000 L ethanol fermentation bioreactor;

11. Microfiltration; 12. 1000 L xylitol fermentation bioreactor; 13.

Microfiltration; 14. Ultrafiltration; 15. Nanofiltration; 16. Ion exchange

resin; 17. Rotary evaporator; 18. Crystallization reactor

4.5   Proposed process of producing xylitol from bagasse.

The process of producing xylitol is proposed in the diagram 4.47. Firstly bagasse is pretreated with dilute alkali to hydrolyze hemicellulose, then it is centrifuged to separate the pulp and enter the microfiltration system. Next, use ethanol to precipitate the xylane. The xylan is then centrifuged and dried to obtain xylan solid form. Next, xylanase is used to hydrolyze xylan to xylose. The sugar mixture is then removed from the glucose by fermentation of ethanol. The xylose purification process is done by removing the cells by microfiltration and then concentrating on preparing for the next process. *C. guiliermondii* has been used for xylitol fermentation, the fermentation is carried out at a pilot scale with 500 L bioreactor. After fermentation, the fermentation broth is passed through systems of microfiltration, ultrafiltration and nanofiltration. After filtration, xylitol is desalinated and decolorized by ion exchange resin before concentration to super-saturated to perform crystallization. The crystallization method is performed by seeding crystals at low temperatures. After crystallization, filter and dry to obtain solid xylitol crystals.

CHAPTER V

CONCLUSION

From the above results, we conclude as follows:

Xylitol can be produced from sugarcane bagasse hemicellulosic hydrolysate by *Candida guilliermondi* TISTR 5068. This strain has produced xylitol with high efficiency at pilot scale. Yield, concentration and xylitol productivity were 0.87 $g_{xylitol}/g_{xylose}$, 23.24 g/L and 0.14 g/L.h, respectively.

High fermentation efficiency has facilitated downstream processes including microfiltration, ultrafiltration, nanofiltration, ion exchange resin and crystallization. Membrane processes have been used to efficiently separate cells, polymers and partial colorants. As a result, the ion exchange resin process has eliminated 99.94% of ions and 99.63% of color compounds.

The high purification efficiency of the above processes facilitates the crystallization process to produce high purity xylitol crystals. The cooling method combined with seeding has been studied to obtain xylitol crystals of 99.64% purity with a crystallization recovery rate of 85.03%. The combination of processes based on membrane processes, ion exchange resin, and crystallization has efficiently delivered the desired xylitol product without the need for any the auxiliary components.

The results obtained in this study may be useful in protecting the environment, reducing the cost of xylitol production from inexpensive biomass to the bio xylitol product. On the other hand, the results in this study also open up the prospect of applying xylitol production from bagasse on an industrial scale.
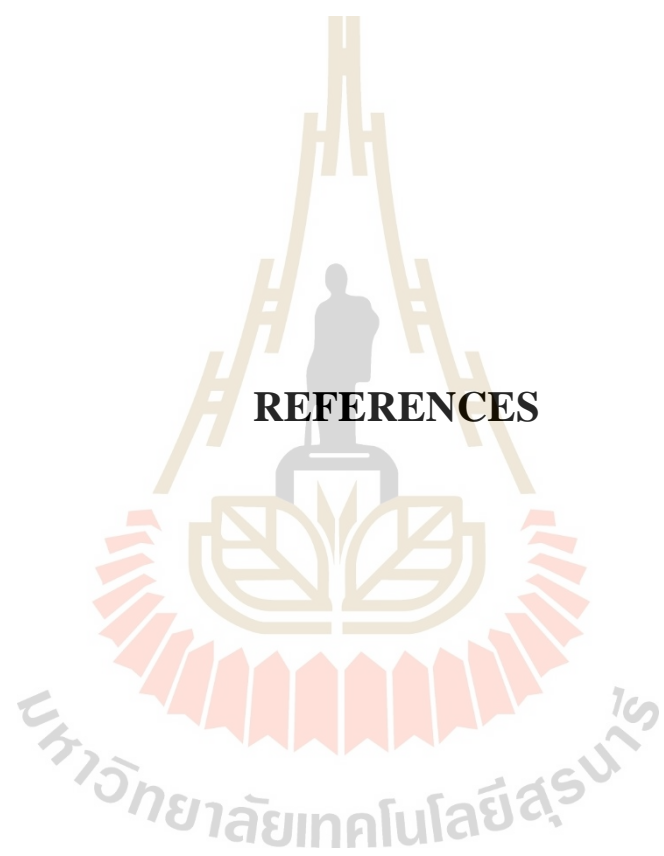
REFERENCES

REFERENCES

Abril, A. and E. A. Navarro (2013). Etanol a partir de biomasa lignocelulósica. Aleta Ediciones, 102

Affleck, R. P. (2000). Recovery of xylitol from fermentation of model hemicellulose hydrolysates using membrane technology. Blacksburg, Virginia, Virginia Polytechnic Institute and State University. **M.Sc. thesis:** 114.

Antunes, F. A. F., et al. (2017). Biotechnological Production of Xylitol from Biomass. **Production of Platform Chemicals from Sustainable Resources, 7:** 311-342.

Bensouissi, A., et al. (2010). Effect of conformation and water interactions of sucrose, maltitol, mannitol and xylitol on their metastable zone width and ease of nucleation. **Food Chemistry**, 122(2): 443-446.

Bothast, B. S. a. R. (1999). Production of xylitol by *Candida peltatasaha.* **Journal of Industrial Microbiology & Biotechnology**, 22: 633–636.

Canilha, L., et al. (2008). Clarification of a wheat straw-derived medium with ion-exchange resins for xylitol crystallization. **Journal of Chemical Technology & Biotechnology**, 83(5): 715-721.

Canilha, L., et al. (2013). Bioconversion of Hemicellulose from Sugarcane Biomass Into Sustainable Products. Sustainable Degradation of Lignocellulosic Biomass - Techniques, Applications and Commercialization. **1**: 15-45.

Cerceau Alves, Y. P., et al. (2021). From by- to bioproducts: selection of a nanofiltration membrane for biotechnological xylitol purification and process optimization.

Food and Bioproducts Processing, 125: 79-90.

Chandel, A. K., et al. (2018). The path forward for lignocellulose biorefineries: Bottlenecks, solutions, and perspective on commercialization. **Bioresour Technol**, 264: 370-381.

Cingi, C., et al. (2014). Comparison of nasal hyperosmolar xylitol and xylometazoline solutions on quality of life in patients with inferior turbinate hypertrophy secondary to nonallergic rhinitis. **International Forum of Allergy & Rhinology**, 4(6): 475-479.

da Silva, D. D. V. and M. d. G. de Almeida Felipe (2006). Effect of glucose:xylose ratio on xylose reductase and xylitol dehydrogenase activities from *Candida guilliermondii* in sugarcane bagasse hydrolysate. **Journal of Chemical Technology & Biotechnology**, 81(7): 1294-1300.

Dalli, S. S., et al. (2017). Development and evaluation of poplar hemicellulose prehydrolysate upstream processes for the enhanced fermentative production of xylitol. **Biomass and Bioenergy**, 105: 402-410.

de Cássia Lacerda Brambilla Rodrigu, R., et al. (2012). Statistical Approaches for the Optimization of Parameters for Biotechnological Production of Xylitol. D-Xylitol. Springer, Berlin, Heidelberg, 133-160.

De Faveri, D., Perego, P., Converti, A., & Del Borghi, M. (2002). Xylitol recovery by crystallization from synthetic solutions and fermented hemicellulose hydrolyzates **Chemical Engineering Journal**, 90(3): 291-298.

Delgado Arcaño, Y., et al. (2020). Xylitol: A review on the progress and challenges of its production by chemical route. **Catalysis Today**, 344: 2-14.

Desiriani, R., et al. (2017). Membrane-Based Downstream Processing of Microbial Xylitol Production. **International Journal of Technology**, 8(8)

Dominguez, J. M., et al. (1997). Production of Xylitol from D-Xylose by *Debaryomyces hanseniidominguez*. **Biotechnology for Fuels and Chemicals**, 117-127.

Faneer, K. A., et al. (2018). Influence of pluronic addition on polyethersulfone membrane for xylitol recovery from biomass fermentation solution. **Journal of Cleaner Production**, 171: 995-1005.

Faneer, K. A., et al. (2017). Evaluation of the operating parameters for the separation of xylitol from a mixed sugar solution by using a polyethersulfone nanofiltration membrane. **Korean Journal of Chemical Engineering**, 34(11): 2944-2957.

Faria LF, G. M., Nobrega R, Pereira N Jr. (2002). Influence of oxygen availability on cell growth and xylitol production by *Candida guilliermondii*. **Appl Biochem Biotechnol**, 98: 449-458.

Fatehi, P., et al. (2014). Simulation analysis of producing xylitol from hemicelluloses of pre-hydrolysis liquor. **Chemical Engineering Research and Design**, 92(8): 1563-1570.

Fehér, A., et al. (2018). Treatments of Lignocellulosic Hydrolysates and Continuous-Flow Hydrogenation of Xylose to Xylitol. **Chemical Engineering & Technology**, 41(3): 496-503.

Felipe Hernandez-Perez, A., et al. (2019). Xylitol bioproduction: state-of-the-art, industrial paradigm shift, and opportunities for integrated biorefineries. **Crit Rev Biotechnol**, 39(7): 924-943.

Guirimand, G., et al. (2016). Cell surface engineering of *Saccharomyces cerevisiae* combined with membrane separation technology for xylitol production from rice

straw hydrolysate. **Appl Microbiol Biotechnol**, 100(8): 3477-3487.

Gurgel, P. V., Mancilha, I. M., Peçanha, R. P., & Siqueira, J. F. M. (1995). (1995). Xylitol recovery from fermented sugarcane bagasse hydrolyzate **Bioresource Technology**, 52(3): 219-223.

Hao, H., et al. (2006). Effect of solvent on crystallization behavior of xylitol. **Journal of Crystal Growth**, 290(1): 192-196.

Hernández-Pérez, A. F., et al. (2019). Sugarcane Syrup Improves Xylitol Bioproduction from Sugarcane Bagasse and Straw Hemicellulosic Hydrolysate. **Waste and Biomass Valorization**, 11(8): 4215-4224

Hernandez-Perez, A. F., et al. (2016). Biochemical conversion of sugarcane straw hemicellulosic hydrolyzate supplemented with co-substrates for xylitol production. **Bioresour Technol**, 200: 1085-1088.

Hernández-Pérez, A. F., et al. (2020). Biotechnological production of sweeteners. Biotechnological Production of Bioactive Compounds, **Elsevier B.V,** 261-292.

Hong, E., et al. (2016). Optimization of dilute sulfuric acid pretreatment of corn stover for enhanced xylose recovery and xylitol production. **Biotechnology and Bioprocess Engineering**, 21(5): 612-619.

Hou-Rui, Z. (2012). Key Drivers Influencing the Large Scale Production of Xylitol. D-Xylitol. **Springer, Berlin, Heidelberg,** 267-289.

Hyvönen, L., et al. (1982). Food Technological Evaluation of Xylitol. Advances in Food Research Volume 28**:** 373-403.

Ikeuchi, T. A., M.; Kato, J.; Ooshima, H. (1999). Screening of microorganisms for xylitol production and fermentation behavior in high concentrations of xylose. **Biomass Bioeng**, 16: 333–339.

Izumori, K. and K. Tuzaki (1988). Production of xylitol from D-xylulose by *Mycobacterium smegmatis izumori*. **Journal of Fermentation Technology**, 66(1): 33-36.

Jandera, P., & Churáček, J (1974). Ion-exchange chromatography of aldehydes, ketones, ethers, alcohols, polyols and saccharides. **Journal of Chromatography A**, 98(1): 55–104.

Jeon, Y. J., et al. (2011). Xylitol production from a mutant strain of *Candida tropicalis*. **Lett Appl Microbiol**, 53(1): 106-113.

Jiang, X., et al. (2016). High-efficient xylitol production by evolved *Candida maltosaadapted* to corncob hemicellulosic hydrolysate. **Journal of Chemical Technology & Biotechnology**, 91(12): 2994-2999.

Kim, J. H., et al. (2002). Optimization of fed-batch fermentation for xylitol production by *Candida tropicalis*. **J Ind Microbiol Biotechnol**, 29(1): 16-19.

Kim, S.-Y., Kim, J.-H., & Oh, D.-K. (1997). Improvement of xylitol production by controlling oxygen supply in Candida parapsilosis. **Journal of Fermentation and Bioengineering**, 83(3): 267–270.

Ko, B. S., et al. (2011). Enhancement of xylitol production by attenuation of intracellular xylitol dehydrogenase activity in Candida tropicalis. **Biotechnol Lett**, 33(6): 1209-1213.

Kogje, A. B. and A. Ghosalkar (2017). Xylitol production by genetically modified industrial strain of *Saccharomyces cerevisiae* using glycerol as co-substrate. **J Ind Microbiol Biotechnol**, 44(6): 961-971.

Kresnowati, M. T. A. P., et al. (2017). Ultrafiltration of hemicellulose hydrolysate fermentation broth. **AIP Conference Proceedings**, 1818: 020024

Kresnowati, M. T. A. P., et al. (2019). Combined ultrafiltration and electrodeionization techniques for microbial xylitol purification. **Food and Bioproducts Processing**, 114: 245-252.

Kumar, S., et al. (2015). Bioprocessing of bagasse hydrolysate for ethanol and xylitol production using thermotolerant yeast. **Bioprocess Biosyst Eng**, 38(1): 39-47.

Kumar, V., et al. (2018). Efficient detoxification of corn cob hydrolysate with ion-exchange resins for enhanced xylitol production by *Candida tropicalis* MTCC 6192. **Bioresour Technol**, 251: 416-419.

Kumar, V., et al. (2019). Improved upstream processing for detoxification and recovery of xylitol produced from corncob. **Bioresour Technol**, 291: 121931.

Kyaw Wunna, K. N., Joseph L. Auresenia, Leonelia C. Abella (2017). Effect of Alkali Pretreatment on Removal of Lignin from

Sugarcane Bagasse. **Chemical Engineering Transactions**, 56: 1831-1836.

Lenhart, A. and W. D. Chey (2017). A Systematic Review of the Effects of Polyols on Gastrointestinal Health and Irritable Bowel Syndrome. **Adv Nutr**, 8(4): 587-596.

Little, P., et al. (2017). Probiotic capsules and xylitol chewing gum to manage symptoms of pharyngitis: a randomized controlled factorial trial. **CMAJ**, 189(50): 1543-1550.

Liu, Y.-Y., et al. (2016). Reinforced alkali-pretreatment for enhancing enzymatic hydrolysis of sugarcane bagasse. **Fuel Processing Technology**, 143: 1-6.

Lopez-Linares, J. C., et al. (2018). Xylitol production by *Debaryomyces hansenii* and *Candida guilliermondii* from rapeseed straw hemicellulosic hydrolysate. **Bioresour Technol**, 247: 736-743.

Lugani, Y., et al. (2017). Xylitol: A Sugar Substitute for Patients of Diabetes Mellitus.

World Journal of Pharmacy and Pharmaceutical Sciences, 6(4), 741-749

Lugani, Y. and B. S. Sooch (2018). Insights into Fungal Xylose Reductases and Its Application in Xylitol Production. Fungal Biorefineries. **Springer, Cham,** 121-144.

Ly, K. A., et al. (2006). Xylitol, Sweeteners, and Dental Caries. **Pediatric Dentistry**, 28(7): 154-163.

Markets, R. a. (2018). Xylitol Market: Global Industry Trends, Share, Size, Growth, Opportunity and Forecast 2018-2023. Available from: https://www.researchandmarkets.com/, research/2wbg5g/global_xylitol?w=4

Martínez, E. A., et al. (2015). Strategies for xylitol purification and crystallization: A Review. **Separation Science and Technology**, 50(14): 2087-2098.

Martínez, E. A., et al. (2007). Downstream process for xylitol produced from fermented hydrolysate. **Enzyme and Microbial Technology**, 40(5): 1193-1198.

Martínez, E. A., et al. (2009). Batch cooling crystallization of xylitol produced by biotechnological route. **Journal of Chemical Technology & Biotechnology**, 84(3): 376-381.

Martínez, E. A., et al. (2003). The influence of pH and dilution rate on continuous production of xylitol from sugarcane bagasse hemicellulosic hydrolysate by *C. guilliermondii*. **Process Biochemistry**, 38(12): 1677-1683.

Maryana, R., et al. (2014). Alkaline Pretreatment on Sugarcane Bagasse for Bioethanol Production. **Energy Procedia**, 47: 250-254.

Misra, S., et al. (2011). Comparative study on different strategies involved for xylitol purification from culture media fermented by *Candida tropicalis*. **Separation and Purification Technology**, 78(3): 266-273.

Mohamad, N. L., et al. (2014). Xylitol Biological Production: A Review of Recent Studies. **Food Reviews International**, 31(1): 74-89.

Morais Junior, W. G., et al. (2019). Xylitol production on sugarcane biomass hydrolysate by newly identified *Candida tropicalis* JA2 strain. **Yeast**, 36(5): 349-361.

Muller Molnar, C., et al. (2020). An optimized green preparation method for the successful application of Raman spectroscopy in honey studies. **Talanta**, 208: 120432.

Mussatto, S. I. (2012). Application of Xylitol in Food Formulations and Benefits for Health. D-Xylitol**:** 309-323.

Mussatto, S. I., et al. (2006). A study on the recovery of xylitol by batch adsorption and crystallization from fermented sugarcane bagasse hydrolysate. **Journal of Chemical Technology & Biotechnology**, 81(11): 1840-1845.

Pal, S., et al. (2016). Molecular strategies for enhancing microbial production of xylitol. **Process Biochemistry**, 51(7): 809-819.

Prakash, G., et al. (2011). Microbial production of xylitol from D-xylose and sugarcane bagasse hemicellulose using newly isolated thermotolerant yeast *Debaryomyces hansenii*. **Bioresour Technol**, 102(3): 3304-3308.

Pulicharla, R., et al. (2016). Production of Renewable C5 Platform Chemicals and Potential Applications. Platform Chemical Biorefinery. **Elsevier**, 201-216.

Rafiqul, I. S. M. and A. M. M. Sakinah (2013). Processes for the Production of Xylitol—A Review. **Food Reviews International**, 29(2): 127-156.

Salli, K., et al. (2019). Xylitol's Health Benefits beyond Dental Health: A Comprehensive Review. **Nutrients**, 11(8): 1813

Sampaio, F. C., et al. (2006). Xylitol crystallization from culture media fermented by

yeasts. **Chemical Engineering and Processing: Process Intensification**, 45(12): 1041-1046.

Sampaio;, F. C., et al. (2003). Screening of filamentous fungi for production of xylitol from D-xylosesampaio. **Brazilian Journal of Microbiology**, 34: 325-328.

Silva, D. D. V., et al. (2020). Production and purification of xylitol *by Scheffersomyces amazonenses* via sugarcane hemicellulosic hydrolysate. **Biofuels, Bioproducts and Biorefining**, 14(2): 344-356.

Silva, D. D. V. d., et al. (2007). Improvement of biotechnological xylitol production by glucose during cultive of *Candida guilliermondii* in sugarcane bagasse hydrolysate. **Brazilian archives of Biology and Technology**, 50: 207-215.

Suzuki, S., et al. (2002). Novel enzymatic method for the production of xylitol from D-arabitol by *Gluconobacter oxydans*. **Biosci Biotechnol Biochem**, 66(12): 2614-2620.

Tada, K., et al. (2012). Enhanced Production of Bioxylitol from Corn Cobs by *Candida magnoliae*. **Industrial & Engineering Chemistry Research**, 51(30): 10008-10014.

Tamburini, E., et al. (2010). Cosubstrate effect on xylose reductase and xylitol dehydrogenase activity levels, and its consequence on xylitol production by *Candida tropicalis*. **Enzyme and Microbial Technology**, 46(5): 352-359.

Tamburini, E., et al. (2015). Optimized Production of Xylitol from Xylose Using a Hyper-Acidophilic *Candida tropicalis*. **Biomolecules**, 5(3): 1979-1989.

Tochampa, W., et al. (2005). A model of xylitol production by the yeast Candida mogii. **Bioprocess Biosyst Eng**, 28(3): 175-183.

Umino, Y., et al. (2019). Modulation of lipid fluidity likely contributes to the

fructose/xylitol-induced acceleration of epidermal permeability barrier recovery. **Arch Dermatol Res**, 311(4): 317-324.

Unrean, P. and N. Ketsub (2018). Integrated lignocellulosic bioprocess for co-production of ethanol and xylitol from sugarcane bagasse. **Industrial Crops and Products**, 123: 238-246.

Ur-Rehman, S., et al. (2015). Xylitol: a review on bioproduction, application, health benefits, and related safety issues. **Crit Rev Food Sci Nutr**, 55(11): 1514-1528.

Vallejos, M. E., et al. (2016). Strategies of detoxification and fermentation for biotechnological production of xylitol from sugarcane bagasse. **Industrial Crops and Products**, 91: 161-169.

Vaz de Arruda, P., et al. (2017). Scale up of xylitol production from sugarcane bagasse hemicellulosic hydrolysate by *Candida guilliermondii* FTI 20037. **Journal of Industrial and Engineering Chemistry**, 4: (297-302.

Venkateswar Rao, L., et al. (2016). Bioconversion of lignocellulosic biomass to xylitol: An overview. **Bioresour Technol**, 213: 299-310.

Wang, H., et al. (2016). Xylitol production from waste xylose mother liquor containing miscellaneous sugars and inhibitors: one-pot biotransformation by *Candida tropicalis* and recombinant Bacillus subtilis. **Microb Cell Fact**, 15(1): 1-12.

Wang, Y., et al. (2019). Electrodialysis-Based Separation Technologies in the Food Industry. Separation of Functional Molecules in Food by Membrane Technology, **Elsevier,** 349-381.

Wannawilai, S., et al. (2017). Furfural and glucose can enhance conversion of xylose to xylitol by *Candida magnoliae* TISTR 5663. **J Biotechnol**, 241: 147-157.

Wei, J., et al. (2010). Purification and crystallization of xylitol from fermentation broth

of corncob hydrolysates. **Frontiers of Chemical Engineering in China**, 4(1): 57-64.

Xu, L., et al. (2018). Xylitol Production by *Candida tropicalis* 31949 from Sugarcane Bagasse Hydrolysate. **Sugar Tech**, 21(2): 341-347.

Yewale, T., et al. (2016). Enhanced xylitol production using immobilized *Candida tropicalis* with non-detoxified corn cob hemicellulosic hydrolysate. **3 Biotech**, 6(1): 75.

Yi, G. and Y. Zhang (2012). One-pot selective conversion of hemicellulose (xylan) to xylitol under mild conditions. **ChemSusChem**, 5(8): 1383-1387.

Yunhui Gong, M., et al. (2015). Xylitol Gum Chewing to Achieve Early Postoperative Restoration of Bowel Motility After Laparoscopic Surgery. **Surg Laparosc Endosc Percutan Tech**, 25: 303-307.

Zhang, B., et al. (2016). Simultaneous fermentation of glucose and xylose at elevated temperatures co-produces ethanol and xylitol through overexpression of a xylose-specific transporter in engineered Kluyveromyces marxianus. **Bioresour Technol**, 216: 227-237.

Zhang, J., et al. (2012). Xylitol production from D-xylose and horticultural waste hemicellulosic hydrolysate by a new isolate of *Candida athensensis* SB18. **Bioresour Technol**, 105: 134-141.

BIOGRAPHY

Mr. Nguyen Cao Cuong was born on 23rd February 1985 in Nghe An, Viet Nam. In 2000, he graduated an upper secondary degree at Quy Hop School, Nghe An, Viet Nam. In July 2008, he graduated a Bachelor degree in Storage and Processing of Agricultural Products at Hue University of Agricultural and Forestry, Hue province, Viet Nam. In September 2008, he has become a lecturer at Hue University of Agricultural and Forestry. In July 2019, he got a scholarship for a Master program from Assoc. Prof. Dr. Apichat Boontawan, Suranaree University of Technology, Thailand. He studied in the field of Bioprocessing engineering at School of Biotechnology, Institute of Agricultural Technology, Suranaree University of Technology from July 2019 to February 2021 with the thesis entitled "Production and Purification of Xylitol from Sugarcane Bagasse".